

Copyright

by

Andrea Johanna Ryan

2011

**The Thesis Committee for Andrea Johanna Ryan
Certifies that this is the approved version of the following thesis:**

Modeling Hydrodynamic Fluxes in the Nueces River Delta

**APPROVED BY
SUPERVISING COMMITTEE:**

Supervisor:

Ben R. Hodges

George H. Ward, Jr.

Modeling Hydrodynamic Fluxes in the Nueces River Delta

by

Andrea Johanna Ryan, B.S.

Thesis

Presented to the Faculty of the Graduate School of

The University of Texas at Austin

in Partial Fulfillment

of the Requirements

for the Degree of

Master of Science in Engineering

The University of Texas at Austin

August 2011

Acknowledgements

I would like to thank my advisor, Ben R. Hodges for his direction and guidance in my graduate studies. Rachel Chisolm was a wonderful resource to me in understanding the model, and George Ward's knowledge of the history of the Nueces Delta helped me greatly. I am also appreciative of the help of the other students at the Center for Research in Water Resources.

I would also like to express my appreciation for the Coastal Bend Bays and Estuaries Program, the Army Corps of Engineers, and the City of Corpus Christi for providing the funding needed for this project.

Lastly, I am incredibly grateful for my family's constant support and love throughout my education and graduate studies.

Abstract

Modeling Hydrodynamic Fluxes in the Nueces River Delta

Andrea Johanna Ryan, M.S.E.

The University of Texas at Austin, 2011

Supervisor: Ben R. Hodges

Increasing municipal and regional water demands have reduced freshwater inflows to the Nueces Delta. These flow reductions impair the marsh ecosystem's functionality. As part of a United States Army Corps of Engineers multi-agency collaboration to restore the Nueces River and its tributaries, we have developed a mass-conservative hydrodynamic model to analyze fate and transport of freshwater and tidal inflows to the Nueces Delta. The model is built upon the LIDAR bathymetric data collected by the Coastal Bend Bays and Estuaries Program (CBBEP). Input data includes tidal, salinity, and wind data obtained from the Texas Coastal Ocean Observation Network (TCOON), pumping data from the Nueces River Authority, precipitation data from NOAA, and river flow from the USGS.

The underlying modeling method uses conservative finite-difference/volume discretization on a Cartesian rectangular grid to simulate the movement of water and salt fluxes across the delta. Sub-models to represent the hydraulic influence of flow constrictions (e.g. railroads trestles, culverts) have been developed. The model's

response to forcing from wind, precipitation, and roughness were analyzed. The time to spin up for the model was analyzed and found to be approximately seven days. Preliminary validation of the model was qualitative but the overall trend of the tide coming in appears correct at the monitoring stations analyzed, indicating that the lowest frequency forcing of the tide and wind are correct. The effects of pumping into the delta were investigated under different pumping conditions to reveal the area inundation and impacts on salinity from pumping.

Table of Contents

List of Tables	x
List of Figures	xi
Chapter 1: Introduction	1
1.1 Overview	1
1.2 Background	1
1.3 History.....	4
1.3.1 Introduction.....	4
1.3.2 Nueces Delta Mitigation Project.....	4
1.3.3 Rincon Bayou Demonstration Project	5
1.3.4 Overflow Channel Reopened.....	6
1.3.5 Allison Wastewater Treatment Plant Diversion Project	6
1.3.6 Rincon Pipeline Calallen Diversion.....	6
1.4 Hydrodynamic Model	8
1.4.1 Introduction.....	8
1.4.2 Prior Models.....	9
1.4.3 PC2 Method	11
1.5 Objectives	11
1.6 Approach.....	12
Chapter 2: Methodology	13
2.1 Overview	13
2.2 Model Input.....	14
2.2.1 Overview	14
2.2.2 Bathymetry.....	14
2.2.3 Roughness	16
2.2.4 Forcing Data.....	19
2.2.5 Initial Conditions	21
2.3 Simulations	21

2.4 Analysis Methods.....	24
2.4.1 Metrics for Analysis.....	24
2.4.2 Spin Up	28
2.4.3 Comparison to Field Data	29
Chapter 3: Results & Discussion	30
3.1 Overview	30
3.2 Spin Up	30
3.3 Qualitative Comparison to Field Data	33
3.4 Model Response to Forcing	35
3.4.1 Model Response to Rainfall.....	35
3.4.2 Model Response to Wind.....	38
3.4.3 Model Response to Roughness	40
3.5 Effects of Pumping	42
Chapter 4: Conclusions and Future Work.....	51
4.1 Findings.....	51
4.2 Future Work.....	52
Appendix A: Input Data Sources and Manipulation.....	56
A.1 Bathymetry.....	56
A.2 Barriers.....	64
A.3 Forcing Input.....	66
A.3.1 Overview.....	66
A.3.2 Tidal Data.....	66
A.3.3 Inflow Data	67
A.3.4 Wind Data	69
A.3.5 Precipitation Data.....	71
A.3.6 Salinity	72
A.3.7 Land Cover.....	72
A.4 Data Collection Limitations	73
A.5 Plots of Forcing Input	74

A.5.1 Rainfall Input	74
A.5.2 Wind Input	75
A.5.3 Tidal Input.....	79
Appendix B: Additional Information used in Analysis	81
B.1 Inundated Area Depth Cutoff.....	81
B.2 Vertical Datums.....	83
B.3 Soil infiltration Algorithm.....	84
B.4 Model’s Response to Rainfall: Total Volume.....	84
B.5 Model’s Response to Wind: Percent Change in V_T	86
Appendix C: Additional information for Future Work.....	87
C.1 Culvert Data	87
C.2 Meteorological Data	89
C.2.1 Sources for Meteorological Data in the Nueces Delta	89
C.2.2 Water Temperature Data	91
Appendix D: Matlab Scripts	92
D.1 Script for Analyzing Spin Up.....	92
D.2 Script for Analyzing Model Response to Rainfall	94
D.3 Script for Analyzing Model Response to Wind	97
D.4 Script for Analyzing Model Response to Wind	100
D.5 Script for Analyzing Pumping	102
References.....	111

List of Tables

Table 1.1: Prior numerical models created for simulating estuarine environments	10
Table 2.1: Roughness Variations used in Simulations.....	19
Table 2.2: Data Sources for Input values for the years simulated	20
Table 2.3: Conditions used in the simulations of the delta	23
Table A.1: Manning’s n values associated with various Land Cover types	73
Table B.1: Values used to estimate the NAVD88 datums for the monitoring stations	84

List of Figures

Figure 1.1: Location of the Nueces Delta	2
Figure 1.2: Major Rivers and Reservoirs in the Nueces Basin	3
Figure 1.3: Significant projects in the Nueces Delta	8
Figure 2.1: Image of the bathymetry used in the model	16
Figure 2.2: Image of roughness matrix based on land cover	17
Figure 2.3: Examples of two 15 x 15 m grids and their subgrid-scale topography.	18
Figure 2.4: Locations of TCOON salinity monitoring stations in the delta	21
Figure 2.5: Plot demonstrating the methodology for calculating the μ_{300D} and σ_{300D}	27
Figure 3.1: Comparison of 10 day and 17 day simulations to investigate spin up	31
Figure 3.2: Mean difference in depths at each grid per day.....	32
Figure 3.3: Comparison of Simulated Surface Elevations with estimated Field Surface Elevations for Preliminary Validation	34
Figure 3.4: A_i , ΔA_i , and depth of rainfall for various rain scenarios	36
Figure 3.5: Snapshots of the flow in the uplands during a rainfall event for the rain scenario and heavy rain scenarios.....	37
Figure 3.6: μ_{300D} and σ_{300D} errorbar plot for April 17, 2009, the 7 th simulated day	39
Figure 3.7: Comparison of Total Volume of Water in the System for different Roughness Scenarios	41
Figure 3.8: Inundated Area from pumping with 2 pumps over seven days with varying cutoffs for minimum fraction of pumped water in a cell	43
Figure 3.9: Inundated area in the delta from pumping through time compared with the volume pumped at that point.....	45
Figure 3.10: V_{FW} through time for various pumping scenarios	47

Figure 3.11: Volume of brackish water in the system for various pumping scenarios, increase in brackish water from pumping, and net increase in brackish water from pumping.....	49
Figure A.1: The bathymetry originally received from CBBEP with a color scale from -5 to 25 m.....	57
Figure A.2: The bathymetry originally received from CBBEP with a color scale from -1 to 4 m.....	58
Figure A.3: 1 x 1 m bathymetry displaying the location of Section A in the delta60	
Figure A.4: Section A shown at a 1 x 1 m data set.....	61
Figure A.5: Section A shown at a 15 x 15 m grid.....	62
Figure A.6: Images of the 15 x 15 m bathymetry with varying standard deviations used for channelization	63
Figure A.7: Location of the monitoring station at White Point	66
Figure A.8: Locations of the USGS Gage and the Rincon Pipeline Outfall in the Study Area	68
Figure A.9: Locations of the USGS Gage and the pipeline outfall in reference to where the Nueces River splits.....	69
Figure A.10: Locations of the weather stations measuring wind data	70
Figure A.11: Comparison of wind data from various weather stations with NUDEWX	71
Figure A.12: Rainfall in April 2008.....	74
Figure A.13: Rainfall in April 2009.....	75
Figure A.14: Rainfall in April 2010.....	75
Figure A.15: Wind Speed in April 2008.....	76
Figure A.16: Wind Direction in April 2008.....	76

Figure A.17: Wind Speed in April 2009.....	77
Figure A.18: Wind Direction in April 2009.....	77
Figure A.19: Wind Speed in April 2010.....	78
Figure A.20: Wind Direction in April 2010.....	78
Figure A.21: Tidal Boundary Condition in April 2008	79
Figure A.22: Tidal Boundary Condition in April 2009	79
Figure A.23: Tidal Boundary Condition in April 2010	80
Figure B.1: Inundated Area from Simulation 6 over seven days with varying cutoffs for minimum depth	82
Figure B.2: Depiction of the TCOON monitoring station vertical datums.....	83
Figure B.3: Depiction of the estimation method for approximating TCOON vertical datum.....	83
Figure B.4: Plots of V_T , ΔV_T , and daily rainfall depth for various rain scenarios.	85
Figure B.5: Percent Change in V_T for different wind scenarios	86
Figure C.1: Possible culvert flow conditions.....	87

Chapter 1: Introduction

1.1 OVERVIEW

In this work we developed the Nueces Delta Hydrodynamic Model to simulate the hydrodynamic conditions in the Nueces Delta in Corpus Christi, Texas. This model addresses the effects of pumping, tides, wind and precipitation on the delta while accounting for wetting and drying processes and is based on the PC2 Hydrodynamic Code, v6.0. The Nueces Delta Hydrodynamic Model was created in response to a series of projects designed to restore the ecosystem in the delta. Particularly, there is a need to increase freshwater inflows to reduce high salinities in the upper areas of the delta. These high salinities are a result of reduced freshwater inflows from the Nueces River into the delta. The Nueces Delta Hydrodynamic Model builds a framework for understanding the conditions in the delta and allows for investigating the potential impacts of restoration projects.

1.2 BACKGROUND

An estuary is the transition zone where salt water from the sea mixes with freshwater inflows from rivers (Montagna, Merryll, et al. 2002, Montagna, Hill and Moulton 2009). Estuaries typically have low salinity at the outlet of the river and increase in salinity closer to the sea. Without sufficient freshwater inflows, salt water can intrude farther upstream, increasing salinity in an estuary (Alber 2002). In extreme cases, a reverse estuary condition can occur, in which salinity patterns are reversed, and higher salinities occur upstream rather than downstream near the tidal source (Montagna, Kalke and Ritter 2002, Palmer, Montagna and Kalke 2002). High evaporation rates coupled with low rainfall can create hypersaline conditions. Since freshwater inflows are critical to the ecological health of estuaries and river deltas (Montagna, Merryll, et al.

2002, Alber 2002), studies involving deltas and estuaries experiencing these issues are becoming increasingly necessary.

The Nueces Estuary, located near Corpus Christi in southeast Texas, includes the Nueces Delta, the Nueces River tidal segment, one primary bay: Corpus Christi Bay, one secondary bay: Nueces Bay, and two tertiary bays: Oso Bay and Redfish Bay (Montagna, Hill and Moulton 2009, Bureau of Reclamation 2000a). The Nueces Delta, also known as the Nueces Marsh, covers approximately 75 square kilometers and consists of vegetated marshes, mudflats, tidal creeks and shallow ponds (Bureau of Reclamation 2000b). The location of the Nueces Delta along the Texas Coastal Bend is shown in Figure 1.1.

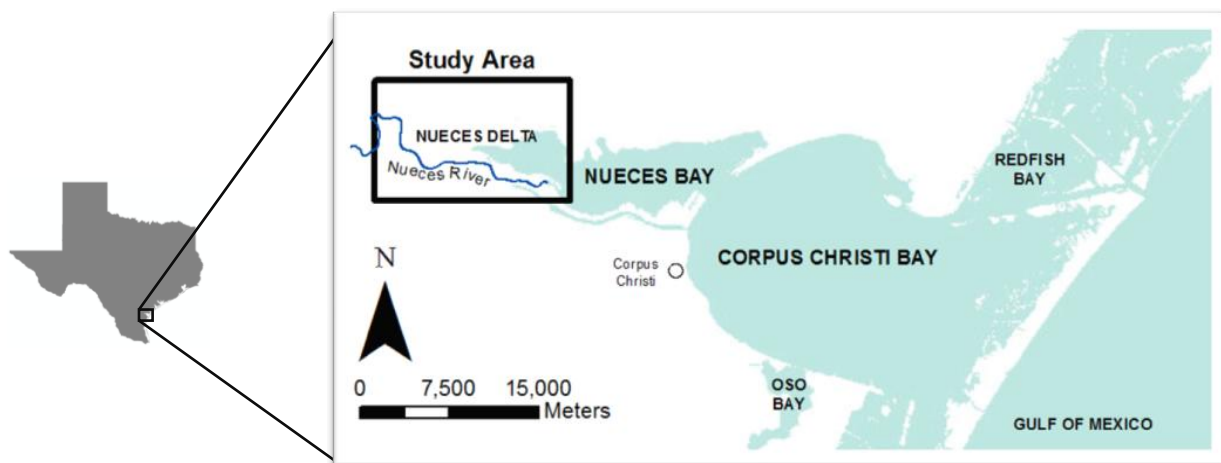


Figure 1.1: Location of the Nueces Delta

The climate in this area is considered semi-arid with mean precipitation near 75 cm/y (Rasser 2009). The Nueces Delta has been experiencing extreme reductions in freshwater inflows over the past thirty years. Since 1982, average annual freshwater inflows to the upper delta have decreased by over 99% compared to inflows prior to 1958

(Irlbeck and Ward 2000). In 1958, the Wesley Seale Dam was constructed on the Nueces River creating Lake Corpus Christi, and in 1982 the Choke Canyon Dam was constructed on the Frio River creating the Choke Canyon Reservoir (Bureau of Reclamation 2000b). Both dams contributed to reductions in river flow in the Nueces Basin. Decreasing river flow by the installation of reservoirs often has a negative effect on estuarine ecology (Copeland 1996). The locations of these reservoirs in the Nueces Basin are displayed in Figure 1.2.



Figure 1.2: Major Rivers and Reservoirs in the Nueces Basin

The Rincon Bayou, a creek located in the Nueces River Delta, has high variability, with salinity ranging from 0 ppt to 160 ppt and temperatures as high as 40°C (Montagna, Kalke and Ritter 2002). The Rincon Bayou was historically the main channel of the Nueces River, but now the main channel is south of the delta, separated by embankments that limit flooding (Heilman, et al. 2000). Without increases in the

frequency of flooding events to the upper Nueces Delta, the hypersaline conditions will continue to affect the ecosystem negatively (Alexander and Dunton 2002). The occurrence of freshwater flooding events in the upper Nueces Delta requires that the water level exceeds the minimum flooding threshold of the Nueces River in that area (Bureau of Reclamation 2000b). Therefore, freshwater inflow to the Nueces Delta is limited to discrete events when flow in the river is sufficient to overbank. This lack of freshwater inflow to the delta has led to a deterioration of the ecosystem in the Nueces Delta.

1.3 HISTORY

1.3.1 Introduction

In its recent history, there have been several attempts to restore the ecology of the Nueces Delta. The Rincon Bayou Demonstration Project, the reopening of the Rincon Overflow Channel, and the Rincon Pipeline Diversion are projects designed to increase freshwater inflows to the delta. The Allison Wastewater Treatment Plant Diversion involved piping nutrient-rich water to the delta, and the Nueces Delta Mitigation Project excavated an area to restore a salt marsh habitat. These projects were all carried out as efforts to improve the ecosystem in the delta. Outlined in Sections 1.3.2 – 1.3.6 are the significant restoration projects conducted since 1987.

1.3.2 Nueces Delta Mitigation Project

The United States Army Corps of Engineers (USACE) and the Corpus Christi Port Authority conducted the Nueces Delta Mitigation Project in March 1987 as an effort to reduce wetland losses due to dredging in the Corpus Christi Ship Channel (Alan Plummer Associates, Inc. 2007). The objective was to create a salt marsh that could provide a wetland habitat. In this project, the USACE excavated an $80 \times 10^3 \text{ m}^2$ (198

acre) area of to create a network of channels and ponds with maximum water circulation to simulate natural salt marshes (Nicolau, et al. 1996). The project was considered to be complete in August 1997, when many levees on the Nueces Delta Mitigation Project had new growth. While the Nueces Delta Mitigation Project did not replace *Spartina alterniflora*, an important plant species in the delta, the project did produce a non-vegetated bay bottom habitat (Nicolau, et al. 1996).

1.3.3 Rincon Bayou Demonstration Project

The Nueces River flows south of the Nueces Delta directly into the Nueces Bay. Before increases in pumping from the Nueces River, the river flooded frequently into the delta. From 1940-1957 the mean annual river flow into the upper Nueces Delta was $158 \times 10^6 \text{ m}^3$ (127,997 acre-ft), whereas the mean annual flow from 1983-1996 was only $662 \times 10^6 \text{ m}^3$ (537 acre-ft). Since the completion of the Choke Canyon Dam in 1982 until 1999, the Nueces River only significantly overbanked into the delta five times (Ward, Irlbeck and Montagna 2002). The U.S. Bureau of Reclamation conducted the Rincon Bayou Demonstration Project in October 1995 to increase freshwater inflows from the Nueces River to the Nueces Delta (Bureau of Reclamation 2000a). Within the demonstration project, the Nueces Overflow Channel was excavated from the Nueces River to the headwaters of the Rincon Bayou with a bottom elevation at approximately mean sea level (Bureau of Reclamation 2000b). A second overflow channel, the Rincon Overflow Channel, was created to provide a spillway from the upper Rincon Bayou to the tidal mudflat areas.

The more frequent diversion of freshwater from the demonstration project had a positive effect on the ecology of the Rincon Bayou and the upper Nueces Delta, and eventually reduced the salinities in the delta. However, the project did not have

permanent easements and the channel was closed in September 2000 (Montagna, Hill and Moulton 2009).

1.3.4 Overflow Channel Reopened

Because of the success of the Rincon Bayou Demonstration Project, the City of Corpus Christi re-opened the overflow channels in October 2001, and the channels are now permanent features of the Nueces Delta (Alan Plummer Associates, Inc. 2007).

1.3.5 Allison Wastewater Treatment Plant Diversion Project

The Allison Wastewater Treatment Plant, located on the south bank of the Nueces River tidal reach, has historically discharged secondary treated municipal wastewater effluent to the Nueces River since the plant's construction in 1966 (Alan Plummer Associates, Inc. 2007). In an effort to provide high-nutrient freshwater to the delta, the City of Corpus Christi created a pipeline under the Nueces River to divert water from the treatment plant to the delta. In August 1997, the City constructed three earthen cells to receive treated effluent in the Lower Nueces River Delta. The diversion began in October 1998, diverting approximately 2.0×10^6 gallons per day (Montagna, Hill and Moulton 2009). A study on the effects of the wastewater diversion project found that there were no detrimental impacts on the marsh, but that more wastewater must be diverted if substantial reduction in salinity downstream is the primary goal (Alexander and Dunton 2006). The Allison Wastewater Treatment Plant Diversion Project was completed in August 2003 (Nicolau, et al. 2002).

1.3.6 Rincon Pipeline Calallen Diversion

The Calallen pool was formed from a dam constructed by the Corpus Christi Water Supply Company to prevent saltwater from the Nueces Bay from intruding upstream and impacting drinking water in the late 1800's. The Calallen Dam is located

approximately 10 miles upstream from the mouth of the river, a few hundred feet downstream of the Missouri Pacific Railroad crossing of the river. The dam successfully prevents normal tides from impacting the water upstream of it (Cunningham 1999). Because the saltwater barrier maintains freshwater in the Calallen pool, the City constructed a pipeline to divert water from the Calallen pool to the upper Rincon Bayou to deliver freshwater to the delta on a more controllable basis. The pipeline was completed in 2008.

Only two estuarine systems on the Texas Gulf Coast, the Nueces Estuary and the Colorado Estuary, have explicit bay and estuary freshwater inflow volume requirements attached to water rights in their respective basins (Tolan 2007). Based on the 1995 Agreed Order by the Texas Natural Resource Conservation Commission, the City of Corpus Christi is required to “pass through” freshwater to the bays and estuaries (Adams and Tunnell 2010). The Calallen Diversion Project pump station and pipeline are designed to divert up to 3,000 acre-feet from upstream of the saltwater barrier dam to the Rincon Bayou. The Nueces River Authority monitors the volume of water that is diverted from the river to the Rincon Bayou. The locations of the restoration projects conducted in the Nueces Delta are displayed in Figure 1.3.

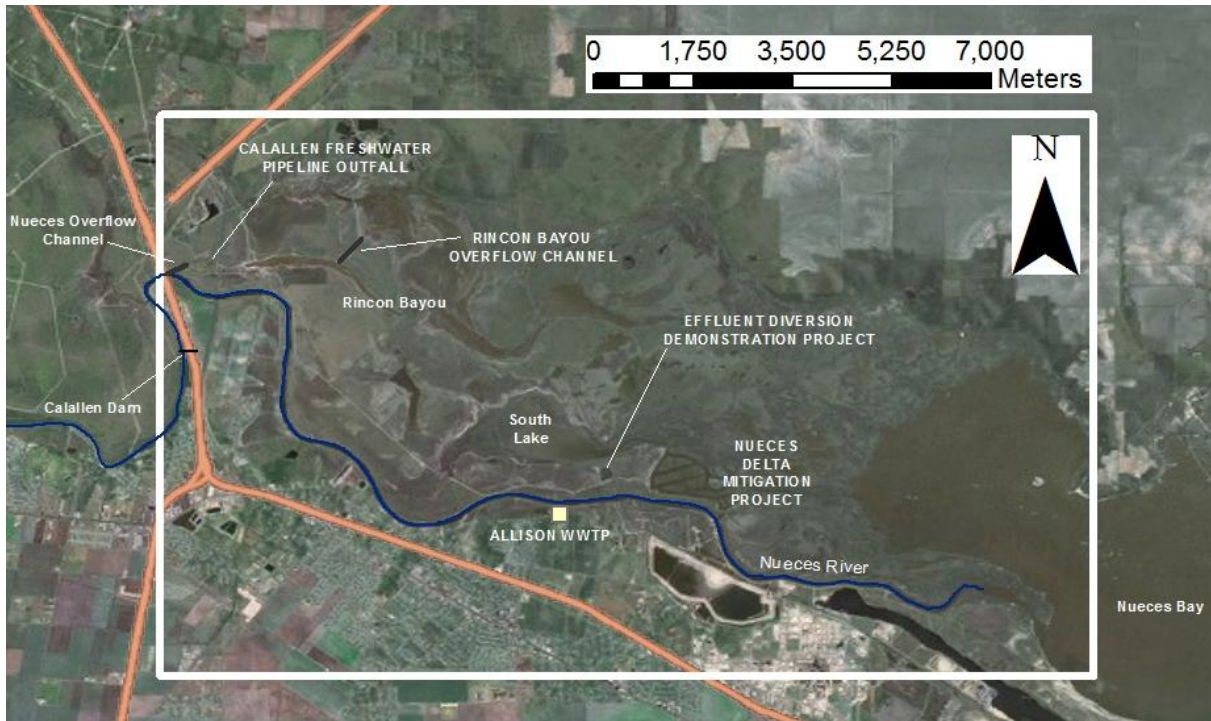


Figure 1.3: Significant projects in the Nueces Delta

1.4 HYDRODYNAMIC MODEL

1.4.1 Introduction

Prior to the present study, a comprehensive numerical model of flow hydrodynamics in the Nueces Delta using the shallow-water equations had not been attempted. The Bureau of Reclamation report for the Rincon Bayou Demonstration Project notes the opportunity for a numerical model to integrate the data components of the study and improve understanding of the marsh under various conditions (Bureau of Reclamation 2000b). The study presented here fills the need for a hydrodynamic model of the Nueces Delta to examine the impacts of changes in flow to the Delta, including inflows from the Rincon Pipeline, tidal flows, and rainfall.

1.4.2 Prior Models

Numerical models have been used extensively to simulate hydrodynamic conditions in estuaries (Roman, Garvine and Portnoy 1995, Yang and Khangaonkar 2009, Chen, Liu and Beardsley 2003, Xia, Falconer and Lin 2010, Zheng, Chen and Zhang 2004, Zhang, Baptista and Myers 2004, Ji, Morton and Hamrick 2001). Recent advancements allow for more accurate modeling of estuarine conditions. A principal challenge for estuaries, simulating wetting and drying processes, has been addressed by a number of models (Yang and Khangaonkar 2009, Battjes 2006, Ji, Morton and Hamrick 2001, Oey 2006, Casulli and Zanolli 2002). These developments in numerical modeling of estuarine environments have been used to model estuaries across the globe, with each model having a different focus. Table 1.1 provides examples of these numerical models cited in the current literature.

Model	Area	Dimensionality	Focus	Cited by:
FVCOM	Skagit River Estuary, Puget Sound, WA	3D	Tidal circulation & transport processes	Yang and Khangaonkar 2009, Chen, Liu and Beardsley 2003
ECOM-si	Satilla River Estuary, Georgia	3D	semi-implicit finite difference scheme; realistic vertical turbulent mixing parameters	Zheng, Chen and Zhang 2004
ELCIRC	Columbia River Estuary	3D	turbulence closure schemes; includes terms for the tidal potential and atmospheric pressure gradients, and provides a detailed description of air-water exchanges	Zhang, Baptista and Myers 2004
Environmental Fluid Dynamics Code (EFDC)	Morro Bay, James River Estuary (might need more citations)	3D	Provides a hydrodynamic model with water quality model, sediment transport model, and toxics model capabilities	Ji, Morton and Hamrick 2001
Princeton Ocean Model (POM) with wetting and drying scheme	Cook Inlet, Alaska	3D	Movable land-sea boundaries	Oey 2006
Delft-FLS	Polders of Tiel and Culemborg, Netherlands	2D	Specifically suited to simulate overland flow over initially dry land	Stelling, Kernkamp and Laguzzi 1998
TRIM	Barbamarco Lagoon, Italy	3D	A stable semi-implicit finite difference method of discretization computationally suitable for spatially fine grids with relatively large time steps	Casulli and Cattani 1994, Casulli and Cheng 1992
ELCOM-CAEDYM	Barbamarco Lagoon, Italy	3D	Provides a hydrodynamic model coupled with an aquatic ecosystem model; includes external environmental forcing	Spillman, Hamilton, Hipsey and Imberger 2008

Table 1.1: Prior numerical models created for simulating estuarine environments

1.4.3 PC2 Method

The Estuarine models in Table 1.1 all use the hydrostatic Navier-Stokes equations (also known as the shallow water equations) to solve conservation of momentum and mass. A common numerical approach in several models is the semi-implicit algorithm using implicit discretization for the free surface (barotropic mode) and explicit discretization for the velocity and baroclinic forcing (internal wave), e.g. Casulli and Cheng (1992). This approach is generally implemented in a first-order accurate scheme for unsteady and baroclinic flows (Hodges 2004). By restructuring the semi-implicit algorithm for a predictor-corrector sweep, the semi-implicit θ -method (Casulli and Cattani, 1994) can be improved to 2nd order for both barotropic and baroclinic flow (Hodges and Rueda 2008). The PC2 Hydrodynamic Code used for the Nueces Delta Hydrodynamic Model employs predictor-corrector methods using two time-levels of information (Hodges and Rueda 2008). It has volume-consistent discretization of both barotropic and baroclinic modes, along with mass-conserving scalar transport. The model can be implemented in either 2D or 3D, and using either first-order or second-order accurate numerical algorithms. During development of the Nueces Delta Hydrodynamic Model, the PC2 Hydrodynamic Code was applied in 2D (depth-averaged) with first-order algorithms. This approach ensured the fastest model simulation time, which is an advantage during model development.

1.5 OBJECTIVES

The main objectives of this research are:

1. Create a model that reasonably represents the hydrodynamic conditions in the Nueces Delta.

2. Demonstrate the possible effects of pumping in the delta through the Rincon Pipeline.

1.6 APPROACH

To allow for the PC2 Hydrodynamic Code, v6.0 to simulate conditions in the Nueces Delta, the code requires input specific to the delta and analysis of the model results to understand the model's success. Section 2.1 presents the model input used to create the Nueces Delta Hydrodynamic Model. Within this section, the methodology for determining the input to the model is defined. Details on input sources and manipulation techniques are outlined in Appendix A. Using variations of the model input detailed in Section 2.3, the model simulates different scenarios, and the model's response to different forcing mechanisms is analyzed based on the output of these scenarios. The methods for analyzing the model results are described in Section 2.4 and the results of analysis are discussed in Section 3.2 – 3.4. The possible effects of pumping in the delta are analyzed and described in Section 3.5.

Chapter 2: Methodology

2.1 OVERVIEW

This project is intended to investigate the influences of freshwater inflow on the hydrodynamics of the Nueces Delta by running the PC2 Hydrodynamics Code configured as the Nueces Delta Hydrodynamic Model to simulate various scenarios. Comparing different simulations allows for a greater insight into the effects of different forcing conditions on the Nueces Delta. In formulating Nueces Delta Hydrodynamic Model, the input files are developed to reflect realistic bathymetric, inflow, and meteorological conditions in the delta. Hydraulic effects, such as overtopping of dikes or flow through bridge piers, are not readily represented by the shallow water equations at the model resolution, so are handled by customized submodels. The input files and configuration are described in Section 2.2. The methods for analyzing the model results are described in Section 2.4. Matlab scripts for recreating the results are included in Appendix D. The results are analyzed to aid in understanding the model's response to boundary forcing and the influence of initial conditions on the output. Four model scenarios are used to evaluate the relative influence of different pumping options for the Rincon Pipeline.

Due to the lack of sufficient field data, the Nueces Delta Hydrodynamic Model could neither be calibrated nor validated for the present study. Discussion of the types of data needed for calibration and validation are provided in Section 4.2. However, because the model is mechanistic, the uncalibrated results are useful in model-model comparisons to investigate the system's sensitivity to different forcing conditions.

2.2 MODEL INPUT

2.2.1 Overview

The input to the model includes boundary data, such as bathymetric data and roughness, and forcing data, which accounts for wind, tide, precipitation and inflows. Input also includes parameters that change the model representation of the physics, such as the time step and the wind drag coefficient. The initial conditions consist of the salinity across the delta and the initial water depth. April 2008, 2009, and 2010 are the time periods of interest for simulation. The methodology for determining the boundary data, initial conditions, and forcing data is outlined in Sections 2.2.2 – 2.2.5, as this data is specific to the Nueces Delta. The details on the manipulations of this data, such as the removal of NaN values and step by step processes for data preparation, and information on the model parameters are available in Appendix A. Data manipulation and model parameters are important to model function but are not the central focus of this work, and are included in the appendix for this reason.

2.2.2 Bathymetry

The available bathymetry for this project was a 1 x 1m raster data set prepared by J. Gibeaut at Texas A&M Corpus Christi from LiDAR data collected under a project funded by the Coastal Bend Bays and Estuary Program. This bathymetry was previously processed and validated against field measurements by J. Gibeaut (personal comm). The 1 x 1 m data set consists of 105×10^6 elevations within the Nueces Delta and the nearby uplands. Extrapolating from recent experience, in its present configuration the PC2 Hydrodynamic Code running on a 3 GHz processor would require about 1500 GB of memory and 10 minutes of computer time for every second of model simulated time (i.e. only $1/600^{\text{th}}$ of real time so that it takes 600 hours on the computer to model one hour in

the delta). By creating a coarser 15 x 15 m bathymetry data set for the Nueces Delta Hydrodynamic Model, the computer memory required is more manageable (5 GB) and the computational time is 0.14 seconds for every second modeled in the delta (i.e. 7 times faster than real time, so that 1 hour of computation will model 7 hours in the delta). Upscaling from the 1 x 1 m data to the 15 x 15 m data was accomplished using the mean elevation value with adjustments for subgrid scale features. Channelization effects along grid cell diagonals for subgrid features was approximated using a statistical analysis to identify affected cells in the 15 x 15 m data set and adjust to the cell elevation to the mean of the lowest 15 data points in the 1 x 1 m grid. The PC2 Hydrodynamic Code has edge features that can be used to account for subgrid-scale blocking topography that is lost in the upscaling process. The two railways crossing the Nueces Delta are 3 to 4 m wide, so they are represented by elevations on cell edges in the 15 x 15 m grid. Where piers allow flow under the railways, the mean elevation in the grid cell was used, with a hydraulic model applied to represent the drag associated with the piers. Details on the bathymetry modeling are provided in Appendix A.1. The bathymetry used in the model is displayed in Figure 2.1.

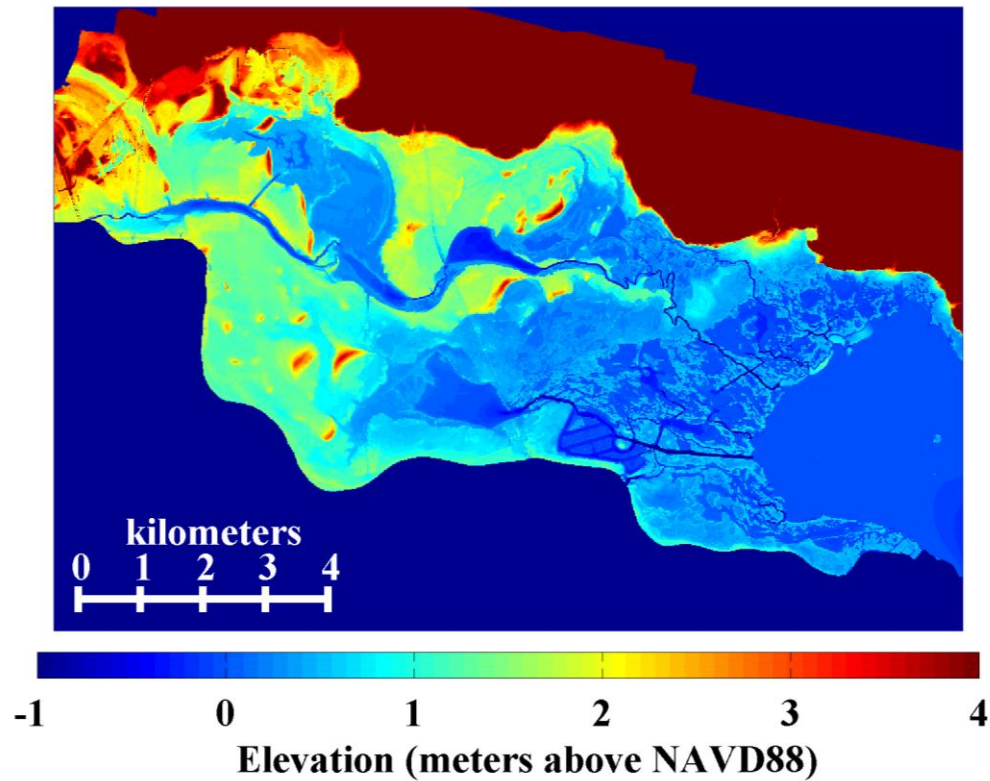


Figure 2.1: Image of the bathymetry used in the model

2.2.3 Roughness

The roughness in the model was developed from the 2001 National Land Cover Dataset. Manning's roughness coefficient values associated with simulating flow across the 2001 NLCD were gathered from literature and translated to a matrix corresponding with bathymetry in the delta (Hossain, Jia and Chao 2009). The impacts of piers and culverts under barriers are incorporated into the land cover matrix as adjusted Manning's roughness coefficients. Details on the methodology used to create the roughness matrix are given in Appendix A.3.7. Figure 2.2 displays the baseline roughness matrix used in the model. The variable used to describe this roughness matrix is $n_B(k)$.

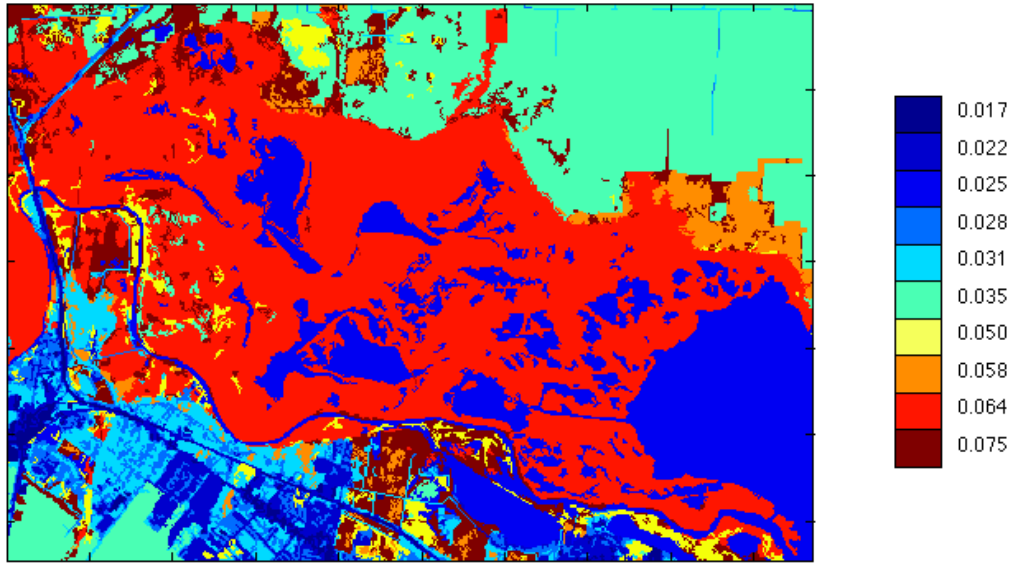


Figure 2.2: Image of roughness matrix based on land cover

There are weaknesses associated with this roughness matrix. Because the 15 x 15 m grid was rasterized from the 1 x 1 m grid, we have the ability to understand the subgrid-scale topography. Figure 2.3 gives an example of two 15 x 15 m grids containing two-hundred and twenty-five 1 x 1 meter data values. The two grids have the same mean elevation of 2.1 m, with the grid on the left having a standard deviation of 0.70 m and the grid on the right having a standard deviation of 0.02 m.

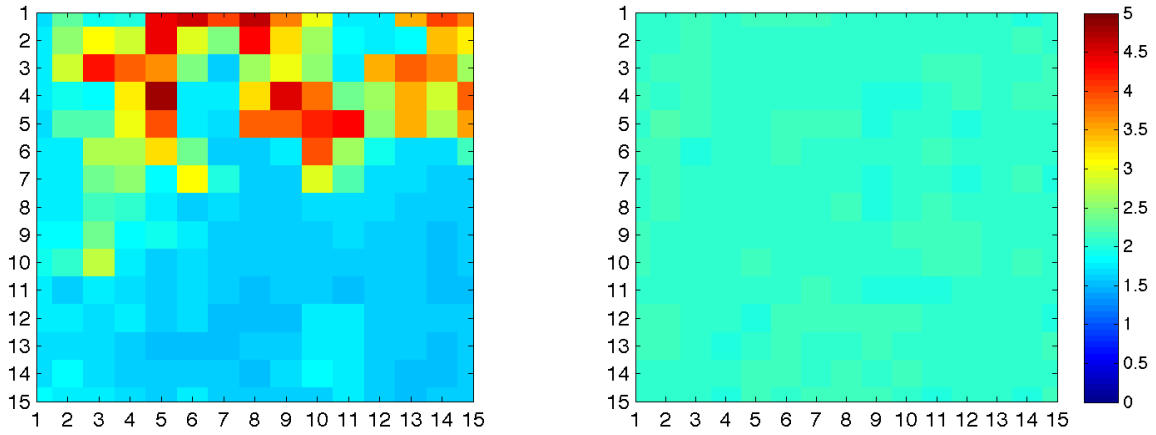


Figure 2.3: Examples of two 15 x 15 m grids and their subgrid-scale topography.

The flow across these two grids would be different because of elevation change within the cell. However, methods for understanding the impacts of subgrid-scale topography on model roughness are not defined. This issue is discussed in Section 4.2 as future work. Although the methods for improving the roughness are currently unknown, and the affects of subgrid-scale topography on flow have not yet been investigated, there is still merit to testing the model’s response to changing the roughness in areas with high standard deviations caused by subgrid-scale elevation changes. The different manipulations of the roughness are outlined in Table 2.1. The matrix $n_B(k)$ is used as roughness ID R_B , the base roughness. To create variations of this roughness, matrix $n_B(k)$ is adjusted by multiplying grid cells with standard deviations in subgrid-scale elevation greater than a cutoff value by a factor of two to create matrix R_{σ_2} and by a factor of ten to create matrix $R_{\sigma_{10}}$. The entire matrix $n_B(k)$ is multiplied by a factor of ten to create matrix R_{10} and by a factor of one hundred to create matrix R_{100} .

Roughness ID	Adjustment of Roughness
R_B	$n_B(k)$
$R_{\sigma 2}$	$n_{\sigma 2}(k) = \begin{cases} 2n_B(k) & : \sigma_Z(k) \geq c_\sigma \\ n_B(k) & : \sigma_Z(k) < c_\sigma \end{cases}$
$R_{\sigma 10}$	$n_{\sigma 10}(k) = \begin{cases} 10n_B(k) & : \sigma_Z(k) \geq c_\sigma \\ n_B(k) & : \sigma_Z(k) < c_\sigma \end{cases}$
R_{10}	$n_{10}(k) = 10n_B(k)$
R_{100}	$n_{100}(k) = 100n_B(k)$

Table 2.1: Roughness Variations used in Simulations

The variable $n_B(k)$ is the baseline Manning's n roughness for $k=\{1\dots N\}$ grid cells, where $k=\{1\dots N\}$ includes the entire system. The standard deviation of the topography in the k^{th} grid cell is defined as $\sigma_Z(k)$, and c_σ is the standard deviation cutoff value, which, as discussed in Appendix A.1, is defined at 20 cm.

2.2.4 Forcing Data

The forcing data in the model includes tidal elevation, wind speed and direction, inflows, salinity, and precipitation. Data sources, time periods of data availability, and data manipulation are outlined in detail in Appendix A.3. Appendix A.5 also provides example plots of the input values used for the simulations. Table 2.2 gives the data sources for the years simulated. Section 2.3 describes the variations of the forcing data for different scenarios.

Input	Source		
	2008	2009	2010
Tide	TCOON	TCOON	TCOON
Salinity	TCOON	TCOON	TCOON
Precipitation	NOAA	NOAA	NOAA
Wind	NOAA	TCOON	TCOON
Inflow	USGS	USGS	USGS
Pumping	Nueces River Authority	Nueces River Authority	Nueces River Authority

Table 2.2: Data Sources for Input values for the years simulated

TCOON monitors the salinity in the delta at the SALT and NUDE stations. The locations of these stations are displayed in Figure 2.4. The salinity data obtained from SALT03 is used as the boundary condition for tidal salinity in the simulations.



Figure 2.4: Locations of TCOON salinity monitoring stations in the delta

2.2.5 Initial Conditions

The initial conditions in the Nueces Delta Hydrodynamic Model include salinity and initial water depth. The monitored salinities at the SALT and NUDE stations in the delta for the day prior to the start of each simulation are averaged and interpolated across the space to create a matrix of salinities as the initial condition. The locations of the salinity monitoring stations and the details on creating the salinity initial condition are given in Figure 2.4 in Section 2.2.4. The initial water depth for the system is set equal to the tidal level at the start of simulation.

2.3 SIMULATIONS

The model runs were chosen to simulate varying conditions in the delta to allow for comparison. All simulations use field measured data for tide, salinity, and USGS gauged inflow input. The input for precipitation, wind speed, and pumping vary depending on the scenario of interest. Inputs for the rainfall scenarios include no rain, the

actual measured rainfall, and heavy rainfall. The methodology for defining heavy rainfall in the delta is outlined in Appendix A.3.5. The wind speed variations include no wind, the actual measured wind speed, and twice the wind speed. Pumping scenarios include using zero to three pumps. More details on the variations of the forcing data are provided in Appendix A.3. The variations in roughness are discussed in Table 2.1 in Section 2.2.3. Table 2.3 displays the input variations for the simulations.

	Simulation Number	Year			Wind			Rain			Days simulated				Roughness					Number of Pumps			
		2008	2009	2010	no wind	baseline wind	2x wind	no rain	baseline rain	heavy rain	7	10	14	17	a	b	c	d	e	0	1	2	3
		Pump Scenarios	1	X				X			X		X				X					X	
	2	X				X			X		X				X						X		
	3	X				X			X		X				X							X	
	4	X				X			X		X				X								X
Rain Scenarios	5		X			X		X			X				X					X			
	6		X			X			X		X				X					X			
	7		X			X				X	X				X					X			
Wind Scenarios	8		X		X				X		X				X					X			
	9		X			X			X		X				X					X			
	10		X				X		X		X				X					X			
Spin Up Scenarios	11		X			X		X				X			X					X			
	12		X			X		X					X		X					X			
Roughness Scenarios	13			X		X			X			X			X					X			
	14			X		X			X			X				X				X			
	15			X		X			X			X				X				X			
	16			X		X			X			X					X			X			
	17			X		X			X			X						X		X			

Table 2.3: Conditions used in the simulations of the delta

The simulations from 2008 compare the pumping scenarios, those from 2009 investigate the models response to forcing from wind and rain and time to spin up, and those from 2010 show the response of the model to variations in roughness. In total, seventeen different conditions were simulated for the Nueces Delta.

2.4 ANALYSIS METHODS

2.4.1 Metrics for Analysis

The analysis of the model results focuses on a few metrics: inundated area, total volume of water in the system, volume of freshwater in the system, volume of brackish water in the system, mean difference in depth between two simulations, and the mean depth across the delta from east to west. The inundated area (A_i) is used to integrate the model behavior over all space into a single metric that evolves through time and has practical meaning for water management. However, the wetting and drying algorithms in the hydrodynamic model will include infinitesimally thin layers (e.g. 10^{-6} m), which may not represent important inundated area and should be removed from the inundated area computation. As a practical measure, the inundated area can be defined as a sum over the N grid cells with individual cell areas $a_k = 225 \text{ m}^2$ given the evolution of the water depth over time $d_k(t)$ as

$$A_i(t) = \sum_{k=1}^N a_k H\{d_k(t) - c_i\} \quad (2.1)$$

where $H\{\}$ is the Heaviside step function and c_i is a cutoff, chosen as 0.02 m for the present study. The methodology for determining 0.02 m as the cutoff for required depth is presented in Appendix B.1. The soil infiltration algorithm in the model, described in Appendix B.3, impacts the A_i by decreasing water depth at a constant rate. By making shallow depths even shallower, the soil infiltration algorithm reduces the number cells with sufficient depths greater than the cutoff for A_i .

The evolution of the total water volume V_T in the delta is computed without a cutoff as small depths will not significantly distort its meaning.

$$V_T(t) = \sum_{k=1}^N a_k d_k(t) \quad (2.2)$$

Analyzing both the total volume of water in the system and the inundated area gives two different perspectives of the behavior of the model. While A_i shows the extent of inundation in terms of spatial extent, the V_T takes the depth into account as well.

The volume of water in the system can be divided into brackish water and freshwater, which is particularly helpful for understanding the effects of pumping. At grid cell k , the fraction of freshwater, F_k , can be calculated by subtracting the salinity, $S_k(t)$, from a reference salinity S_R . S_R is defined here as 30 ppt based on the fact that the tidal water at the boundary condition has a maximum salinity of approximately 30 ppt for April 2008, the month of simulation for pumping scenarios. Equations 2.3 and 2.4 show the calculations for finding $F_k(t)$ and the total volume of freshwater in the system, V_{FW} , where the depth at grid cell k at time t is $d_k(t)$

$$F_k(t) = \frac{S_R - S_k(t)}{S_R} \quad (2.3)$$

$$V_{FW}(t) = \sum_{k=1}^N a_k F_k(t) d_k(t) \quad (2.4)$$

The volume of brackish water in the system, V_B , is calculated by defining a cutoff, c_i , for maximum salinity for defining water as brackish, which for the present study is defined as 15 ppt. The volume of brackish water in a cell, v_{Bk} , is calculated as zero or one depending on if it exceeds the salinity cutoff, c_s . The volume of brackish water in the system is calculated for the varying pumping scenarios as V_{B0} , V_{B1} , V_{B2} , and V_{B3} for the zero pumps, one pump, two pumps, and three pumps scenarios, respectively. The A_i , V_T ,

V_{FW} , and V_B measures each provide a single value for the entire two-dimensional space at each time step for comparison. These calculations are given in Equations 2.5 and 2.6.

$$v_{Bk}(t) = \begin{cases} a_k d_k(t) & : S_k(t) \leq c_s \\ 0 & : S_k(t) > c_s \end{cases} \quad (2.5)$$

$$V_B(t) = \sum_{k=1}^N v_{Bk}(t) \quad (2.6)$$

A depth comparison complements the area and volume comparison so that we can understand the differences across the entire two-dimensional space. Equations 2.7 and 2.8 below show the calculations for finding the mean difference in depth ($\mu_{\Delta D}$) and standard deviation in depth ($\sigma_{\Delta D}$), where the difference between the depths at grid cell k in two different scenarios at time t is defined as $\Delta D_k(t)$, the mean and standard deviation are

$$\mu_{\Delta D}(t) = \frac{1}{N} \sum_k^N \Delta D_k(t) \quad (2.7)$$

$$\sigma_{\Delta D}(t) = \frac{1}{N-1} \sqrt{\sum_k^N [\Delta D_k(t) - \mu_{\Delta D}(t)]^2} \quad (2.8)$$

The $\mu_{\Delta D}(t)$ and $\sigma_{\Delta D}(t)$ demonstrate the spatial differences between two simulations, and is used in understanding the model's spin up, as described in Section 3.2.

The last metric used in analysis is the mean and standard deviation in depth across sections in the delta, μ_{300D} and σ_{300D} . The delta is divided into 300 m north – south sections and the depth is analyzed across these sections. Figure 2.5 demonstrates the method in which the delta is divided into $p=\{1...H\}$ sections.

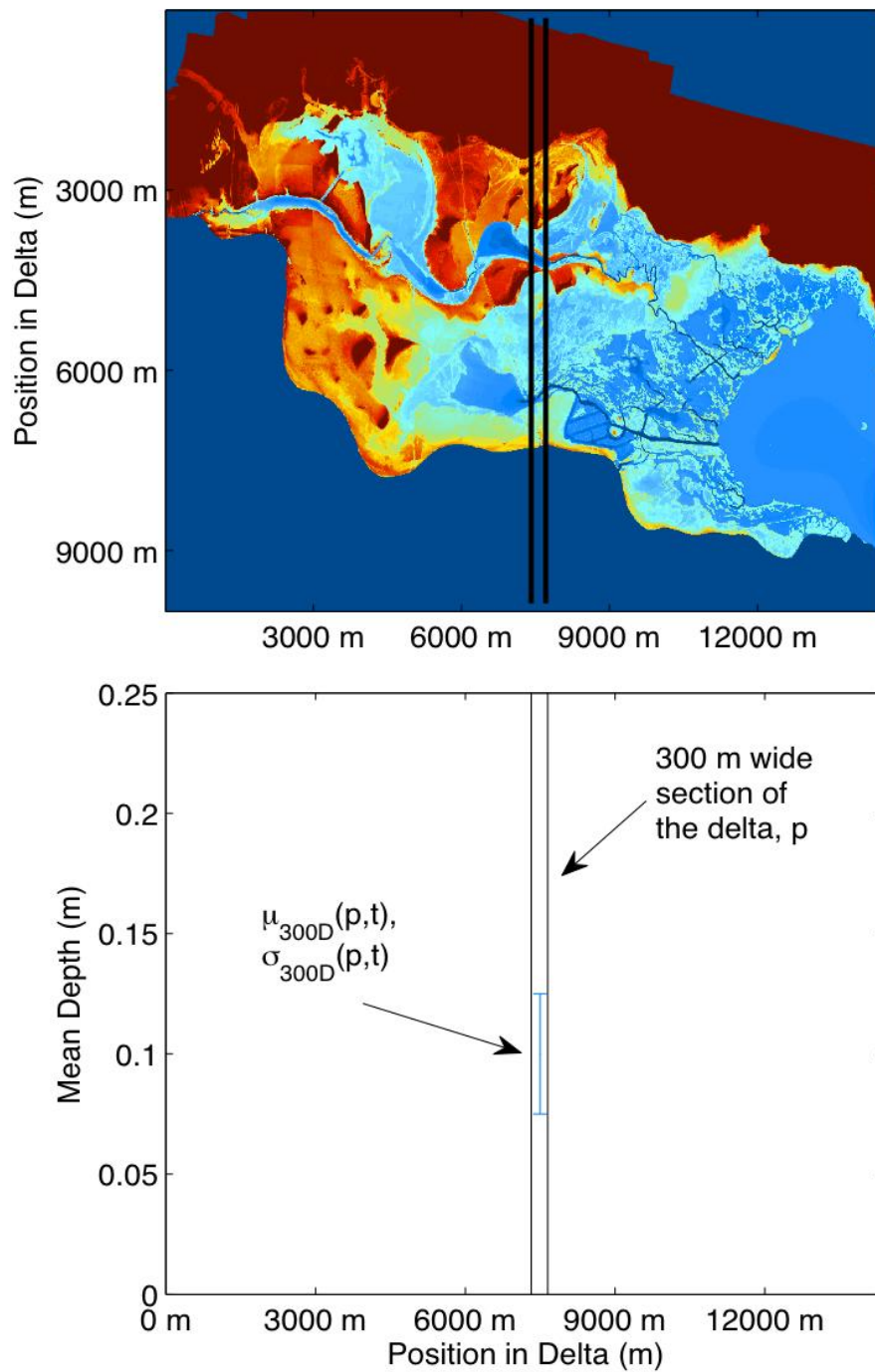


Figure 2.5: Plot demonstrating the methodology for calculating the μ_{300D} and σ_{300D}

For $p=\{1\dots H\}$ 300 m north – south sections in the delta, and $j = \{1\dots N\}$ grids in each section, p , the depth at each grid, j , is defined as $D_j(p)$.

$$\mu_{300D}(p) = \frac{1}{N} \sum_j^N D_j(p) \quad (2.9)$$

$$\sigma_{300D}(p) = \frac{1}{N-1} \sqrt{\sum_j^N [D_j(p) - \mu_{300D}(p)]^2} \quad (2.10)$$

There is no minimum depth cutoff used for μ_{300D} or σ_{300D} . The previous metrics used in analysis, A_i , V_T , and $\mu_{\Delta D}$ and $\sigma_{\Delta D}$, result in a single value for each time step in the model. The μ_{300D} and σ_{300D} , however, give multiple output values for each time step and are best for analyzing the end result of a model at a single time step. This is helpful for understanding the effects of wind on the model, as it displays how wind forces affect the movement of water from east-west in the delta. It is expected that easterly winds will push water into the delta, and the μ_{300D} and σ_{300D} aid in representing how the model responds to wind forces.

2.4.2 Spin Up

Spin up refers to a model's adjustment to forcing such that it can reach a state in which further evolution is approximately independent of the initial conditions. To ensure that inaccuracies in the initial conditions do not dominate the results, the spin-up time is found by comparing results from a simulation beginning on April 3, 2009 and a simulation beginning on April 10, 2009. The initial conditions are defined based on the time the simulation begins, and are described in Section 2.1.5 and Appendix A.3.6. Starting two simulations with the same conditions beginning at different times with different initial conditions allows for comparison. Comparing these scenarios and finding when the results match up helps to define at what time spin up is complete. The metrics for determining the time to spin up are the V_T through time, the A_i through time, and the

$\mu_{\Delta D}$ and $\sigma_{\Delta D}$. The $\mu_{\Delta D}(t)$ is a good tool for analyzing spin up, as the differences between the two simulations spatially at each time step should decrease as the model output becomes less dependent on the initial conditions.

2.4.3 Comparison to Field Data

For insight into model behavior, the modeled water surface elevations were qualitatively compared with data measured at TCOON SALT and NUDE stations. Unfortunately, these stations have not been benchmarked to any vertical geodetic referencing systems. Without data for the sensor elevation relative to a known vertical datum, the depth measurements from SALT and NUDE stations cannot be used for quantitative calibration or validation. However, we can obtain a rough estimate of the sensor elevations by neglecting any mean horizontal gradient in the surface elevation between the sensors, and assuming that the monthly mean water surface elevation at each sensor is approximated by the same as the monthly mean water surface elevation at the White Point TCOON station. Appendix B.2 provides further information on these computations.

Chapter 3: Results & Discussion

3.1 OVERVIEW

The PC2 Model was run to simulate varying conditions in the Nueces River Delta in April 2008, 2009, and 2010. In this chapter we look into the spin up of the model (Section 3.2), compare the initial model output to field data (Section 3.3), and investigate the response of the model to different forcing conditions (Section 3.4). This chapter also includes a section on the effects of pumping (Section 3.5). The methods used for analyzing the results are outlined in Section 2.4.1.

3.2 SPIN UP

Section 2.3 describes the conditions used for understanding spin up in the Nueces Delta Hydrodynamic Model. For this analysis, the V_T and A_i in the delta through time are compared for Simulation 11 and Simulation 12 described in Table 2.3. These metrics are displayed in Figure 3.1.

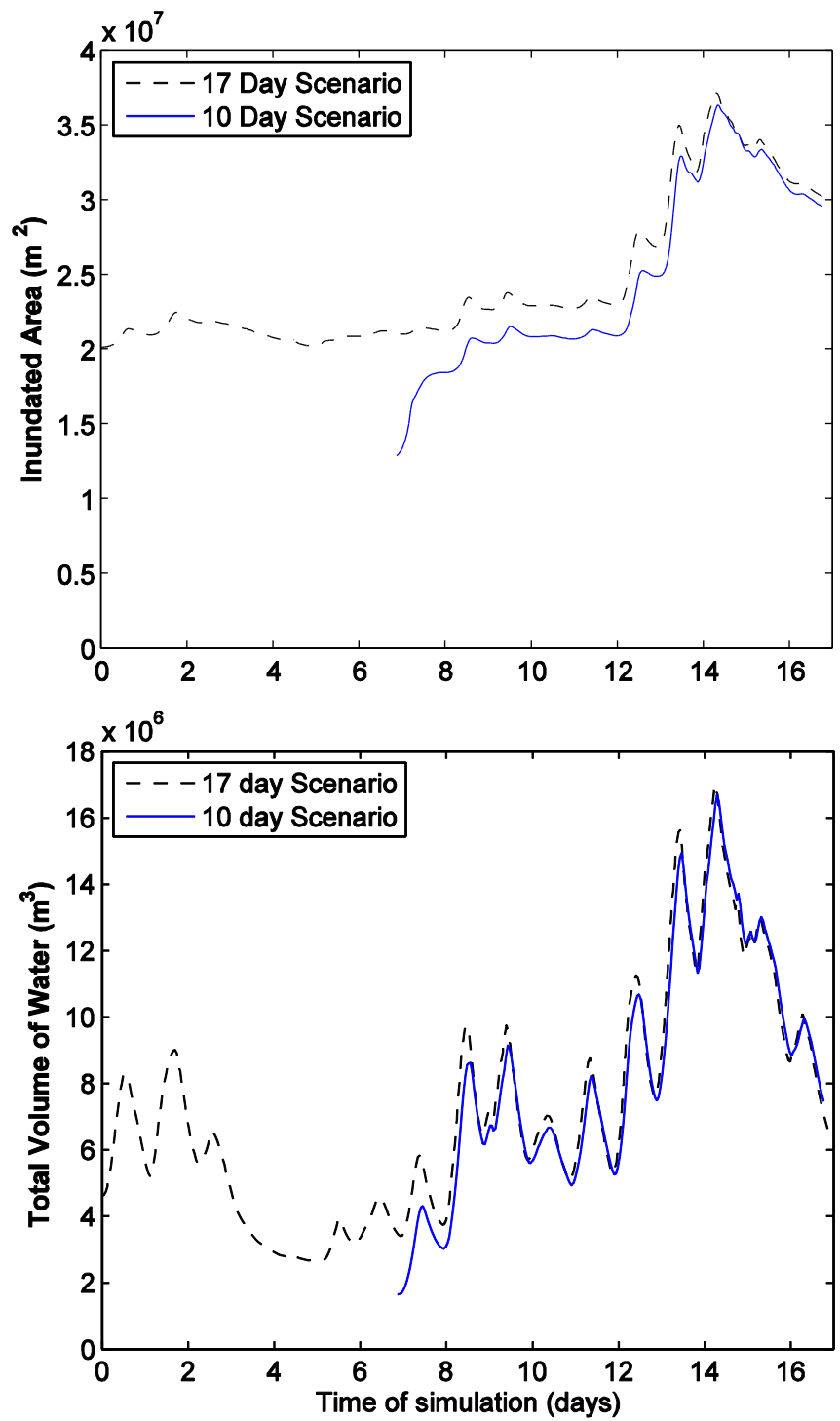


Figure 3.1: Comparison of 10 day and 17 day simulations to investigate spin up

At approximately the 7th day of the April 10, 2009 simulation, which is the 14th day of the simulation starting on April 3, 2009 the output of the two simulations have converged in both inundated area and volume. A more quantitative statistical view can be obtained using the mean difference in depths $\mu_{\Delta D}$ (Equation 2.7), as shown in Figure 3.2, from which it appears that convergence of the two simulations occurs on day 16, when the mean difference is 1.32×10^{-3} m and the standard deviation is 2.62×10^{-3} m.

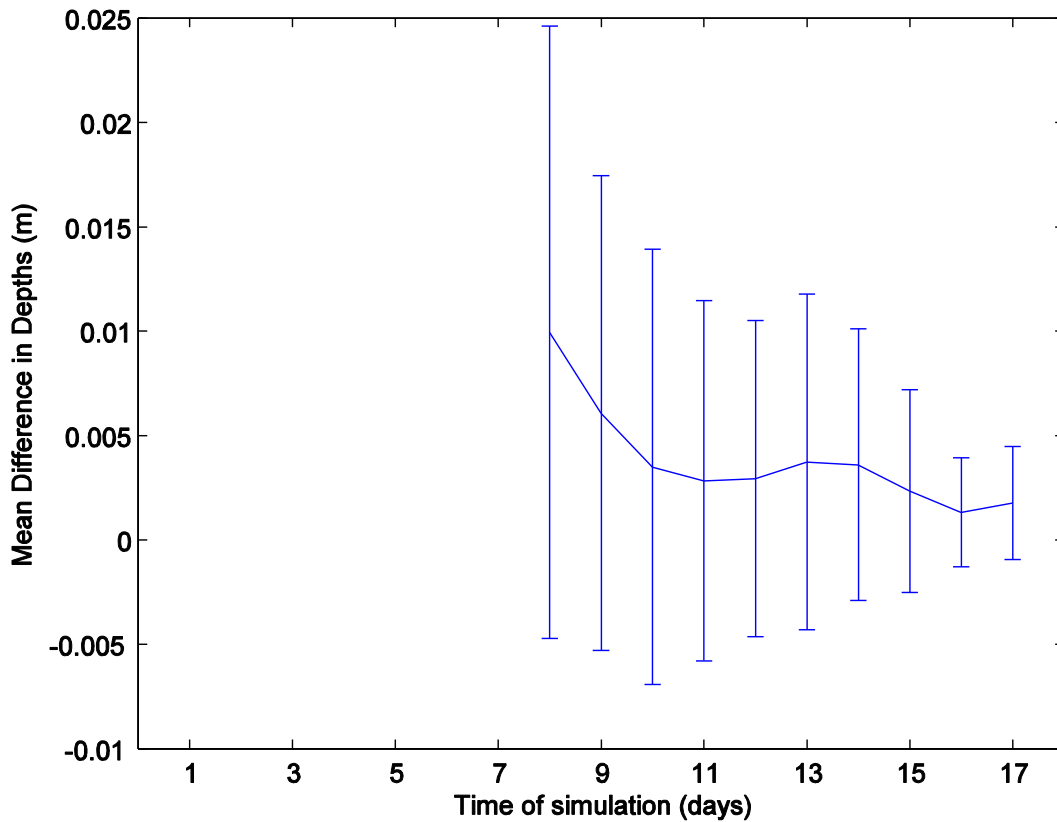


Figure 3.2: Mean difference in depths at each grid per day

Thus, after 7 to 8 days of simulation, the two simulations starting at different times with different initial conditions have converged in terms of A_i , V_T and $\mu_{\Delta D}$. For the

purposes of water surface elevation 8 days can be taken as a reasonable model spin-up time. Spin-up times for salinity have not been analyzed.

3.3 QUALITATIVE COMPARISON TO FIELD DATA

The model output was compared with field data obtained from TCOON to provide insight into its behavior as discussed in Section 2.4.3. The April 2010 simulation with the original roughness matrix, $n_B(k)$, was used for preliminary comparison. As shown in Table 2.3 in Section 2.3, Simulation 13 was the simulation used for comparison with the measured data at the TCOON stations. The locations of these stations are given in Figure 2.4 in Section 2.2.4.

The field-model comparison is made starting on the seventh day of simulation, after spin up was complete. During the time period of simulation, the only stations with available water depth measurements were NUDE2 and NUDE3. Results are shown in Figure 3.3.

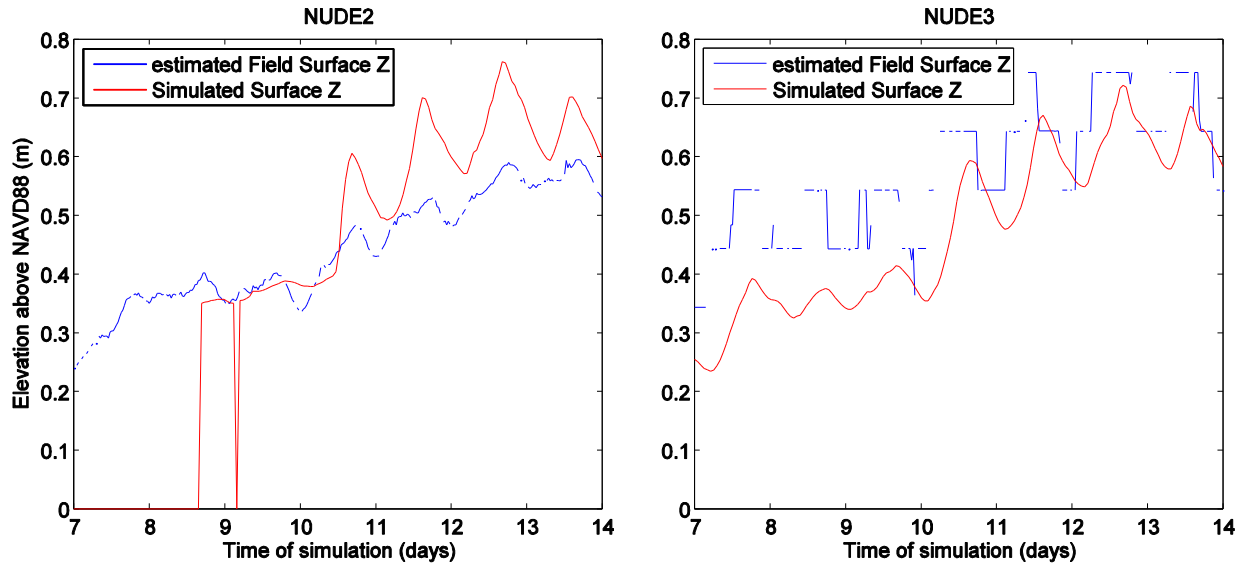


Figure 3.3: Comparison of Simulated Surface Elevations with estimated Field Surface Elevations for Preliminary Validation

As discussed in Section 2.4.3, the comparison in Figure 3.3 is only qualitative because the field data surface elevation is estimated from the depth measurement with an unknown vertical datum. Despite this deficiency, we can still gain insight into the model behavior with the above comparison. The overall increasing trend appears correct at both stations, indicating that the lowest frequency forcing of the tide and wind are correct. The behavior change at day 10 at NUDE3 is apparent in both field and model data, indicating that a sharp change seen in the field was also captured by the model. However, at NUDE2, the field data daily tidal amplitude appears is less than 5 cm, but is more than 15 cm in the model. In contrast, the tidal amplitudes appear reasonable at NUDE3. Since NUDE2 is further upstream in the delta, these results indicate that the model is letting too much tidal energy pass upstream in the marsh and channels between these stations. We speculate this issue is related to bottom roughness, discussed in Section 2.2.3.

3.4 MODEL RESPONSE TO FORCING

In this section the model response to the different forcing conditions discussed in Section 2.4.1 are investigated. The model's response to variations in rainfall, wind, and roughness are tested. Section 3.4.1 discusses the effects of rainfall, Section 3.4.2 presents the model's response to varying wind scenarios, and Section 3.4.3 gives the analysis of the model's response to variations in roughness.

3.4.1 Model Response to Rainfall

The inundated area throughout the seven-day simulation for the varying rain scenarios are presented in Figure 3.4. Equation 2.1 in Section 2.4.1 gives the equation for calculating A_i .

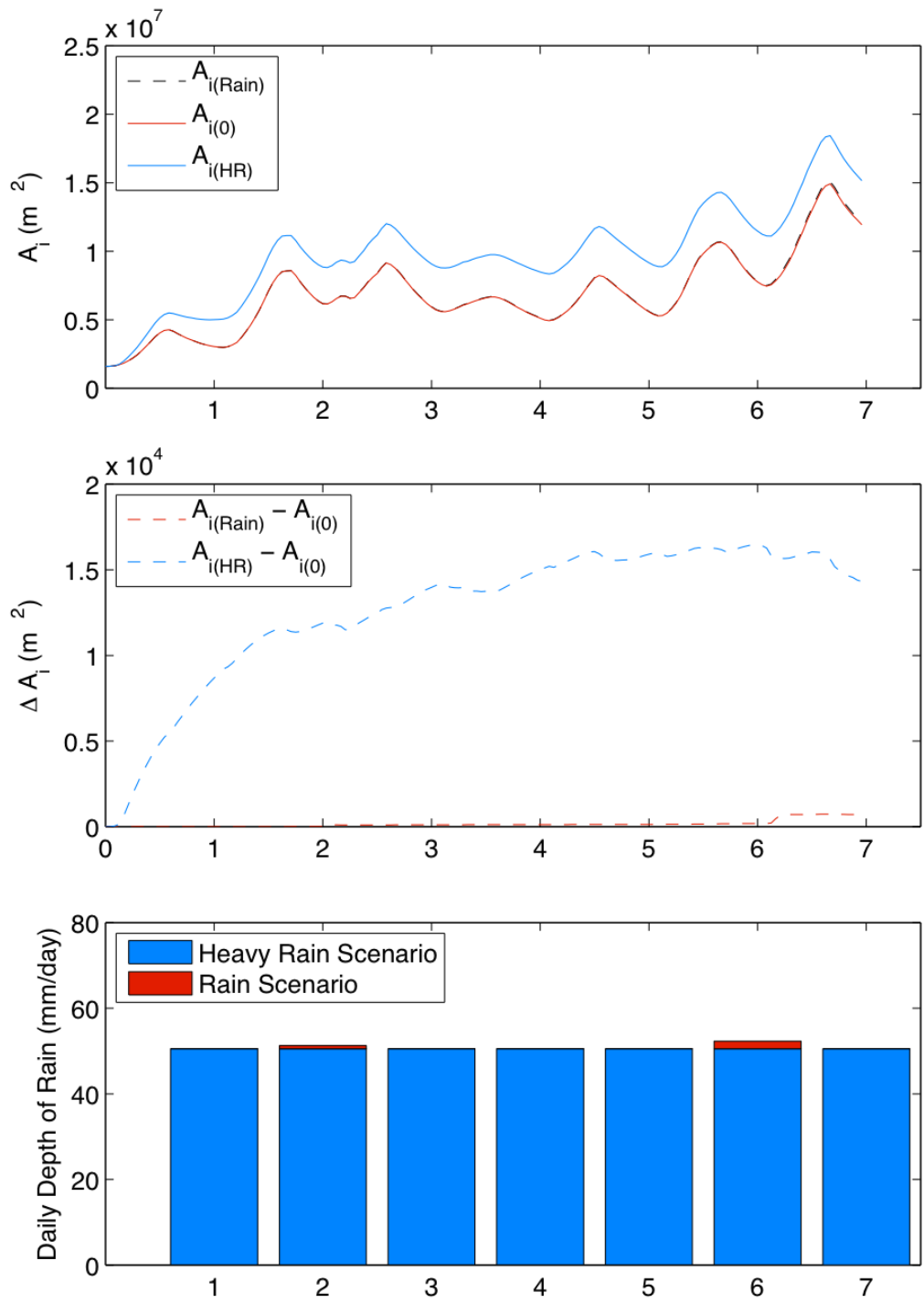


Figure 3.4: A_i , ΔA_i , and depth of rainfall for various rain scenarios

The baseline rainfall in 2009 increased the inundated area by $7.29 \times 10^2 \text{ m}^2$ (0.180 acre) whereas the heaviest rainfall scenario increased the inundated area by over $1.56 \times 10^4 \text{ m}^2$ (3.85 acre). The heavy rain increases the A_i 20% more than the baseline rainfall, demonstrating that the model is able to represent the increased inundation associated with heavy rainfall events. The increased in inundated area for the heavy rainfall may seem small, which is a result of the depth cutoff (2 cm) used in inundated area computations and the uncalibrated soil infiltration model.

Rainfall in the uplands channelizes and flows down to the delta. While the heavy rainfall scenario and the baseline rainfall both develop channelized, the flow depths created by the smaller rainfall event are generally less than those created by heavy rain events. Figure 3.5 displays the channelization of upland flows from rainfall events.

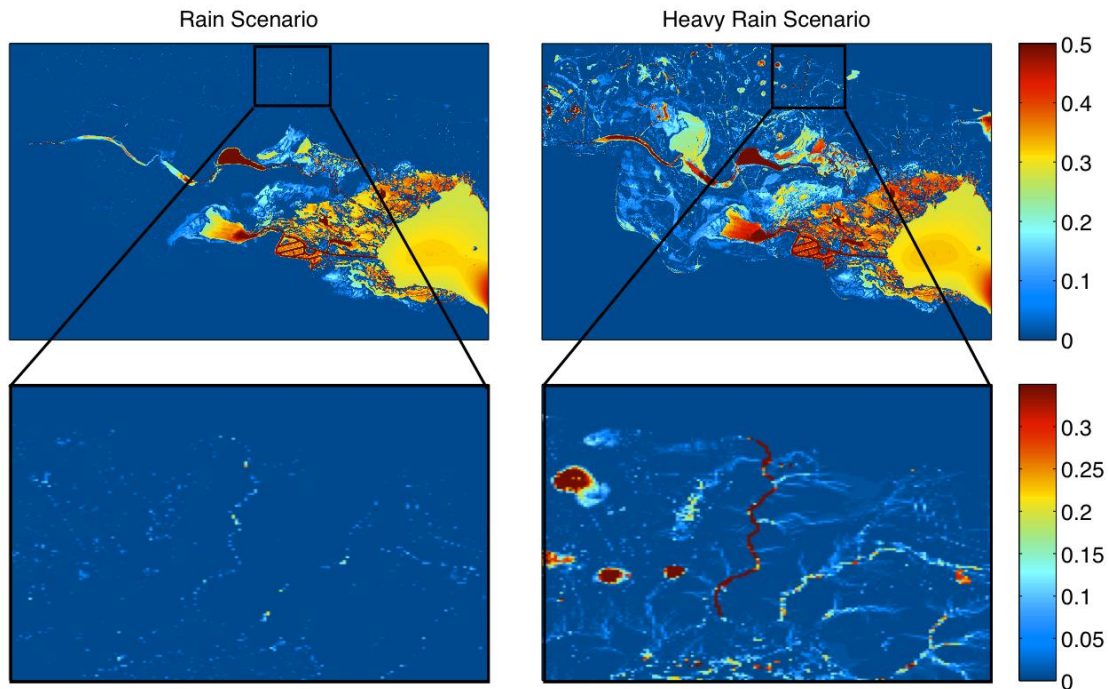


Figure 3.5: Snapshots of the flow in the uplands during a rainfall event for the rain scenario and heavy rain scenarios

The zoomed in area of the uplands shows depths from 0 m to 0.35 m in depth. The baseline rain scenario creates few cells of visible depth, demonstrating why the inundated area is not impacted as much for the small rainfall event as for the heavy rainfall event. Much of small precipitation events is absorbed when it lands on dry areas due to the soil infiltration algorithm discussed in Section 2.3.1 and Appendix B.3. Heavy rainfall events fill up channels that are normally empty, whereas lighter rainfall may not fill these channels above 2 cm. The total volume of water through time was also calculated and is presented in Figure B.4 in Appendix B.4. The heavy rain increases the maximum total volume in the system by 24% from the no rain scenario, whereas the actual rainfall increases the maximum total volume by less than 2%.

3.4.2 Model Response to Wind

Simulations 8 – 10 in Table 2.3 are used to analyze the model's response to wind forcing. The metrics compared for this forcing condition include the A_i through time and the μ_{300D} and σ_{300D} for the end result of the simulation. Figure 3.6 displays the μ_{300D} and σ_{300D} on April 17, 2009, which is the seventh day of simulation.

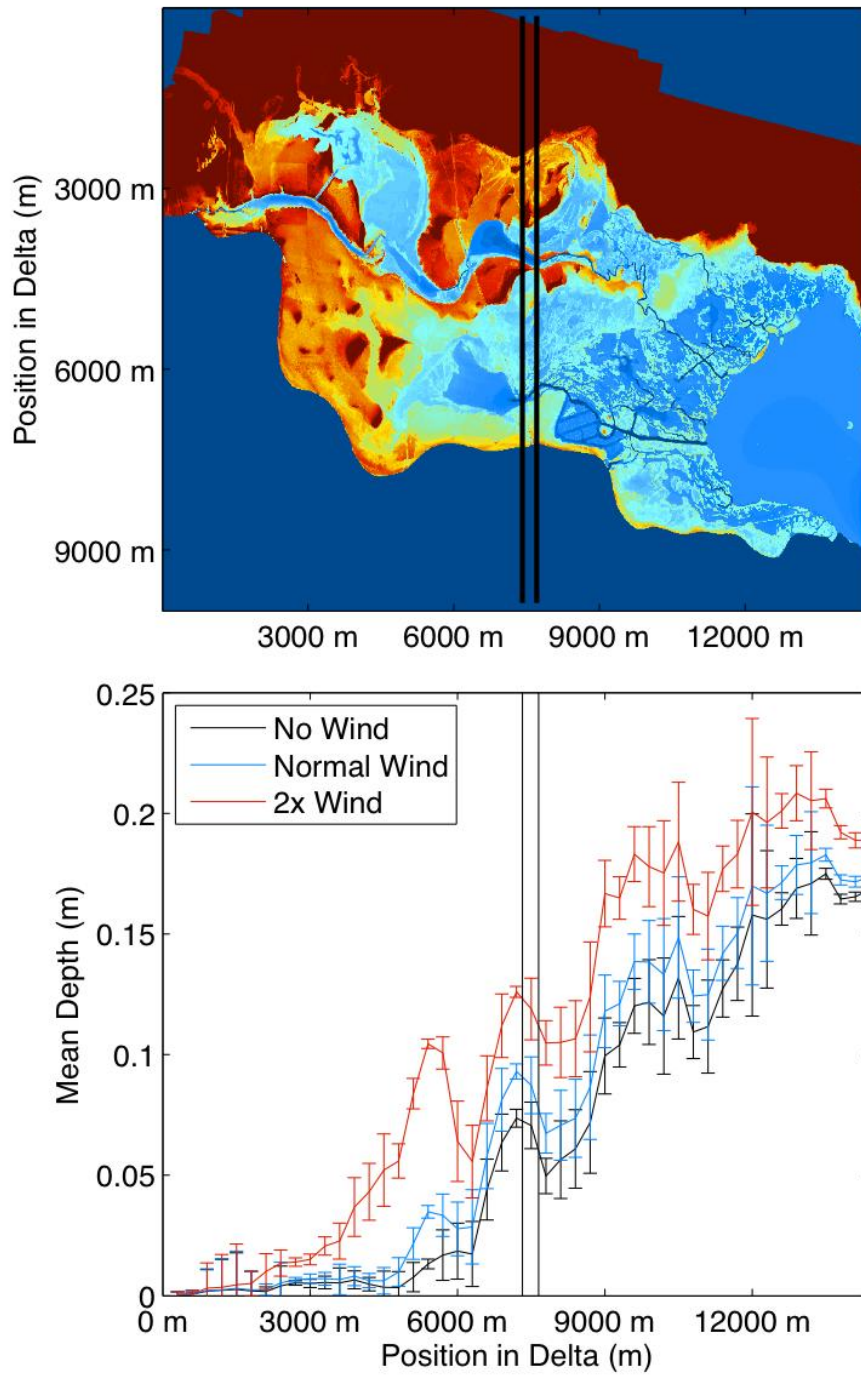


Figure 3.6: μ_{300D} and σ_{300D} errorbar plot for April 17, 2009, the 7th simulated day

Figure 3.6 shows that wind pushes water into the delta for the wind conditions in April 2009 with the stronger wind pushing more water into the delta. As would be expected, there is deeper water in the eastern part of the delta (near Nueces Bay) for all simulations. The wind also causes more water to reach the western parts of the delta. The total volume of water in the delta on the seventh day of simulation is 12% greater for the wind scenario than the no wind scenario and 49% greater for the twice the wind scenario than the no wind scenario. A plot of the percent change in V_T from the no wind scenario is given in Figure B.5 in Appendix B.5. This analysis demonstrates that the wind pushes a substantial volume of water into the delta, and that wind has a strong effect on the output of the model. Plots of the wind speed and direction for April 2009 are given in Appendix A.5.

3.4.3 Model Response to Roughness

The baseline roughness, R_B , and variations of this roughness are described in Section 2.2.3 in Table 2.1. The total volume of water in the delta throughout the seven day simulation was investigated for all roughness scenarios. These results are given in Figure 3.7.

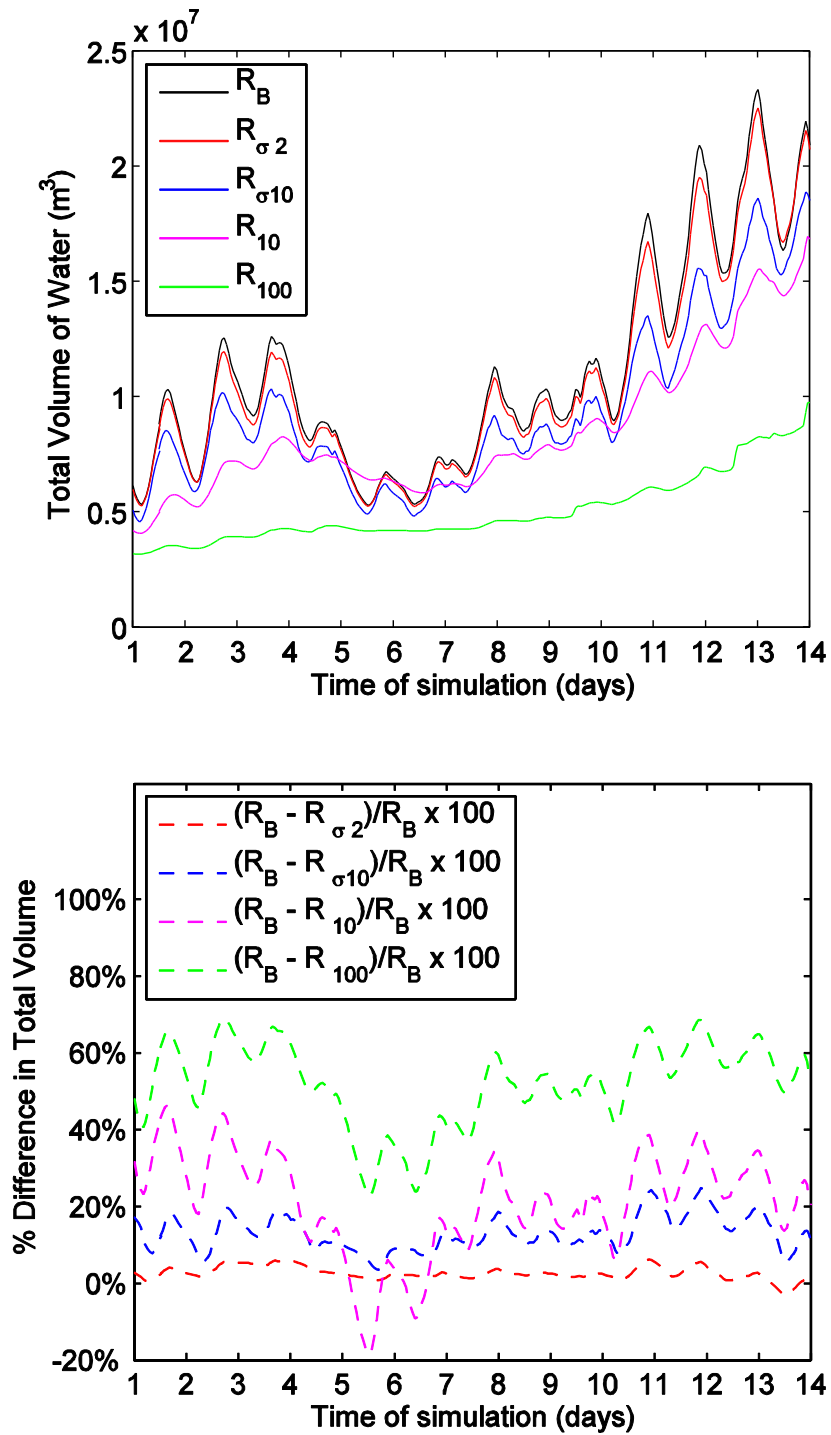


Figure 3.7: Comparison of Total Volume of Water in the System for different Roughness Scenarios

A higher roughness coefficient slows the movement of water so that the motion of the tide coming in and out is not as apparent in the volume of water in the system. In the R_{10} simulation, the movement of the tide out is slow enough such that the simulation with the original roughness reaches a lower volume faster despite the fact that its volume was substantially higher at high tide. The total volume of water in the system reaches a maximum of over $23 \times 10^6 \text{ m}^3$ (1.9×10^4 acre-ft) for R_B , nearly $17 \times 10^6 \text{ m}^3$ (1.4×10^4 acre-ft) for R_{10} , and only $9.7 \times 10^6 \text{ m}^3$ (7.9×10^3 acre-ft) for R_{100} . The simulations with roughnesses adjusted for subgrid-scale topography reach maximum total volumes of $22 \times 10^6 \text{ m}^3$ (1.8×10^4 acre-ft) for R_{σ_2} and $19 \times 10^6 \text{ m}^3$ (1.5×10^4 acre-ft) for $R_{\sigma_{10}}$. The percent difference in total volume given in Figure 3.7 illustrates the response of the model to changes in roughness, and shows that adjustments to the roughness matrix will impact the model's output. Particularly, Figure 3.7 demonstrates how the delta responds to daily tidal oscillation; with higher roughness, the tidal oscillation is damped. Comparing the results here with Figure 3.3 in Section 3.3, there is evidence that the problem at NUDE2 may be that the roughness in the channels leading up to the monitoring station are too small, and require higher roughness to damp the oscillations at that point.

3.5 EFFECTS OF PUMPING

The Rincon Pipeline pumps freshwater from the Calallen weir into the Rincon Bayou with three different pumping rates. The simulations for representing the potential effects of pumping are Simulations 1-4 detailed in Table 2.3. The simulations were started on April 14, 2008 with the baseline conditions with the exception of the pumping data. A tracer was used in the model to track the time-space evolution of water that enters the delta from the pipeline. The tracer concentration in any model grid cell reflects the fraction of that grid cell containing pumped water.

The computed area of inundation affected by the pumped water depends on how we define inundation. One definition for inundation from pumping is based on the fraction of pumped freshwater in each cell. For example, an inundated cell can be defined as having at least 20% of its volume as pumped freshwater, which represents a cutoff fraction of 0.2. Figure 3.8 gives the inundated area from Simulation 3 in Table 2.3 with varying cutoffs for the fraction of pumped water used to define inundation.

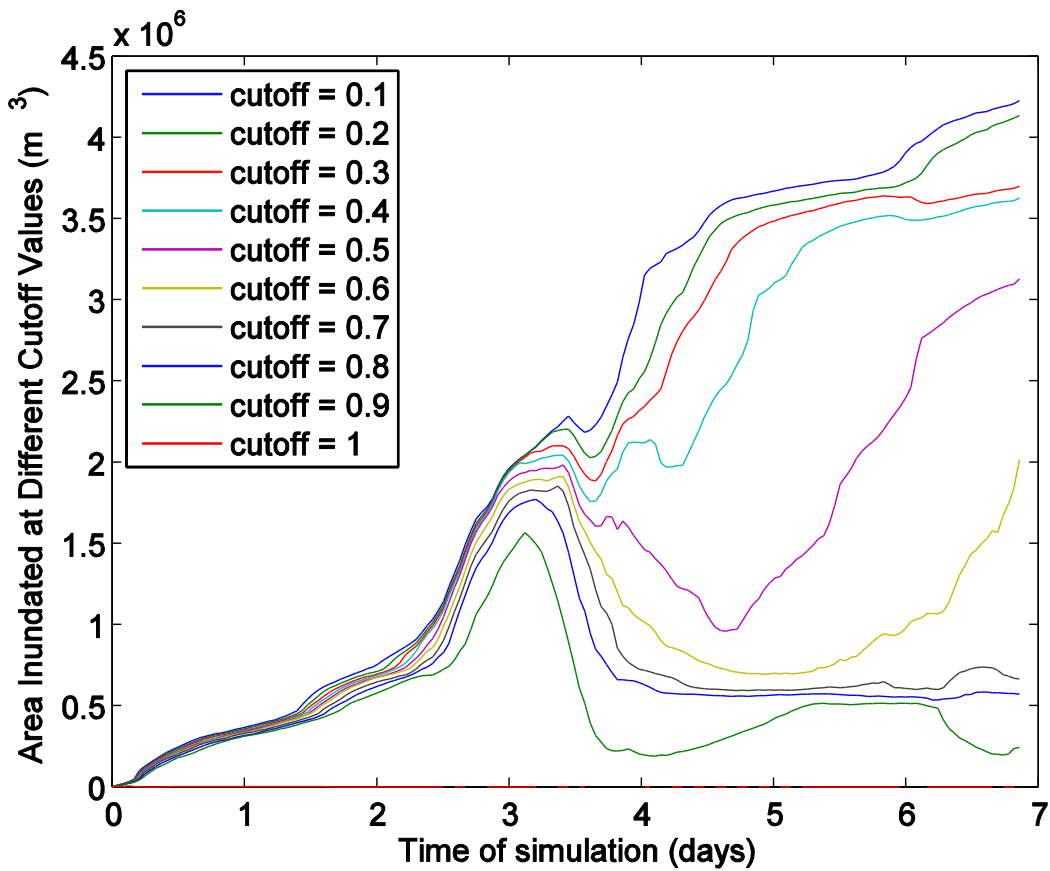


Figure 3.8: Inundated Area from pumping with 2 pumps over seven days with varying cutoffs for minimum fraction of pumped water in a cell

The results plotted in Figure 3.8 show a larger difference between the A_i for a fraction of 0.4 and 0.5 than for the other cutoff values. Either of these fractions would

seem to be a reasonable definition of the area affected by pumped water, but result in qualitatively different behaviors. Because of this sharp reduction in A_i between cutoffs of 0.4 and 0.5, we use 0.4 as the minimum fraction of inundation from pumped water for defining A_i for pumping. A plot of the area inundated by pumping for the three pumping scenarios is given in Figure 3.9, where the inundated area is defined with a pumped freshwater cutoff of 0.4.

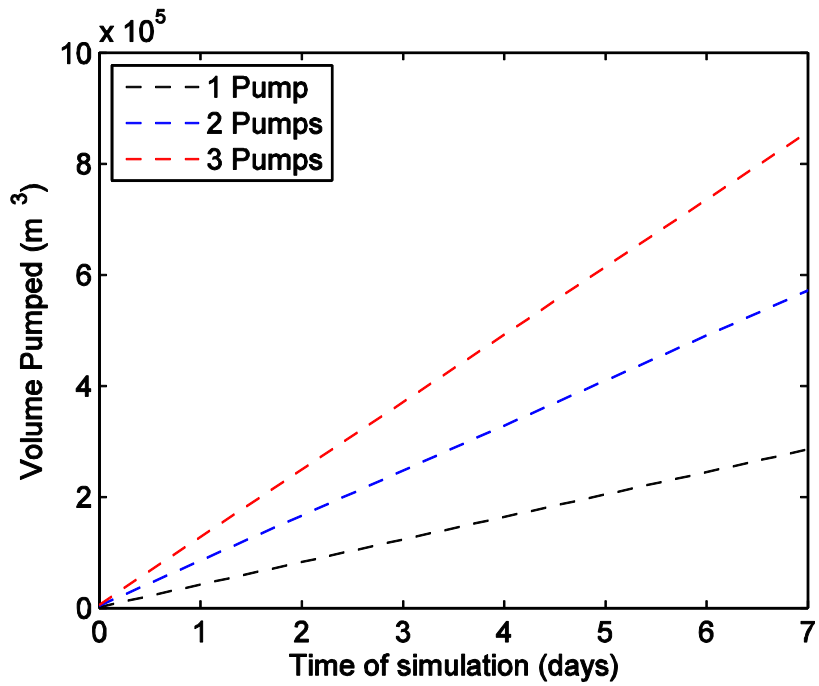
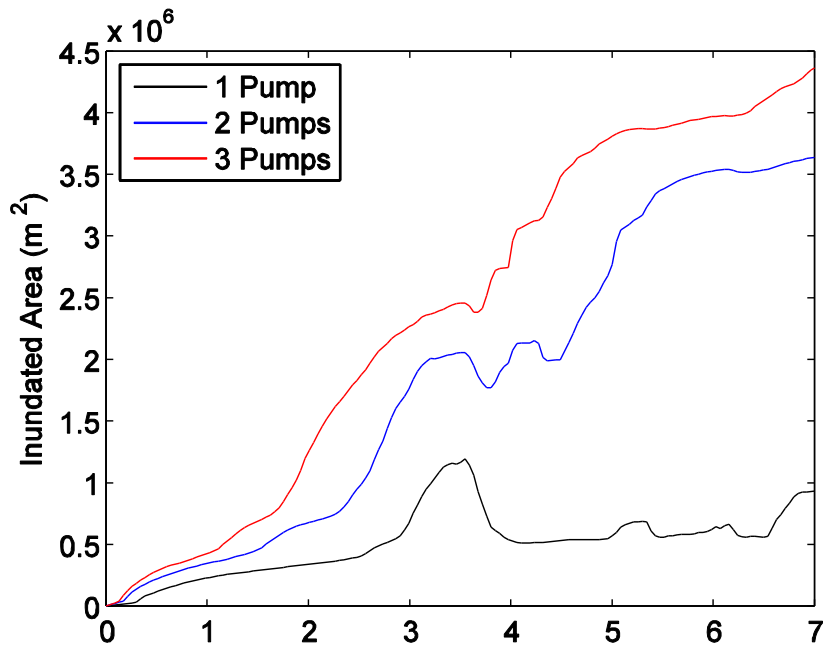


Figure 3.9: Inundated area in the delta from pumping through time compared with the volume pumped at that point

Figure 3.9 considers only cells with at least 40% of the volume consisting of freshwater from pumping to be included in the inundated area calculations. The inundated area shown in Figure 3.9 demonstrates the impacts of the varying pumping scenarios spatially, while taking the amount of water in those cells into account. These results reveal pumping with two or three pumps over seven days as being substantially more effective than pumping with one pump. In the results presented in Figure 3.9, on the seventh day of simulation, April 21, 2008, two pumps inundate 2.8 times and three pumps inundate 3.6 times more area than the one pump simulation, although they only pump one and two times more water than one pump, respectively.

The total volume of freshwater, V_{FW} , in the system is calculated as described in Section 2.4.1, and the results are plotted in Figure 3.10.

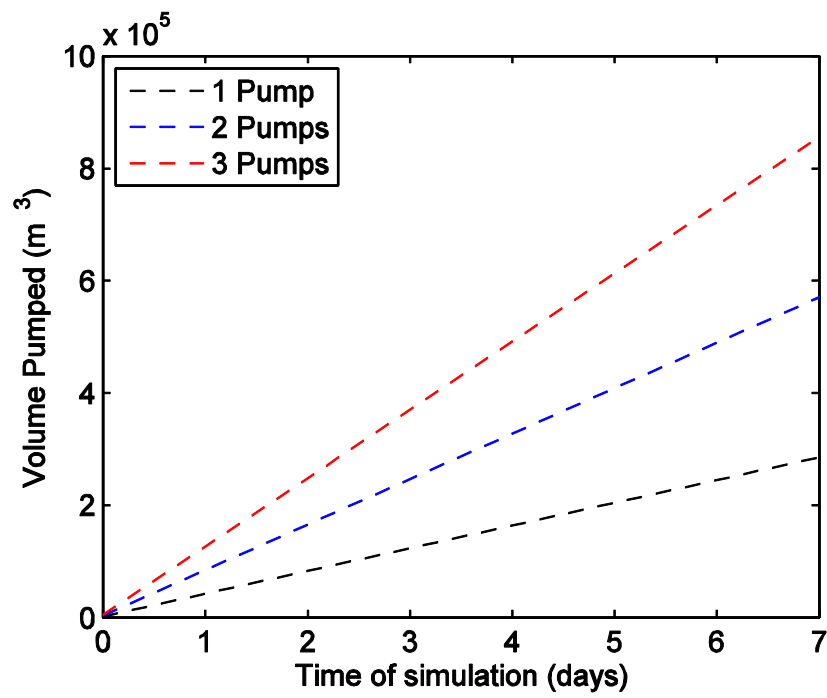
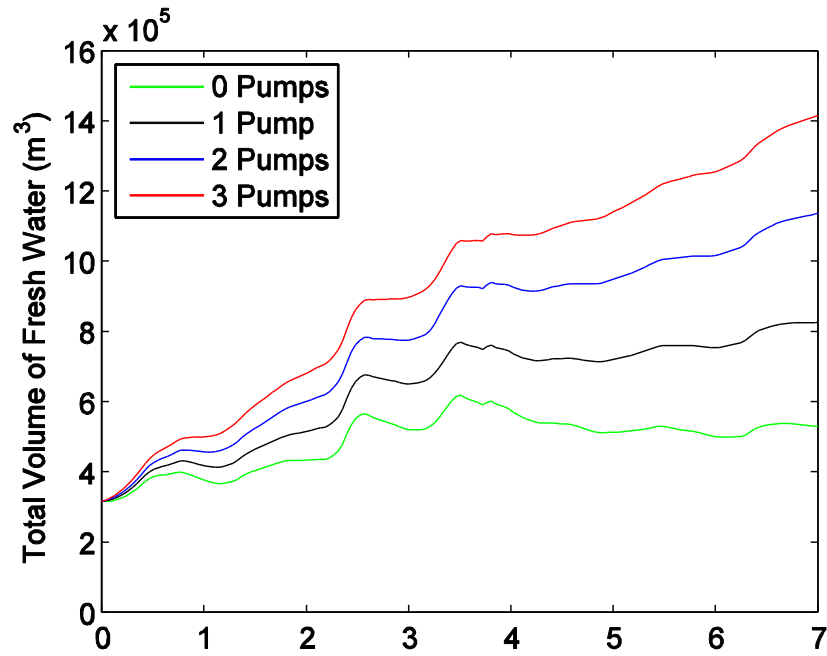


Figure 3.10: V_{FW} through time for various pumping scenarios

The total volume of freshwater in the system increases with increased volume of pumped water, with the difference between the total volume of freshwater in the system for each scenario being approximately equal to the volume of freshwater pumped at that point. While Figure 3.10 provides insight into the delta's freshwater volumes from sources other than pumping, it does not provide insight into the behavior of pumped water in the system. Investigating the volume of brackish water, however, helps in understanding the interaction between the pumped freshwater and the saline water in the delta. The volume of brackish water, V_B , the change in V_B from different pumping scenarios, and the net increase in V_B are given in Figure 3.11.

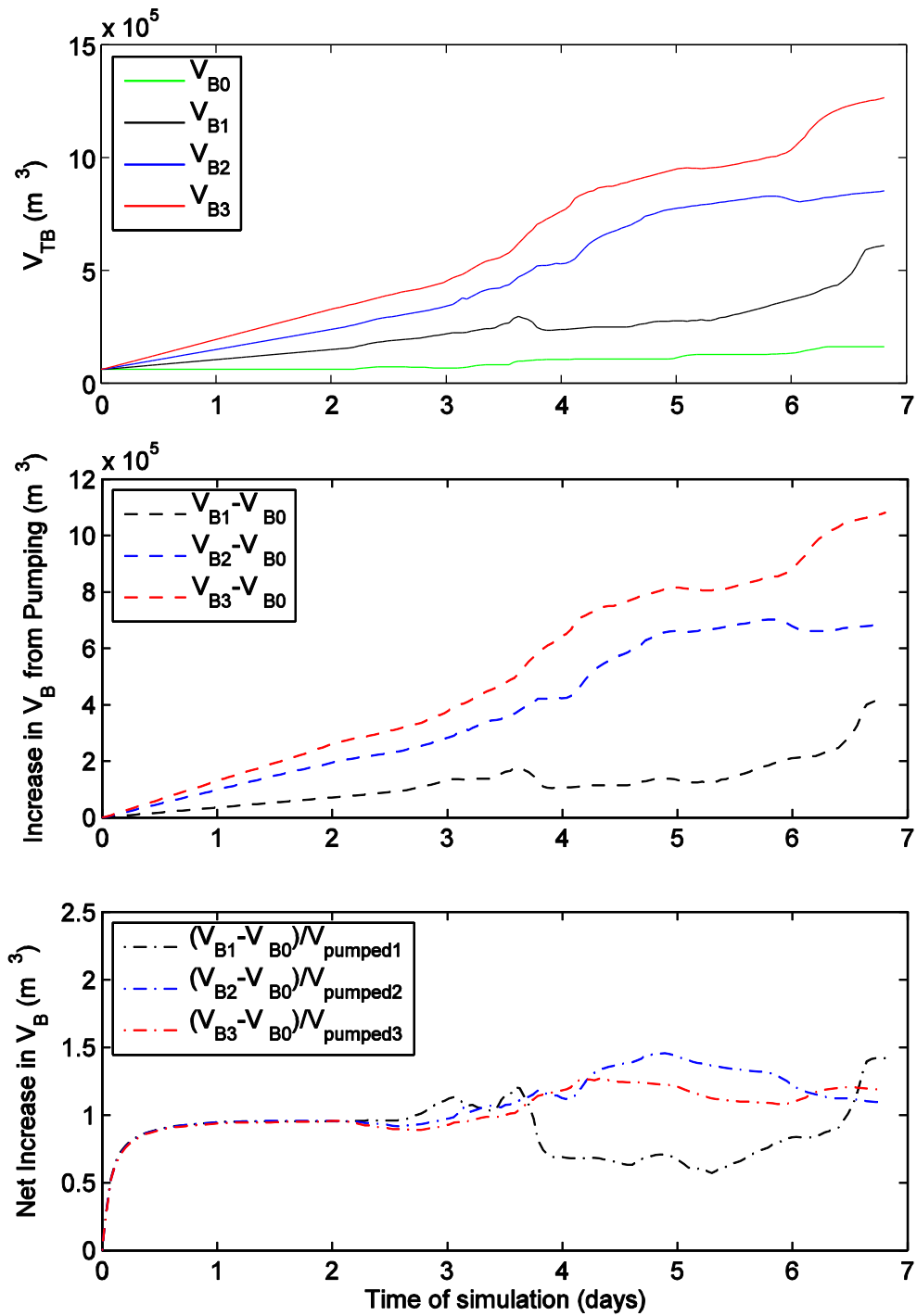


Figure 3.11: Volume of brackish water in the system for various pumping scenarios, increase in brackish water from pumping, and net increase in brackish water from pumping

The net increase in the volume brackish water demonstrates the increase in V_B as a function of the volume of water pumped. The change in the effectiveness of the different pumping scenarios throughout the simulations gives an example of how the spread of pumped water affects the salinity in the delta. The channelized nature of the delta affects the movement of pumped water and therefore the impacts on salinity. The net increase in V_B aids in understanding how effectively different volumes of water pumped can impact the delta's ecosystem, and has implications for use in management of the Rincon Pipeline.

Chapter 4: Conclusions and Future Work

4.1 FINDINGS

The present study created the Nueces Delta Hydrodynamic Model from the PC2 Hydrodynamic Code, v6.0 using input specific to the Nueces Delta. Bathymetry, precipitation, tidal data, wind, roughness, pumping, inflow, and salinity were all input included in the model. Seventeen simulations of the model were run to represent different conditions in the delta. Analysis of the model was based on these simulations.

The preliminary validation of the model was only qualitative; however, it provided a representation of conditions in the delta that reasonably approximates the overall trend of the field conditions at the monitoring stations in the time period tested. The initial Manning's n values used in the model were justified from previous models discussed in the literature, and the land cover data used to create the roughness coefficient matrix was obtained from the National Land Cover Dataset.

With the model to model comparisons that have been completed, the model's response to forcing is better understood. The model's response to changes in wind, rainfall, and roughness on inundated area, total volume of water in the system, and mean depths across the delta were investigated. Variations in roughness included increases in roughness across the entire matrix and increases in roughness for cells with high standard deviations in subgrid-scale topography. These simulations showed the higher roughness values to reduce the tidal influence on the system, which qualitatively appears to be necessary to represent to real conditions in the delta.

Initial testing of the impacts of pumping also lend to understanding of the effects of the Rincon Pipeline on the delta. Analysis metrics for pumping scenarios included area inundated by pumping, total volume of freshwater in the system, and volume of

brackish water in the system. The pumping was analyzed for one, two and three pumps, and the output of these was compared to illustrate the area inundated by of pumping.

4.2 FUTURE WORK

The calibration of the model is incomplete; further work is essential for model reliability. Field studies of the flow through channels and better understanding of the effects of subgrid-scale topography on roughness would lead to improved calibration. Field data may be most helpful in areas where the water surface elevation changes abruptly because these areas may have higher elevation changes in subgrid-scale topography. Field data of flow at eight to twelve points in the delta, and adjusting the roughness in the model based on better understanding from this field data could improve the reliability of the Nueces Delta Hydrodynamic Model.

Additionally, understanding the effect of wind on shallow water may aid in calibration of the model. There is a scarcity of data available that relates the wind stress over shallow water (≤ 20 cm in depth) to the transfer of momentum into the water, which contributes to uncertainty in the model. More extensive field measurements might allow for a better representation of this phenomenon in the model. Further adjustments to the model that may improve its reliability are included in Appendix C.

Eventually, including the Nueces River back into the model and testing the effects of overbanking of the river into the delta is an option that will make the model a more robust tool. The simulations outlined in this paper represent time periods where the Nueces River does not overbank into the river. Overbanking, however, is an occurrence that affects the hydrodynamics in the delta, and incorporation of overbanking events into the model may allow for better understanding of conditions in the delta during high flow events.

The creation of a model that simulates the environmental conditions in the Nueces Delta opens the opportunity for its use as a management tool. Running many simulations with different conditions can provide a basis for controlling engineered flows at the pipeline diversion. It would benefit decision making to recognize which conditions are most effective for restoring the ecosystem using pumped water. Conditions may vary for high or low tide, rate of pumping, duration of pumping, and antecedent moisture conditions. A stronger understanding of where the pumped water spreads under these different conditions might aid in making informed choices.

Results from a calibrated model providing the inundated area in the delta from pumping versus the volume of water pumped (similar to Figure 3.9) may be a valuable management tool. The definition of *inundated area* for the plot can vary depending on the goal of the investigation. For this study, the inundated area was defined to include any area that had a depth greater than 2 cm. Our definition of inundated area did not require a minimum duration of inundation. For pumping, we used a minimum of 40% of the volume of water in a cell coming from pumping as a cutoff point. The possibilities for defining inundated area, however, may lead to understanding different aspects of the ecology, depending on what the goals of analysis are.

In future work the inundated area might be specified based on duration of inundation and depth of inundation. Such an analysis might specify the area inundated at a minimum depth plotted against the length of time that area remains inundated. It may also specify the area inundated for a minimum number of days against the depth at which those areas are inundated. The inundated area may also be defined by the definition used in this study, as any area with a certain depth of standing water and be plotted against duration of pumping and flowrate of pumping.

For more detailed analysis, the land cover in the delta could be considered when analyzing the inundated area. The channelized nature of the Nueces Delta has a strong bearing on which species of vegetation are inundated with freshwater after pumping. The area inundated by freshwater has a major impact on what species of vegetation can grow in that area. Two major species types in the delta, *Borrichia frutescens* and *Salicornia virginica*, have very different conditions for ideal growth. *B. frutescens* is not hindered by flooding and only has a positive growth rate under very low salinity conditions while *S. virginica* is unaffected by increased salinity and has inhibited growth from waterlogged soil (Rasser 2009). Rather than looking only at the inundated area as a one-dimensional metric, the inundated area might be defined as a species-specific value. If the area inundated with water includes only channels with open water, the vegetation and ecology are not impacted as effectively as when water floods into the vegetated areas to flush out more salinity. This approach might allow for improved understanding of the impact and success of different pumping scenarios on the ecology.

A more extensive management tool might eventually be created that is more user friendly for decision making. This tool may incorporate the output of the hydrodynamic model to allow for a more direct comparison of conditions in the delta and the most effective pumping scenario associated with it. The undertaking of this project may involve significant work, but the use of the model as a management tool may prove a valuable asset in decision making. It may be used to help restore the ecosystem using more appropriate allocation of water for a resource and cost effective methodology. The foundation of the user-friendly tool could be formed from many runs of the Nueces Delta

Hydrodynamic Model under varying conditions and transforming the output to a more simple formulation. Incorporating the output of the model into a user-friendly format gives options for making the Nueces Delta Hydrodynamic Model a more robust and reliable management tool.

Appendix A: Input Data Sources and Manipulation

A.1 BATHYMETRY

The available bathymetry was received as the 2007 DEM (Digital Elevation Model) combined with the bathymetric data in ASCII format measured for the Coastal Bend Bays & Estuaries Program (CBBEP). In its original format, the bathymetry is in a 1m x 1m grid gathered using Light Detection and Ranging known as LiDAR. LiDAR systems send pulses of laser energy to surfaces that reflect energy to measure distance (Gibeaut 2003). The bathymetric data is relative to the North American Vertical Datum of 1988 and is given in meters. The North American Vertical Datum of 1988 (NAVD88) was developed by the National Geodetic Survey in 1991 and is the most recently developed vertical datum (Veilleux 2011). NAVD88 is the reference datum for all inputs in the model. Figure A.1 displays the bathymetry in its original format.

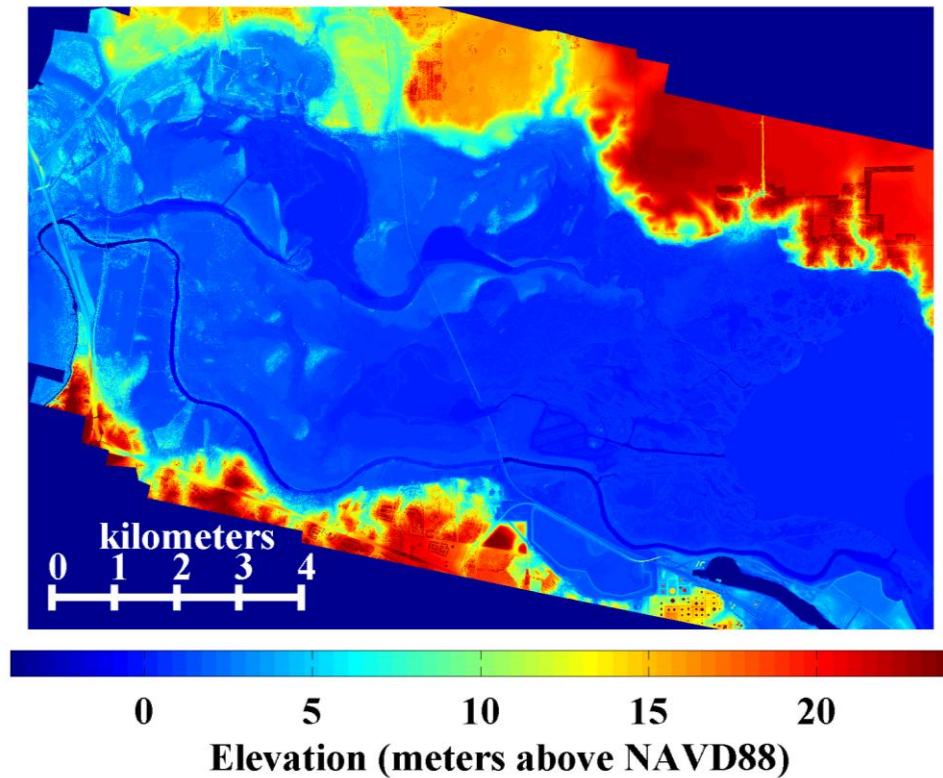


Figure A.1: The bathymetry originally received from CBBEP with a color scale from -5 to 25 m

Figure A.1 gives the bathymetry originally received from CBBEP with an elevation color scale from -5 to 25 m. This shows the detail in the uplands but does not represent the elevations in the delta with detail. Figure A.2 displays the bathymetry originally received from CBBEP with an elevation color scale from -1 to 4 m. This does not represent the differences in elevations in the uplands but allows for greater detail in the lower elevations found in the delta.

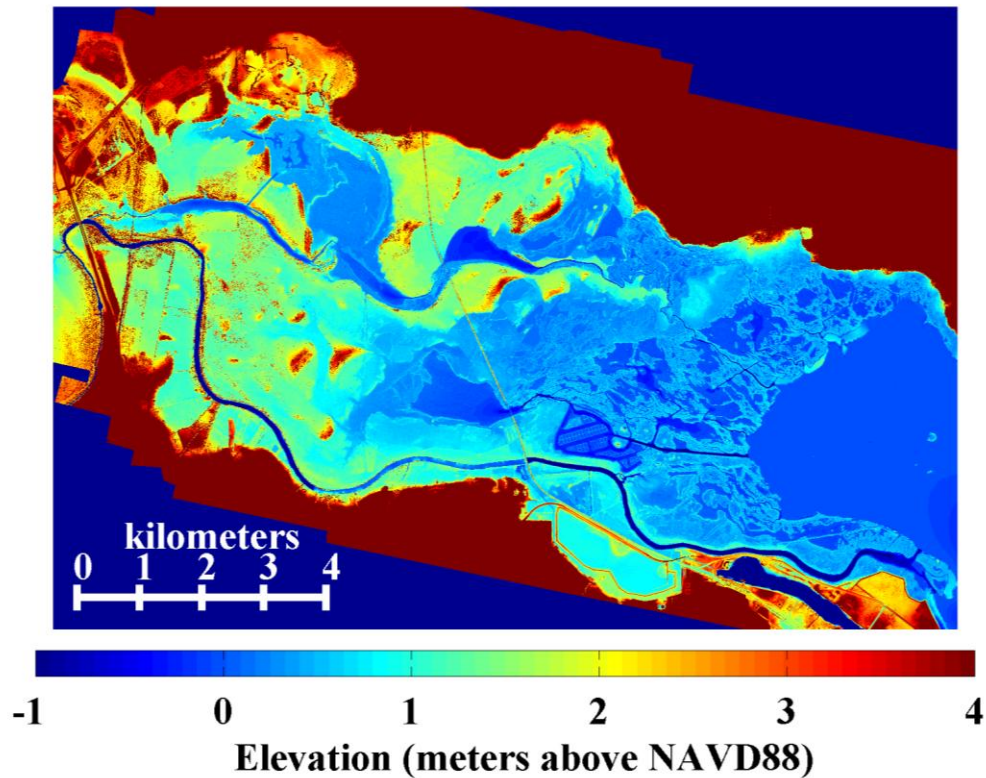


Figure A.2: The bathymetry originally received from CBBEP with a color scale from -1 to 4 m

The 1m x 1m data set is not continuous, and contains NaNs where no LiDAR data was available. We handled this by filling these holes with the average of the eight neighbor values. Where there were adjacent NaN cells, the available neighbor values were averaged to find the first iteration of a value to fill the cells with NaNs. Then the eight values surrounding the cells that originally had NaNs are averaged for a second iteration value to fill the holes.

The original bathymetric data does not have elevation data for the Nueces Bay, an area needed for the tidal data boundary conditions. With 10m x 10m bathymetry data collected from the National Oceanic and Atmospheric Administration (NOAA), the

missing data points in the Nueces Bay are replaced. Because the grid sizes must be consistent, the 10m grid was rasterized to a 1x1 meter grid, assuming all data points within each 10x10 meter section to be uniform. Although there are known inaccuracies associated with this methodology, the 10m x 10m resolution bathymetry is the finest data set available for the bay.

In the original bathymetric data from CBBEP, the bathymetric data for the Nueces River is included. The deeper values in the Nueces River have a tendency to damp the importance of the shallow values in the Nueces Delta when included in the model. Also, the additional computational time needed to include flow at the Nueces River and south slowed the model. For these reasons, the bathymetric data used in the model does not include the Nueces River or the area south of it. Because the Nueces River does not overbank into the delta during the time periods simulated, this adjustment does not affect the appropriateness of the model.

The original data set is 10,012 by 14,564 grid cells in the 1m x 1m data. This fine data set does not allow for the model to be run at faster than real time. Rasterizing this data to a 15m x 15m grid provides a data set of 667 by 971 grid cells. The data is rasterized using the mean of the values within each coarse grid cell. Within each 15 x 15 m grid cell, there are two hundred and twenty five 1 x 1 m grids. Figure A.3 shows the bathymetry at a 1 x 1 m grid with a section of the delta denoted. The section displayed in Figure A.3 is referred to as Section A.

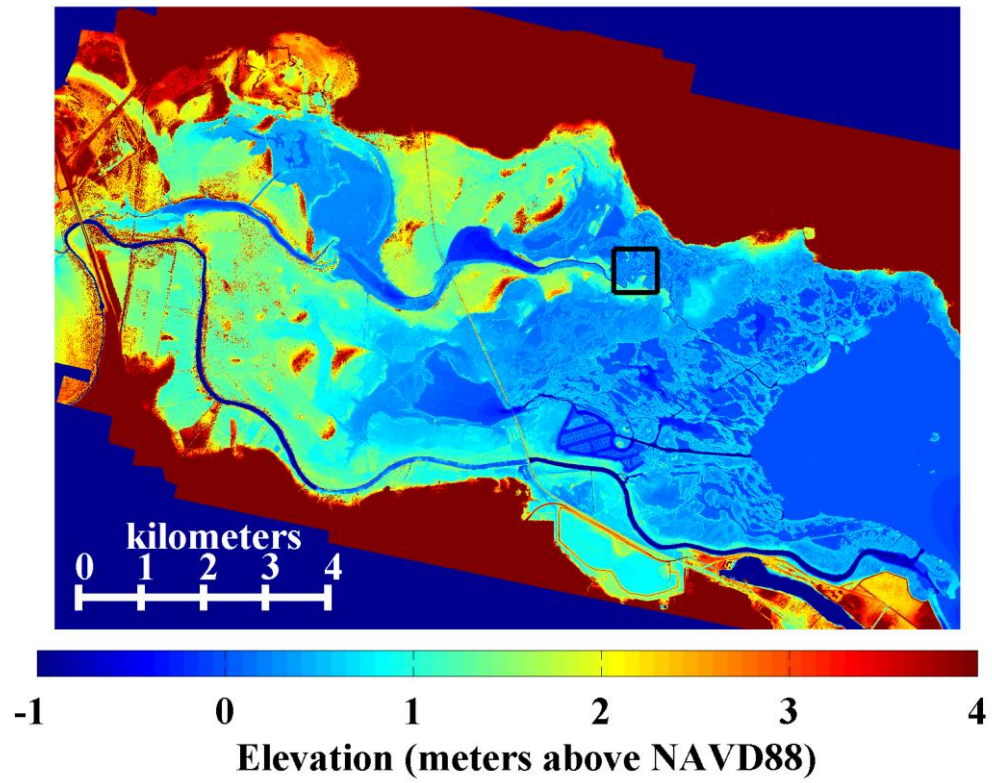


Figure A.3: 1 x 1 m bathymetry displaying the location of Section A in the delta

The section denoted in the box in Figure A.3 is shown at a 1 x 1 m grid in Figure A.4 and at a 15 x 15 m grid in Figure A.5.

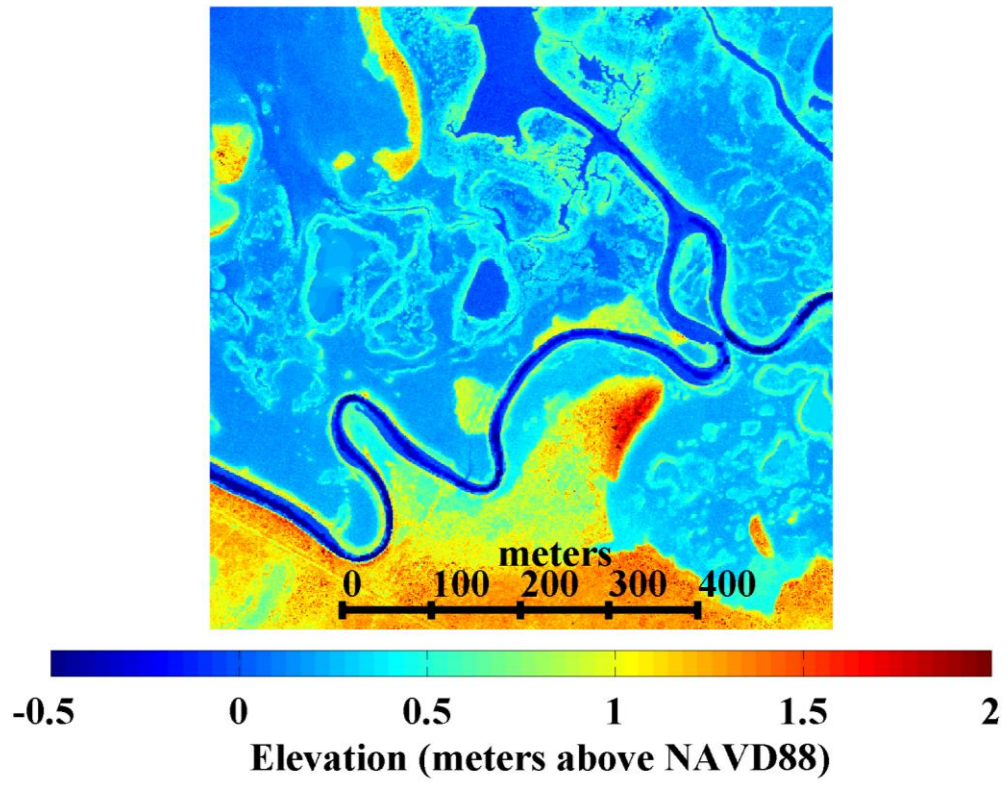


Figure A.4: Section A shown at a 1 x 1 m data set

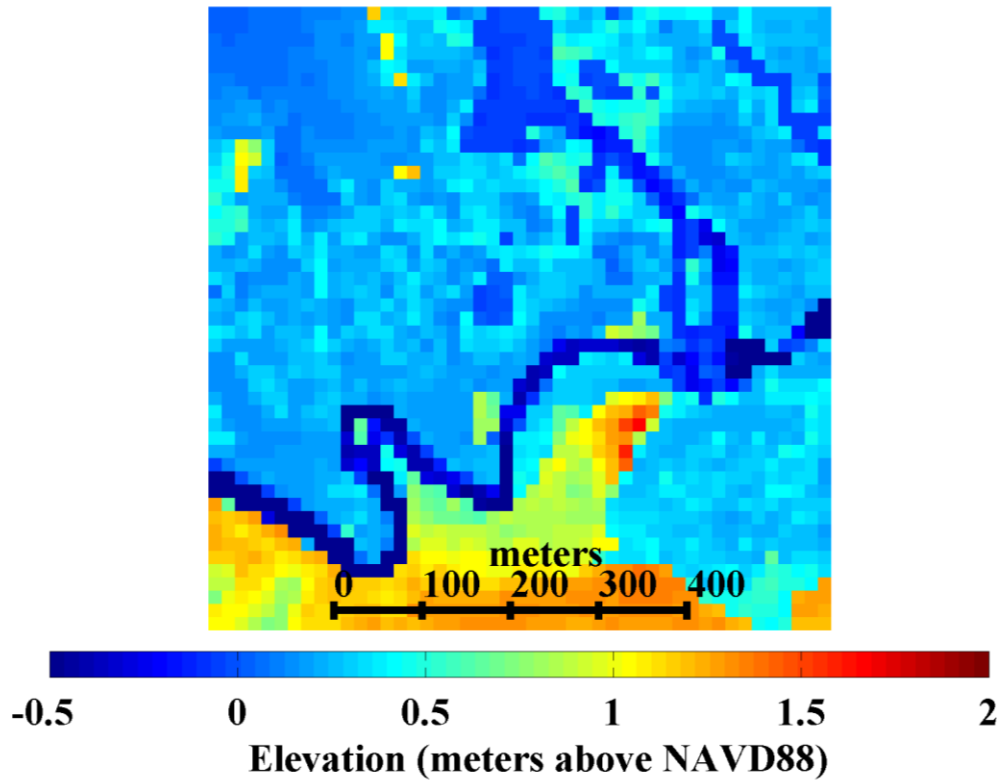


Figure A.5: Section A shown at a 15 x 15 m grid

Figure A.4 and A.5 give an example of the difference in coarseness in the bathymetry, and shows a channel within the bathymetry. In some areas of the bathymetry, the rasterization of the 1 x 1 m data set to a 15 x 15 m grid causes blockages in channels. To help remedy this, for 15 x 15 m grids with a high standard deviation, the mean of the lowest fifteen 1 x 1 m data points in that grid is used as the value for that grid. This adjustment is made so that narrow portions of channels are not incorrectly washed out from high surrounding values.

The bathymetric data was tested with six different standard deviations as the cutoff for ensuring channelization. Plots of the 15 x 15 m bathymetry with standard deviation cutoffs ranging from 5 cm to 30 cm are provided in Figure A.6.

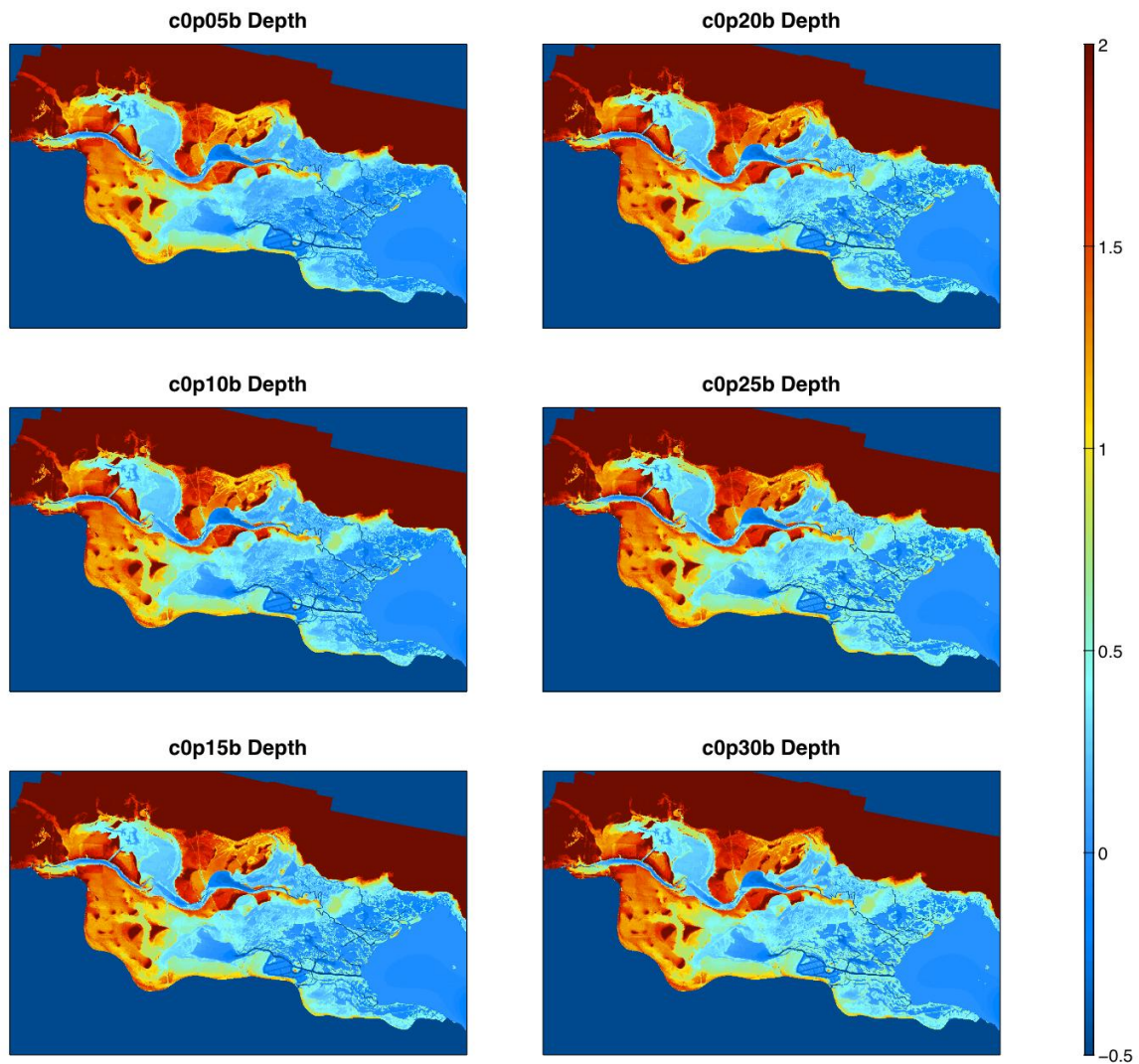


Figure A.6: Images of the 15 x 15 m bathymetry with varying standard deviations used for channelization

This analysis revealed a standard deviation of 20 cm as the cutoff for ensuring channelization. The analysis was based on visual comparison between the 15 x 15 m bathymetry using varying cutoff points with the 1 x 1 m bathymetry.

Additionally, diagonal blockage is checked for and removed. Diagonal blockage refers to any place where cells diagonal to each other are intended to allow flow through. Because the Nueces Delta Hydrodynamic Model only allows flow through the faces of cells, flow is not able to pass through diagonals of cells, and therefore cannot flow through those points in channels. Any location with diagonal blockage is removed by replacing one of the diagonal blocking cells with the average of the elevation of the two rectilinear cells. The rasterization from a 1 x 1 m resolution to a 15 x 15 m resolution helps to make the inaccuracies in the Nueces Bay from methodology of including the 10 x 10 m bathymetry obtained from NOAA into the 1 x 1 m bathymetry negligible.

One area of interest in the bathymetric data is the very deep channel leading from the bay to the delta. While this may seem uncharacteristic to the area, the delta access channel was caused by dredging done for oil exploration (Pulich 2006). This deep channel affects the flow in the delta and remains as a feature in the bathymetry used in the model.

A.2 BARRIERS

Because the bathymetric data was gathered using LiDAR technology which measures surface elevation data using remote sensing from an airplane, the elevation of the bathymetry at the 1m x 1m grid includes all railroads and barriers. Some of the railroads and roads in the delta have piers to allow flow to pass underneath, and the bathymetry in the model must be adjusted accordingly. To more appropriately simulate the conditions of flow at these piers, the bathymetry at these areas in the railroad is manipulated to remove the barrier. The grid cells that were measured as railroad and barrier heights are removed and replaced by averaging the lowest fifteen values at the 1 m x 1 m resolution (as described in Section A.1) to allow flow to pass under the barrier.

Changing the roughness coefficient where the barriers have been removed better represents how culverts and railroad piers affect flow. The railroad piers increase the Manning's roughness coefficient (Manning's n) associated with flow because of backwater effects. The change in Manning's n from bridge piers in subcritical flow was determined in Equation A.1 (Charbeneau and Holley 2001).

$$\frac{\Delta n}{n} = \sqrt{1 + \frac{\phi^2 K y^{4/3}}{g L n^2} (K + 5 Fr^2 - 0.6) (\alpha - 15 \alpha^4)} - 1 \quad (\text{A.1})$$

Where:

L = reach length (the flow length under the bridge)

$\phi = 1$ for SI units

y = depth of flow

n = the original Manning's n value

K = coefficient depending on the pier shape (three circular piers in a row: 1.11)

$Fr = \frac{V}{\sqrt{gy}}$, the Froude number downstream of the pier

α = ratio of the area of the submerged part of the piers to the total flow area

For areas of the bathymetry that have railroads and roads that do not have piers or culverts allowing flow under them, the rasterization of the bathymetry to a coarser grid can dampen the effects of these barriers on flow. The roads and railroads that run through the delta are typically 3-4 meters across. When the 1m x 1m grid is rasterized to a 15m x 15m grid size, the height of the barrier is averaged with the surrounding bathymetry to find the mean in the rasterized grid. Without modification, the height of the barrier is not accurately represented on the coarse grid. Adjustments have been incorporated into the model to block flow across cells containing barriers using sills at the edges of these cells. Sill heights were determined by isolating the barriers and averaging the elevation of the barrier within each cell neglecting the surrounding bathymetry.

These sills allow flow higher than the barrier height to pass over the sill, but block any flows less than this height.

A.3 FORCING INPUT

A.3.1 Overview

The model is run to simulate wet, dry, and average conditions for the Nueces Delta. The input data was collected for April 2008, April 2009, and April 2010. Plots of all forcing input are given in Section A.5.

A.3.2 Tidal Data

The tidal data was obtained from the Texas Coastal Ocean Observation Network (TCOON) platform at White Point, located on the northern shore at the outlet of Nueces Bay as shown in Figure A.7.



Figure A.7: Location of the monitoring station at White Point

The tidal data is in thirty-minute increments as the primary water level at White Point relative to the NAVD88 datum. Missing data points were replaced by taking the linear average of the tidal data surrounding the missing data. This methodology for replacing missing data points in the tidal data is employed for all input parameters. The tidal data is input into the model as water elevations in meters at the boundary condition across the face of the Nueces Bay. The boundary condition where the tide is specified is sufficiently far out in the Nueces Bay that the inaccuracies in the boundary condition become less important at the study area in the delta. The Nueces Bay water surface has a slope (Ward 1997), but that slope is negligible when compared to the changes in water level with time (Ward, Irlbeck and Montagna 2002). Therefore, the tidal data from White Point is appropriate for simulating the tidal conditions in the delta.

A.3.3 Inflow Data

The Nueces River Authority monitors the volume of water pumped in the Calallen Diversion Project. The pumping from the Calallen Diversion Project is a major source of freshwater flow to the Nueces Delta. This inflow is treated by the model as a flow coming up from six grid cells. The inflow is spread out over multiple 15m x 15m grid cells to keep water velocities low enough to not affect the model's stability. This adjustment at the point where inflow comes in does not affect where the inflow travels, and is an appropriate change to maintain stability. The pumping data is collected hourly and was converted from acre-ft/day to cubic meters per second.

Downstream of the Calallen Dam and upstream of where the Calallen Pipeline Diversion Project outfall point is located, the Nueces River splits. Where the Nueces River splits, the majority of flow runs south of the delta and the remaining flow continues east into the delta. The locations of the Rincon Pipeline Outfall and the USGS gage in

the study area are shown in Figure A.8, and a zoomed in figure of the area where the Nueces River splits is displayed in Figure A.9. USGS Gage 08211503 monitors the flow continuing into the delta. The discharge at this point in the river is measured by USGS in cubic feet per second in 15 minute increments and converted to cubic meters per second for input into the model. At times, the discharge is measured as a negative value, representing that the direction of flow at those times is reversed. This change in the direction of flow is caused by saltwater from the Nueces Bay moving up the Nueces River into the Rincon Bayou through the Rincon Bayou Channel during high tide (Ockerman 2001). The negative values in the inflow are removed and replaced with zeros so that the point where this inflow is defined does not become a sink for water at times of reverse flow. The reversed direction of flow is accounted for in the model by the tide coming up into that portion of the delta, pushing the flow inward.



Figure A.8: Locations of the USGS Gage and the Rincon Pipeline Outfall in the Study Area



Figure A.9: Locations of the USGS Gage and the pipeline outfall in reference to where the Nueces River splits

A.3.4 Wind Data

Wind data was taken from TCOON at NUDEWX for 2009 and 2010. The weather station at NUDEWX was not functional during April 2008. To choose the most appropriate weather station to gather wind data for the April 2008 simulation, wind speed and direction values were compared at various stations for April 2009. The weather stations used for comparison were the National Estuarine Research Reserve System station located in the Mission-Aransas Reserve, the TCOON Buoy located in Port Ingleside, and the weather station at the Corpus Christi Airport. The locations of these weather stations are shown in Figure A.10.



Figure A.10: Locations of the weather stations measuring wind data

Because the NUDEWX station is located in the delta, it was considered the most appropriate site for data collection. With the other station data compared to the data at NUDEWX, the data from the Corpus Christi Airport minimized the root mean square difference for both wind speed and wind direction. The wind speed and direction were collected in thirty-minute increments in meters per second and degrees the wind is coming from. The comparison of the root mean square differences when analyzed with respect to the NUDEWX 2009 data is given in Figure A.11.

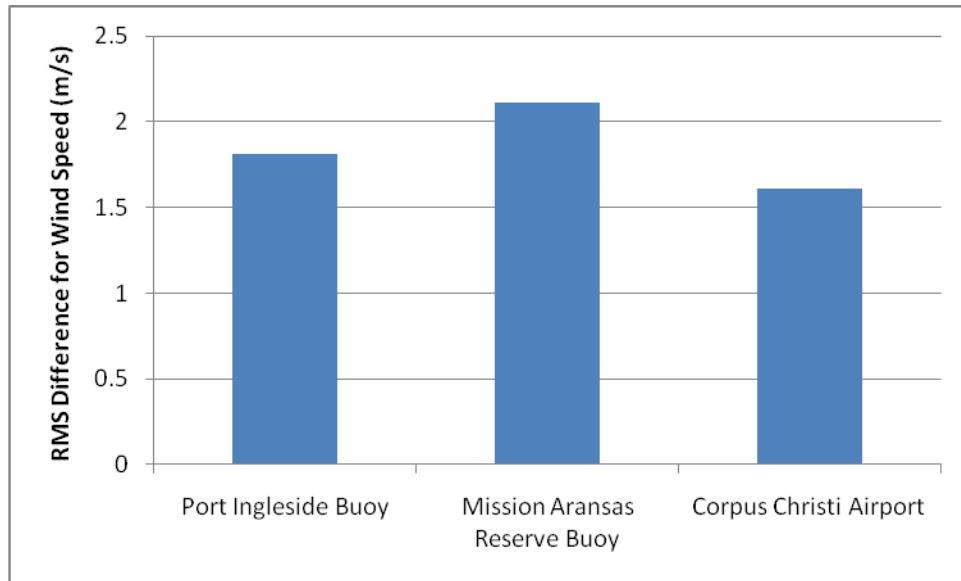


Figure A.11: Comparison of wind data from various weather stations with NUDEWX

A.3.5 Precipitation Data

The precipitation data was collected by NOAA at the Corpus Christi Airport, located approximately 7 miles from the delta at 27°46'N 97°31'W. The time periods for simulation were chosen to introduce and test varying conditions in the model. The average precipitation in the Nueces Delta area for April of 2000 – 2010 was approximately 3.8 inches of precipitation. April 2008 represents a wet condition with 6 inches of rain, April 2009 was dry with less than one inch of rainfall, and April 2010 was slightly above average with 4.85 inches of rain that month. While the rainfall in April 2008 was above average, the conditions were not wet enough to cause the river to overbank into the delta. Knowing that the river will not overbank during the time period of simulation is beneficial for testing the model because it reduces the factors complicating the flow and provides a simpler set of conditions to analyze. The precipitation data was taken from NOAA in hundredths of inches of rainfall per hour and

converted to mm/h for input into the model. All trace precipitation was input as zero precipitation.

Simulations were run for three different rainfall scenarios. Simulations of April 2009 were run with no rain, the actual measured rainfall, and a worst-case scenario of rainfall. The worst-case scenario was determined from the measured rainfall at the NOAA rain gage at Corpus Christi Airport for the last ten years. The highest month of precipitation occurred in July 2007, and the highest consecutive seven days of rainfall in that month had 353 mm of precipitation. This rainfall was averaged out over the seven day simulation for the worst-case scenario.

A.3.6 Salinity

Data for NUDE1, NUDE2, and NUDE3 were only available for 2010. The initial conditions for the salinity in the delta were calculated by interpolating between the salinity monitoring stations. The value used for the initial condition at each station was found using the mean of all salinity values at that station from the day previous to the start of the simulation. Because the salinity is only known at points where there is monitoring data, the interpolation for the initial condition assumes uniform salinity across the delta from north to south, with salinity varying from east to west. The weaknesses associated with the initial condition become less important as the model simulates longer time periods. The time-varying data used for the salinity at the tidal boundary condition was obtained from the salinity at gage SALT03. The salinity for the inflow at the USGS gage 08211503 and for all pumped inflow is approximated as zero salinity.

A.3.7 Land Cover

The land cover data for the delta was gathered from the National Land Cover Dataset (NLCD) from the USGS Land Cover Institute. Manning's roughness coefficient

values associated with simulating flow across the 2001 NLCD were gathered from literature and translated to a matrix corresponding with bathymetry in the delta (Hossain, Jia and Chao 2009). The impacts of piers and culverts under barriers are incorporated into the land cover matrix as adjusted Manning’s roughness coefficients, as discussed in Section 2.2.3. The Manning’s n values used in the model collected from Hossain, Jia and Chao 2009 are given in Table A.1.

Land Cover Description	Manning’s n
Open water	0.025
Concrete/finished	0.015
Bare Earth	0.025
Trees	0.150
Heavy Brush	0.075
Light Brush	0.050
Pasture/Farmland	0.035

Table A.1: Manning’s n values associated with various Land Cover types

The National Land Cover Dataset also includes variations of the land cover types described in Table A.1. These variations depend on the extent of development, and the Manning’s n values given in the table above are adjusted for these variations. Using different Manning’s n values across the delta in the simulations provides a different representation of flow in the delta than using a constant roughness coefficient for the entire area as a starting point for simulation.

A.4 DATA COLLECTION LIMITATIONS

Data collection proved to be a challenging and integral aspect of the model creation process. The bathymetric data collected was at a fine grid scale and required rasterization to a coarser grid for use in the model. Generally speaking, however, the opposite is the case, and the resolution of data available is not fine enough for ideal

incorporation into the model. Much of the other data collected had this problem. The initial conditions for salinity were interpolated from very few data points across the approximately 75 km area. A more representative initial condition in the delta may have aided in the reliability of the starting point of the simulations. It is difficult to strike a balance between having fine enough data to create a reliable model while staying within the model's capabilities. Ultimately, the availability of data and computational capabilities are the two major limiting factors of environmental modeling.

A.5 PLOTS OF FORCING INPUT

A.5.1 Rainfall Input

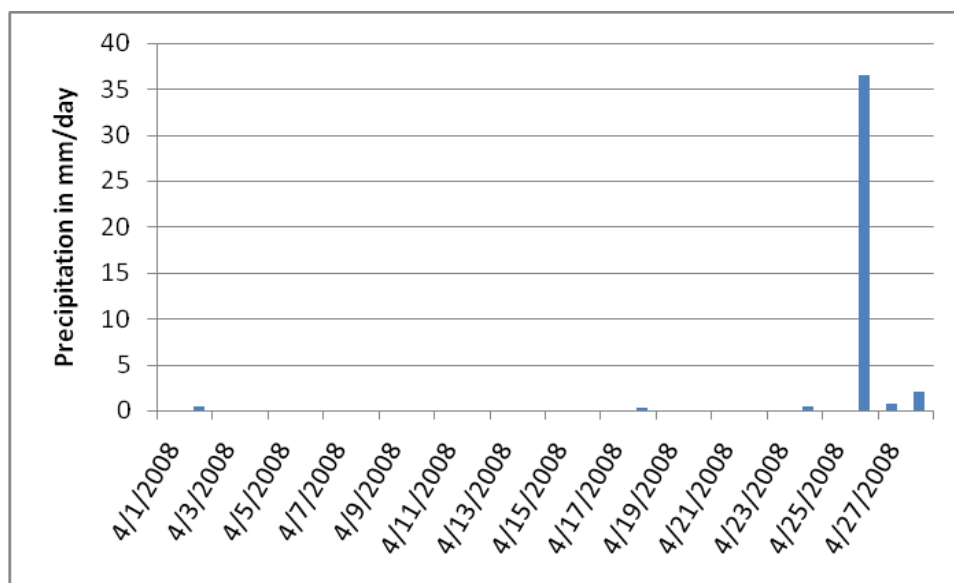


Figure A.12: Rainfall in April 2008

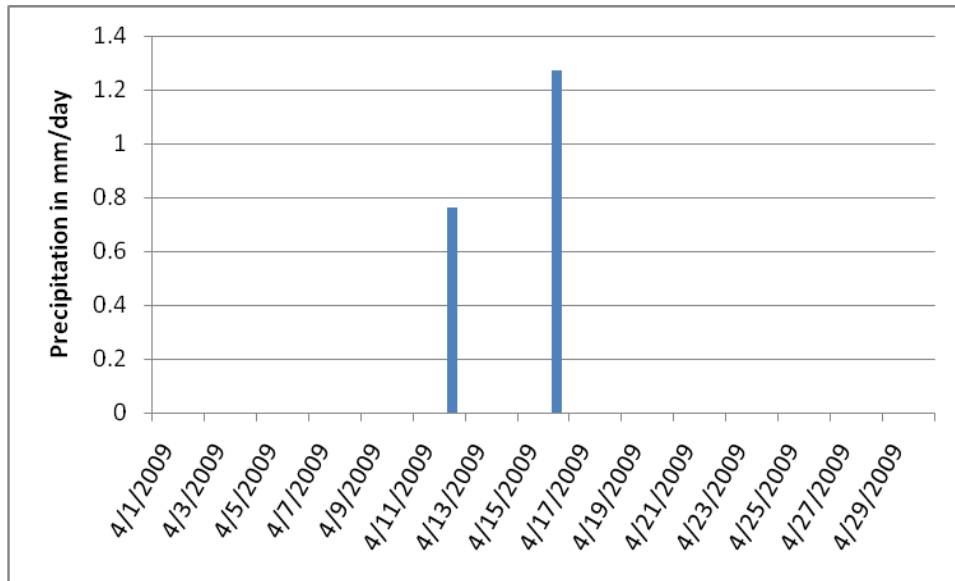


Figure A.13: Rainfall in April 2009

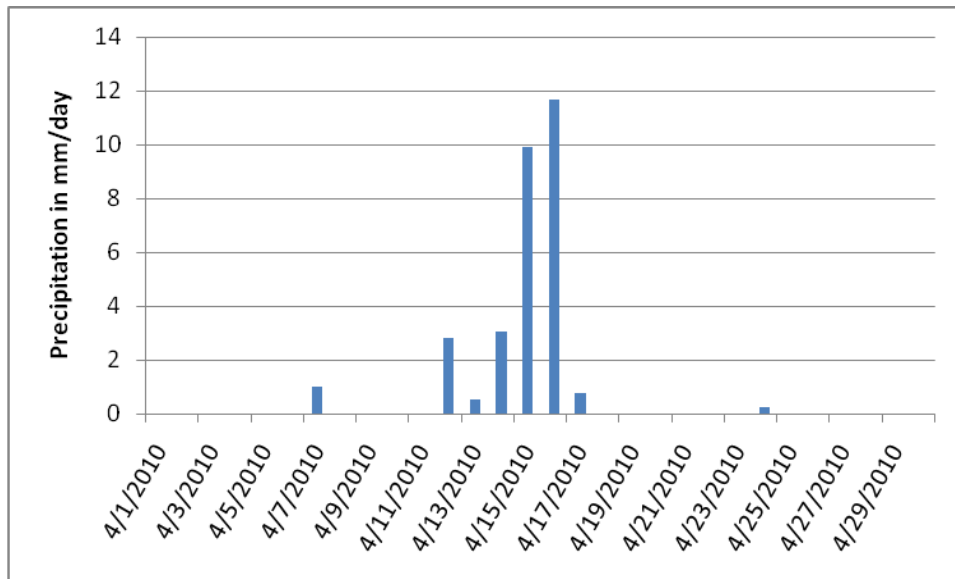


Figure A.14: Rainfall in April 2010

A.5.2 Wind Input

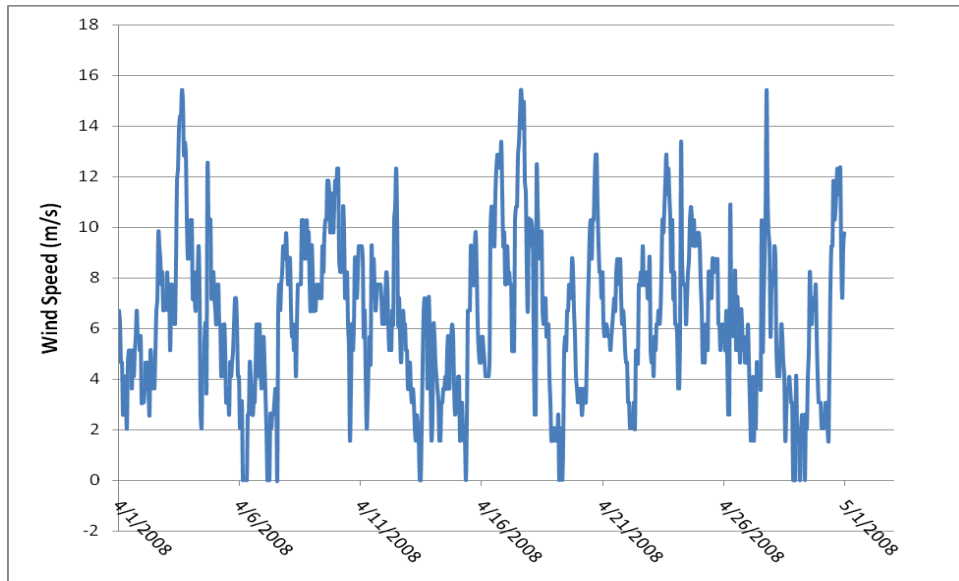


Figure A.15: Wind Speed in April 2008

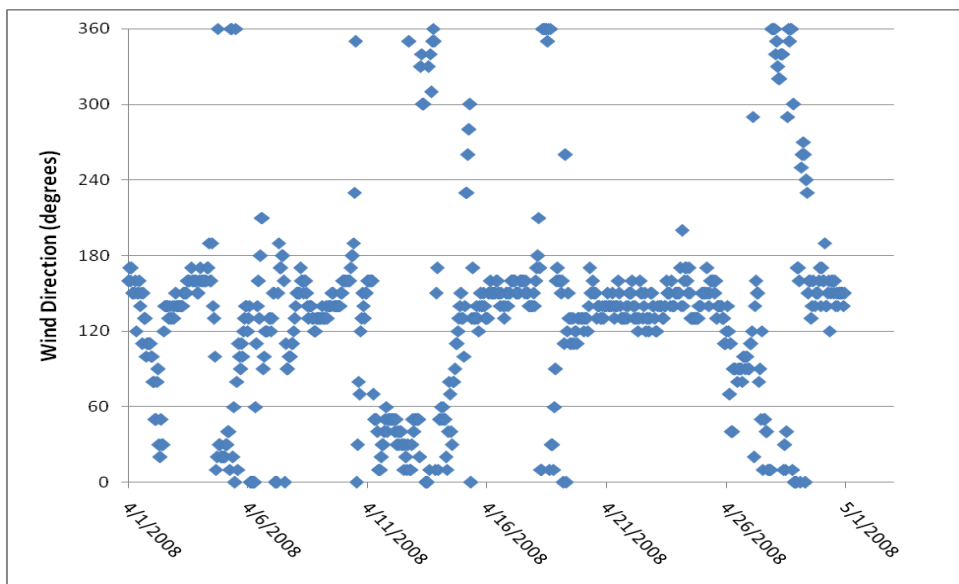


Figure A.16: Wind Direction in April 2008

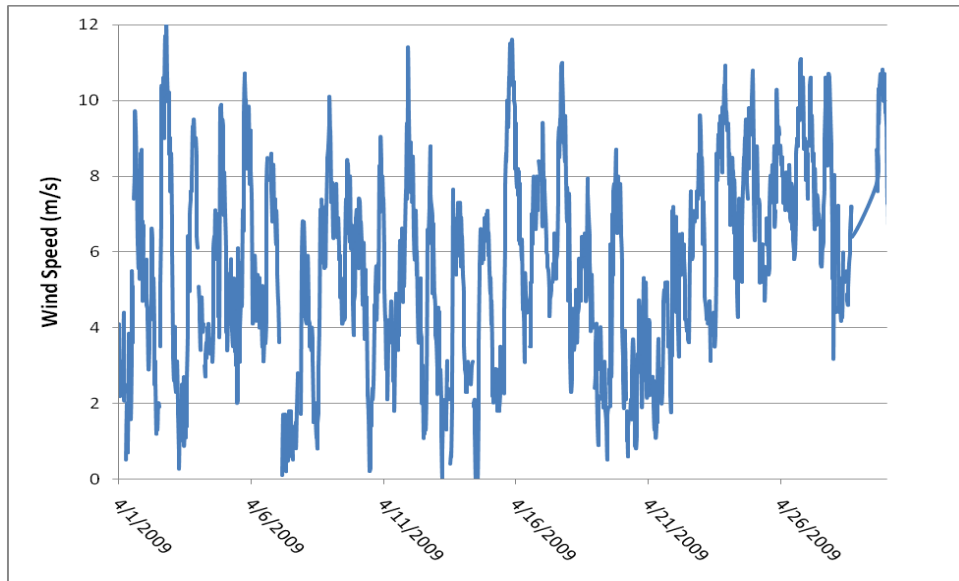


Figure A.17: Wind Speed in April 2009

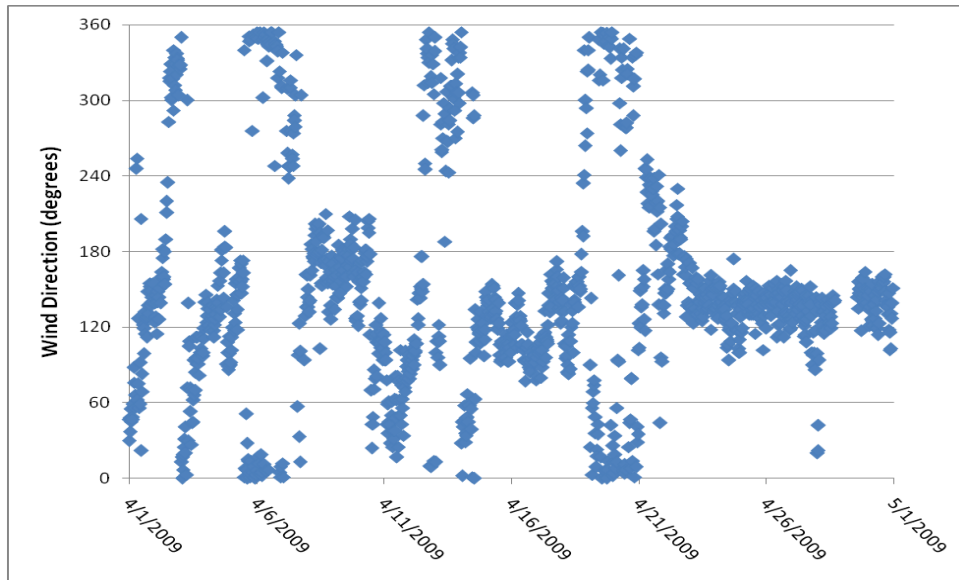


Figure A.18: Wind Direction in April 2009

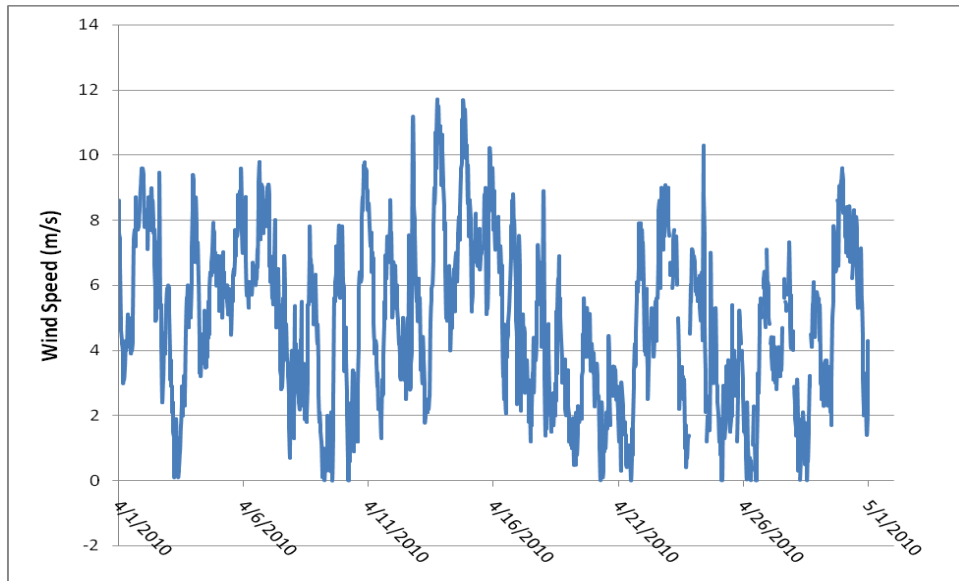


Figure A.19: Wind Speed in April 2010

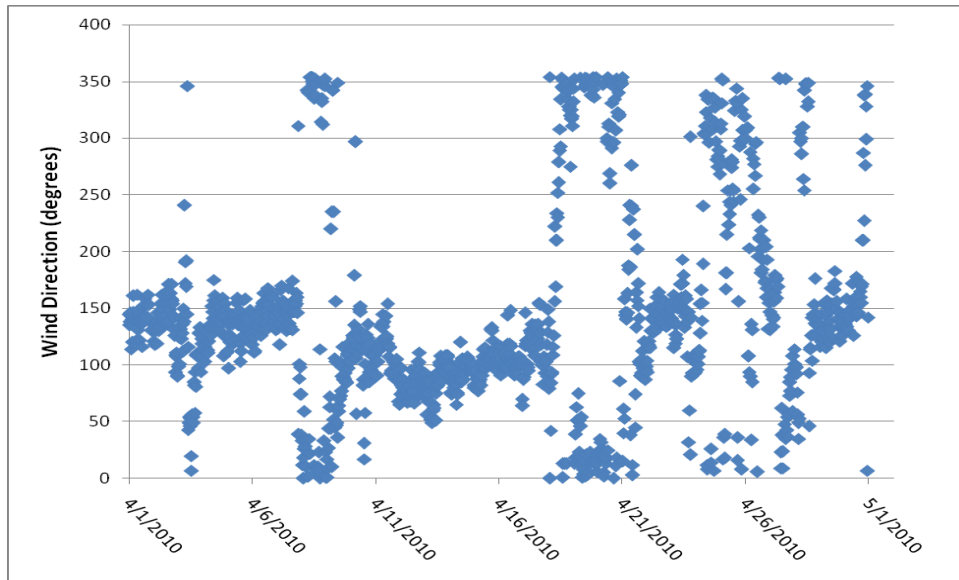


Figure A.20: Wind Direction in April 2010

A.5.3 Tidal Input

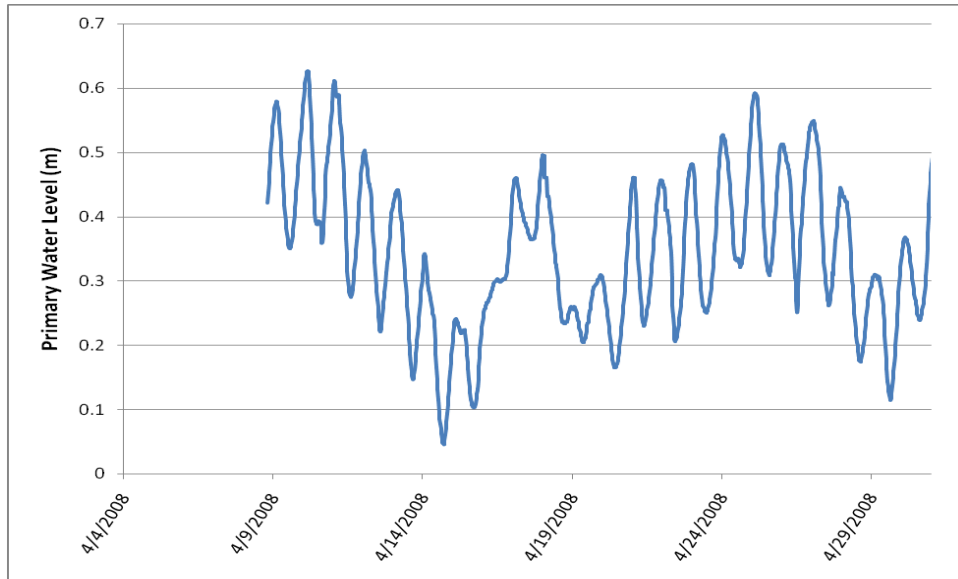


Figure A.21: Tidal Boundary Condition in April 2008

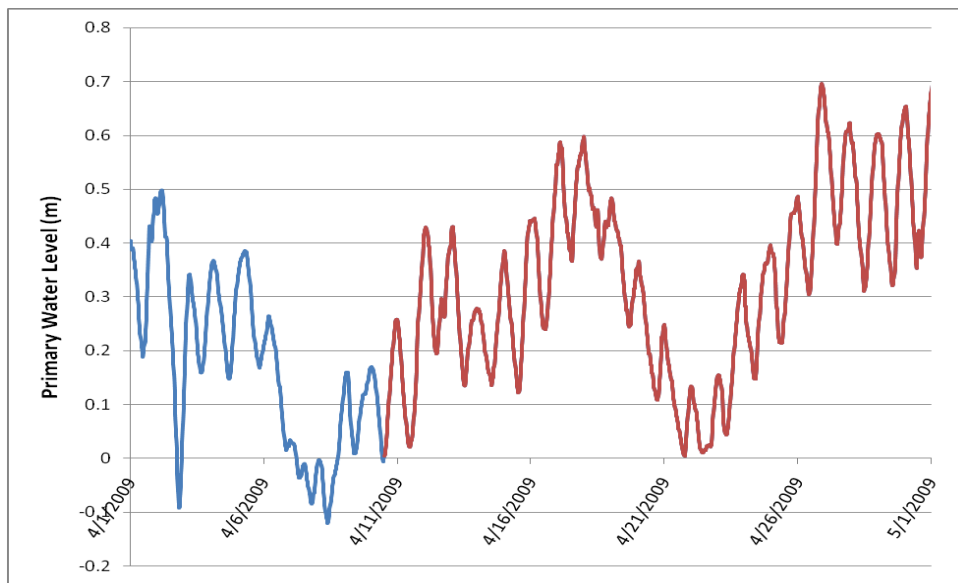


Figure A.22: Tidal Boundary Condition in April 2009

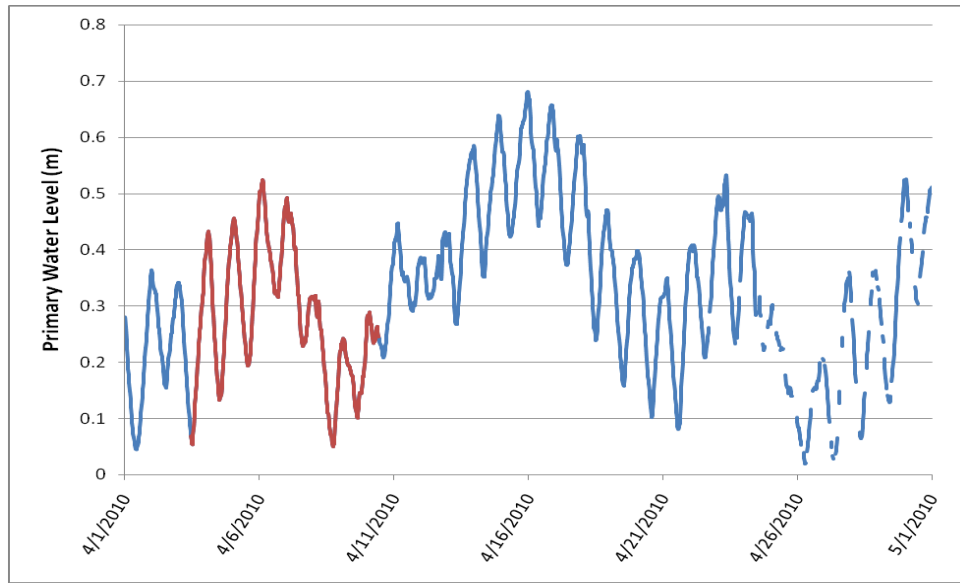


Figure A.23: Tidal Boundary Condition in April 2010

Appendix B: Additional Information used in Analysis

B.1 INUNDATED AREA DEPTH CUTOFF

The area inundated can be defined based on different cutoff values for the minimum depth required. Figure B.1 gives the A_i for Simulation 6 with varying cutoffs for the minimum depth defining inundation. The cutoff values shown in the figure are given in meters. Figure B.1 also gives a close up section of the A_i for the different cutoffs to demonstrate the differences between the output.

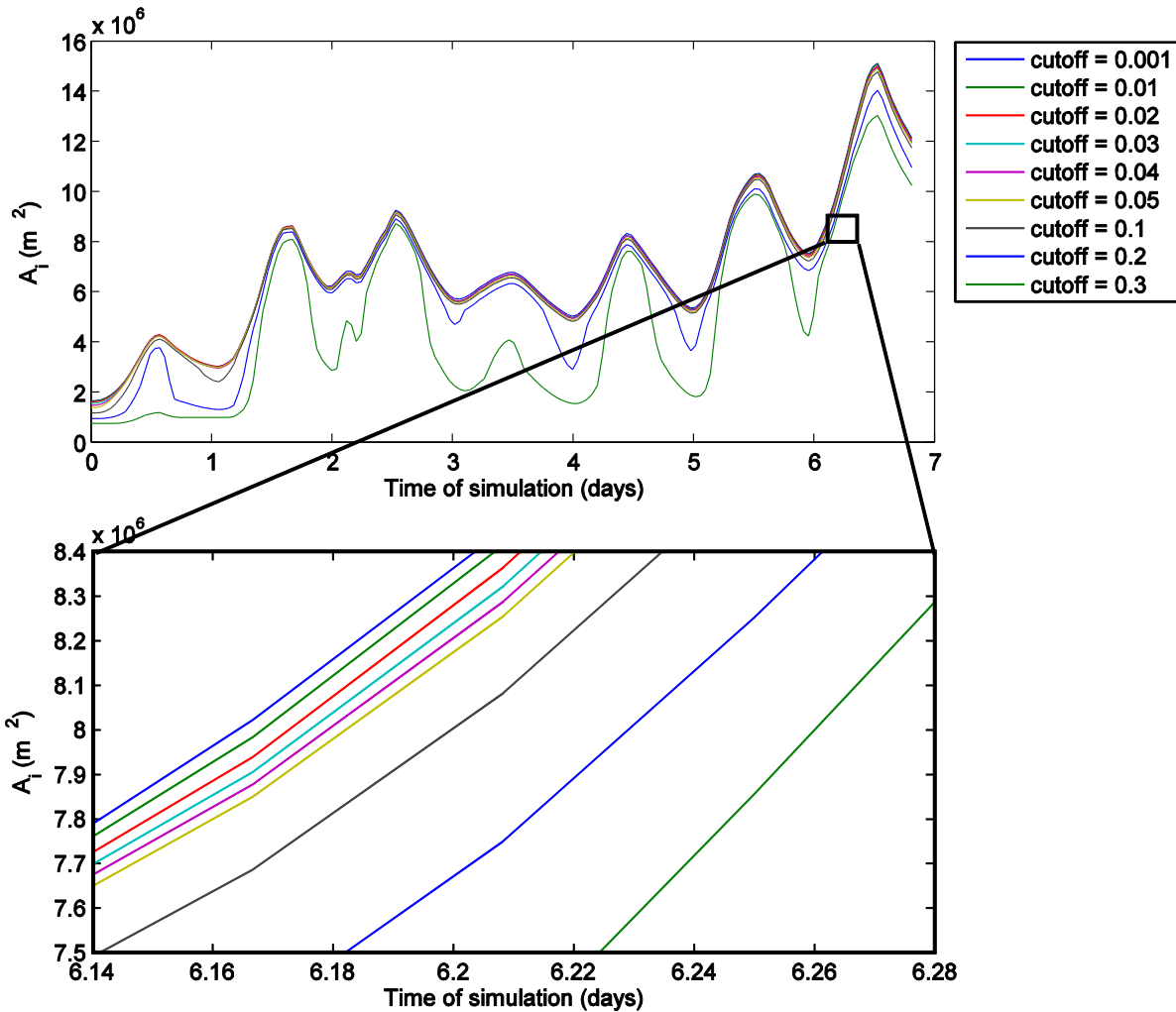


Figure B.1: Inundated Area from Simulation 6 over seven days with varying cutoffs for minimum depth

The plot zoomed in to show only from 6.14 days to 6.28 days shows that cutoffs from 0.001 m (0.039 in) to 0.05 m (1.97 in) have closer results than when the cutoff jumps to 0.1 m (3.94 in) or greater. To maintain results within this range, an intermediate value of 0.02 m (0.787 in) was chosen as the depth cutoff to define inundated area.

B.2 VERTICAL DATUMS

To find the surface elevations for the TCOON SALT and NUDE stations the datum relative to NAVD88, the monthly mean surface elevation at White Point was assumed to be equal to the mean at the salinity stations. The general methodology is presented here:

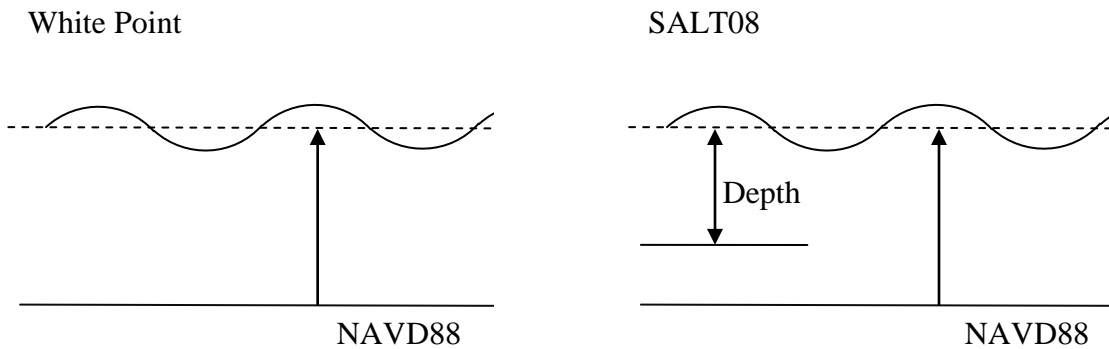


Figure B.2: Depiction of the TCOON monitoring station vertical datums

Monthly mean at White Point = 0.3377 m (primary water level with respect to NAVD88)

Monthly mean at SALT08 = 0.5422 m (depth with respect to station datum)

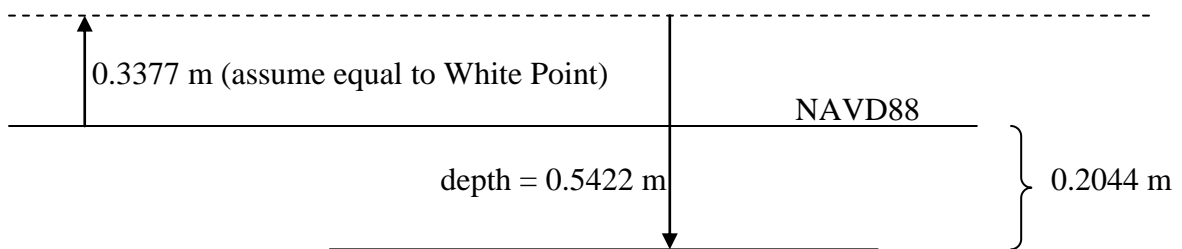


Figure B.3: Depiction of the estimation method for approximating TCOON vertical datum

This methodology is used for NUDE1, NUDE2, and NUDE3 as well. Table B.1 displays the data used to approximate the calculations to transfer the depth data to surface elevations relative to a datum.

Station	Monthly Avg Depth	Transfer data to Surface Elevation
SALT08	0.5422	0.2044
NUDE2	0.1654	-0.1723
NUDE3	0.3946	0.0569

Table B.1: Values used to estimate the NAVD88 datums for the monitoring stations

B.3 SOIL INFILTRATION ALGORITHM

The soil infiltration algorithm in the model incorporates a simple calculation that allows for depths to be absorbed at a constant rate. This algorithm is particularly important in the uplands surrounding the delta, where water depths are shallow.

B.4 MODEL'S RESPONSE TO RAINFALL: TOTAL VOLUME

The V_T from the various rainfall scenarios is given in Figure B.4. Much like the A_i for the rainfall scenarios, the baseline rainfall scenario output matches closely with the zero rainfall scenario. The heavy rainfall, however, has a larger effect on V_T .

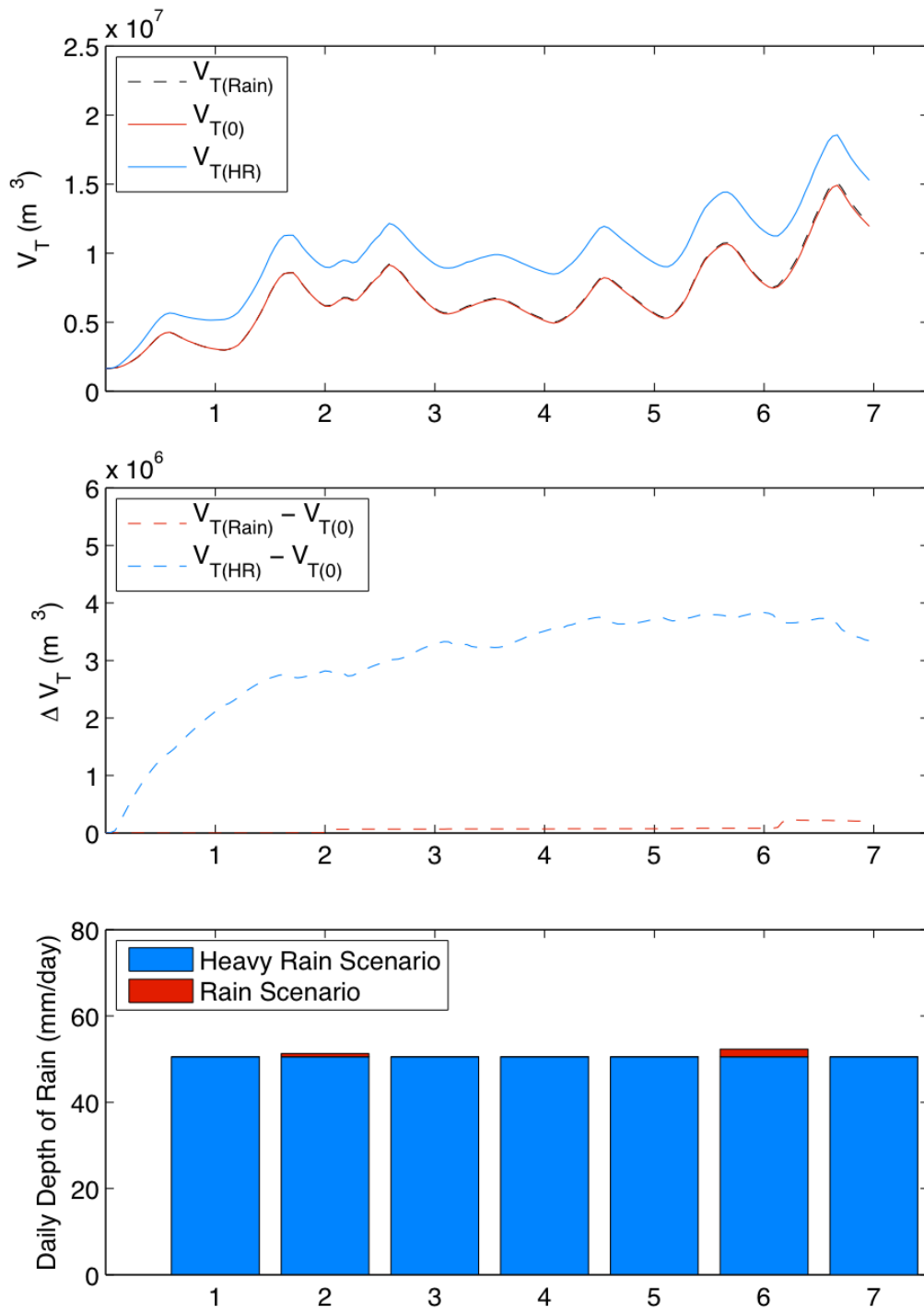


Figure B.4: Plots of V_T , ΔV_T , and daily rainfall depth for various rain scenarios

B.5 MODEL'S RESPONSE TO WIND: PERCENT CHANGE IN V_T

The impacts of changes in wind forcing on the model are investigated here as a percent change from the scenario with no wind, Simulation 8, and are displayed in Figure B.5.

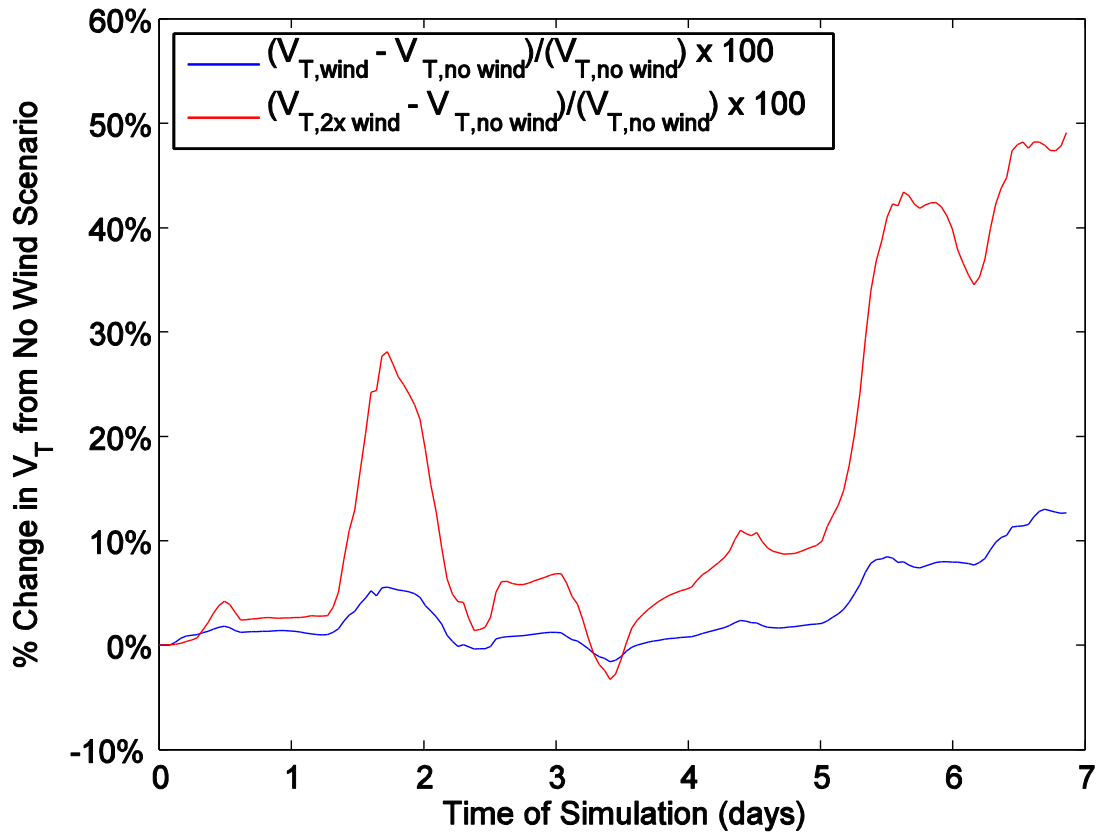


Figure B.5: Percent Change in V_T for different wind scenarios

Appendix C: Additional information for Future Work

C.1 CULVERT DATA

Culverts affect flow by allowing flow through that sufficiently exceeds the height of the bottom of the culvert barrel to flow through. The main culvert in the delta is located at the road that crosses the channel near the Calallen Pipeline outfall. Because these culverts are located in a location that greatly impacts where pumped water flows, one potential addition to the model is incorporating equations specific to the effects of the culverts on the hydraulics.

There are three conditions for culvert flow that could be incorporated into the model. The scenarios considered include a submerged outlet, a free outlet with submerged inlet, and free flow where both the inlet and outlet are unsubmerged. Figure C.1 illustrates the conditions that the model can account for.

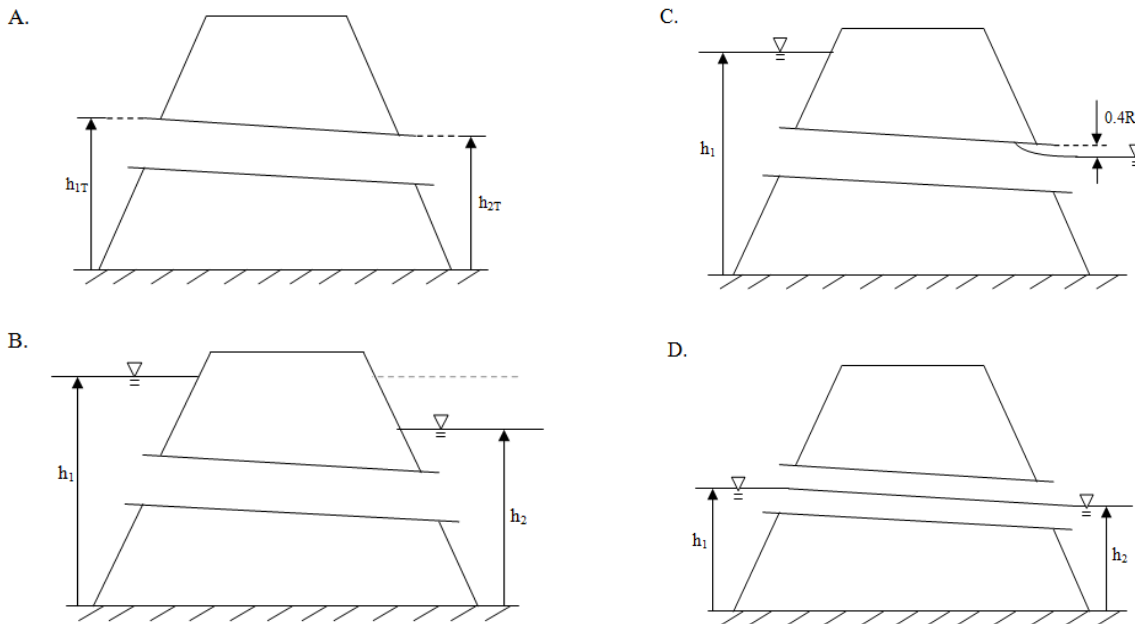


Figure C.1: Possible culvert flow conditions

The equations vary for these conditions. Condition A flow, the submerged outlet, is given as

$$Q = \frac{\pi \left(\frac{d}{2}\right)^2 \sqrt{2g(h_1 - h_2)}}{\sqrt{1.78 + L \left(\frac{1244522 \times n^2}{d^{4/3}}\right)}} \quad (\text{C.1})$$

Where:

d = diameter of the pipe

L = length of culvert barrel

n = Manning's n of the culvert barrel

h_1, h_2, h_{1T}, h_{2T} = displayed in Figure C.1

The calculation for flow through a culvert under Condition B, the submerged inlet with free outlet is

$$Q = \frac{\pi \left(\frac{d}{2}\right)^2 \sqrt{2g(h_1 - h_{2T} + 0.2d)}}{\sqrt{1.78 + L \left(\frac{1244522 \times n^2}{d^{4/3}}\right)}} \quad (\text{C.2})$$

If both the inlet and outlet of the culvert barrel are unsubmerged, the flow is under Condition C the flow is

$$Q = \frac{1}{n} \times A \times R^{2/3} \times S^{1/2} \quad (\text{C.3})$$

$$\text{If } h_1 < \left(h_{1T} - \frac{d}{2}\right)$$

$$P = R \times \theta$$

$$\theta = 2 \arccos\left(\frac{r - y}{y}\right)$$

$$y = h_1 - (h_{1T} - d)$$

$$A = \frac{r^2(\theta - \sin \theta)}{2}$$

$$\begin{aligned}
& \text{If } h_1 > \left(h_{1r} - \frac{d}{2} \right) \\
& P = 2\pi r - (r \times \theta) \\
& \theta = 2 \arccos \left(\frac{y-r}{y} \right) \\
& y = h_1 - (h_{1r} - d) \\
& A = \pi r^2 - \frac{r^2(\theta - \sin \theta)}{2}
\end{aligned}$$

The culverts could be handled in the model by placing a sill at the face of the edge of the cell with the culvert and allow flow based on these equations through the sill.

C.2 METEOROLOGICAL DATA

Meteorological data may aid in accurately simulating heating and cooling in estuary and delta environments. The PC2 Model has capabilities in progress to input shortwave radiation, cloud cover, relative humidity and air temperature data for these calculations.

C.2.1 Sources for Meteorological Data in the Nueces Delta

Cloud cover, relative humidity and air temperature data can be obtained from weather data collected at Corpus Christi International Airport. Shortwave radiation can be calculated using Equations C.4 and C.5 gathered from Bisht et al 2005.

$$R_s^\downarrow - R_s^\uparrow = \frac{S_0 \times (\cos \theta)^2}{d} \quad (\text{C.4})$$

$$d = 1.085 \times \cos \theta + e_0 \times (2.7 + \cos \theta) \times 10^{-3} + 0.1 \quad (\text{C.5})$$

Where:

$$S_0 = 1367 \text{ W/m}^2$$

$$\theta = \text{solar zenith angle}$$

$$e_0 = \text{screen level vapor pressure}$$

The vapor pressure can be calculated using the Antoine Equation with parameters from the National Institute of Standards and Technology (U.S. Secretary of Commerce 2008).

$$\log_{10}(P) = A - \frac{B}{C+T} \quad (\text{C.6})$$

Where:

$$A = 5.40221$$

$$B = 1838.675$$

$$C = -31.737$$

The solar zenith angle can be obtained from the National Solar Radiation Database (NSRDB) from the National Climatic Data Center. Data from the NSRDB is only available up through 2005. The zenith angle at each hour in April varies by a maximum of 0.2 degrees from year to year from 1991-2005. Because the data is consistent from year to year, this data is considered reasonable for calculating the shortwave radiation for the dates simulated. To confirm that this data is accurate for possible input into the model, the solar zenith angle was calculated using equations for calculating the solar zenith angle at a particular latitude point based on the time of day and time of year (Sellers 1965, Wunderlich 1972). The calculations of the solar zenith angle on April 10 at the latitude of the Nueces Delta reveal that the measured solar zenith angles at the Corpus Christi Airport are comparable to the calculated values.

The calculated radiation values are reasonable when compared to solar radiation values measured directly in Sinton, TX, approximately 18 kilometers from the delta. This data was gathered by the Texas A&M AgriLife Extension TexasET system. This data is not appropriate for use as input for the model because varying measurement techniques for shortwave radiation can make data inconsistent in what is being measured. However, it is reasonable to compare this data with our calculated values to confirm that our calculations are legitimate.

C.2.2 Water Temperature Data

The water temperature data for the initial condition is available from TCOON at the salinity stations. As with the initial condition for salinity, the water temperature may be considered uniform from north to south across the delta and varies from east to west as a linear interpolation between the salinity gauging stations. The water temperature at the boundary condition of the incoming tide may be set equal to the water temperature at SALT03 through time. The water temperature for the inflow from at the USGS Station 08211503 is available as daily mean temperature data from USGS. This water temperature data can be used for the inflow at the USGS gage as well as the pumped water since it is pumped from the river. The temperature of rainfall might be considered equal to the average of the air temperature because rainfall temperature data is not available.

Appendix D: Matlab Scripts

D.1 SCRIPT FOR ANALYZING SPIN UP

```
%% Compare 10 day & 17 day runs

load ('/Users/andrearyan/Documents/MATLAB/PC2
20110427/Analysis/Nueces_April2009_17days/OutData2D.mat');
OutData2D_17days = OutData2D; clear OutData2D;
disp ('*****Finished loading first variable*****')

load ('/Users/andrearyan/Documents/MATLAB/PC2
20110427/Analysis/Nueces_April2009_10days/OutData2D.mat');
OutData2D_10days = OutData2D; clear OutData2D;
disp ('*****Finished loading second variable*****')

%% Find volume of water in each time step
length1 = size(OutData2D_17days.depth_time);
mm = length1(2);

length2 = size(OutData2D_10days.depth_time);
length10 = length2(2);

sum_volume_17 = zeros(mm,1);
volume_17 = zeros(667,971,mm);
volume_17_nonan = zeros(667,971);

for n = 1:mm
    volume_17(:,:,n) = OutData2D_17days.depth(:,:,n);
    volume_17_nonan = volume_17(:,:,n);
    aa = isnan(volume_17_nonan);
    volume_17_nonan(aa) = 0; %get rid of nans
    volume_17(:,:,n) = volume_17_nonan;

    sum_volume_17(n,1) = sum(sum(volume_17(:,:,n)));
end

disp ('*****Finished Summing Volume for 17 day Scenario*****')

sum_volume_10 = zeros(length10,1);
volume_10 = zeros(667,971,length10);
volume_10_nonan = zeros(667,971);
for n = 1:length10
    volume_10(:,:,n) = OutData2D_10days.depth(:,:,n);
    volume_10_nonan = volume_10(:,:,n);
    aa = isnan(volume_10_nonan);
    volume_10_nonan(aa) = 0; %get rid of nans
    volume_10(:,:,n) = volume_10_nonan;

    sum_volume_10(n,1) = sum(sum(volume_10(:,:,n)));
end

disp ('*****Finished Summing Volume for the 10 day Scenario*****')
```

```

%% Find inundated area at each time step

depth_cutoff = 0.02; %this is the depth below which will not be included in
inundated area

sum_area_17 = zeros(mm,1);
area_17 = zeros(667,971,mm);

for n = 1:mm
    depth_17 = volume_17(:,:,n);
    cc = find(depth_17 < depth_cutoff);
    depth_17(cc) = 0;
    bb = find(depth_17 > 0);
    depth_17(bb) = 1;
    area_17(:,:,n) = depth_17;

    sum_area_17(n,1) = sum(sum(area_17(:,:,n))).*15.*15; %gives area inundated
at greater than 2 cm
end

disp('*****Finished Finding Inundated Area for 17 day Scenario*****')

sum_area_10 = zeros(length10,1);
area_10 = zeros(667,971,length10);
for n = 1:length10
    depth_10 = volume_10(:,:,n);
    cc = find(depth_10 < depth_cutoff);
    depth_10(cc) = 0;
    bb = find(depth_10 > 0);
    depth_10(bb) = 1;
    area_10(:,:,n) = depth_10;

    sum_area_10(n,1) = sum(sum(area_10(:,:,n))).*15.*15; %gives area inundated
at greater than 2 cm
end

disp('*****Finished Finding Inundated Area for 10 day Scenario*****')

%% Mean & Std. Dev of surface elevation through time

mean_elev_17 = zeros(mm,1);
stdev_elev_17 = zeros(mm,1);
elev_17 = zeros(667,971,mm);

diff = zeros(667,971,length10);
std_dev = zeros(length10,1);
mean_diff = zeros(length10,1);
max_diff = zeros(length10,1);

for n = 1:length10
    time_17 = n + (594000./90./40); %transfer time to work for 17 day scenario
    diff(:,:,n) = abs(volume_17(:,:,time_17) - volume_10(:,:,n));
    std_dev(n,1) = std(std(diff(:,:,n)));

    mean_diff(n,1) = mean(mean(diff(:,:,n)));
    max_diff(n,1) = max(max(diff(:,:,n)));
end

day = 24;

```

```

std_dev_day = [mean(std_dev(1:day,1));mean(std_dev(day+1:day*2,1));...
    mean(std_dev(day*2+1:day*3,1));mean(std_dev(day*3+1:day*4,1));...
    mean(std_dev(day*4+1:day*5,1));mean(std_dev(day*5+1:day*6,1));...
    mean(std_dev(day*6+1:day*7,1));mean(std_dev(day*7+1:day*8,1));...
    mean(std_dev(day*8+1:day*9,1));mean(std_dev(day*9+1:day*10,1))];

mean_diff_day = [mean(mean_diff(1:day,1));mean(mean_diff(day+1:day*2,1));...
    mean(mean_diff(day*2+1:day*3,1));mean(mean_diff(day*3+1:day*4,1));...
    mean(mean_diff(day*4+1:day*5,1));mean(mean_diff(day*5+1:day*6,1));...
    mean(mean_diff(day*6+1:day*7,1));mean(mean_diff(day*7+1:day*8,1));...
    mean(mean_diff(day*8+1:day*9,1));mean(mean_diff(day*9+1:day*10,1))];

% Inundated Area
stddev_diffarea_day =
[mean(diff_area2(1:day,1));mean(diff_area2(day+1:day*2,1));...
    mean(diff_area2(day*2+1:day*3,1));mean(diff_area2(day*3+1:day*4,1));...
    mean(diff_area2(day*4+1:day*5,1));mean(diff_area2(day*5+1:day*6,1));...
    mean(diff_area2(day*6+1:day*7,1));mean(diff_area2(day*7+1:day*8,1));...
    mean(diff_area2(day*8+1:day*9,1));mean(diff_area2(day*9+1:day*10,1))];

mean_diffarea_day =
[mean(diff_area2(1:day,1));mean(diff_area2(day+1:day*2,1));...
    mean(diff_area2(day*2+1:day*3,1));mean(diff_area2(day*3+1:day*4,1));...
    mean(diff_area2(day*4+1:day*5,1));mean(diff_area2(day*5+1:day*6,1));...
    mean(diff_area2(day*6+1:day*7,1));mean(diff_area2(day*7+1:day*8,1));...
    mean(diff_area2(day*8+1:day*9,1));mean(diff_area2(day*9+1:day*10,1))];

% Total Volume
stddev_diffvol_day =
[mean(diff_vol2(1:day,1));mean(diff_vol2(day+1:day*2,1));...
    mean(diff_vol2(day*2+1:day*3,1));mean(diff_vol2(day*3+1:day*4,1));...
    mean(diff_vol2(day*4+1:day*5,1));mean(diff_vol2(day*5+1:day*6,1));...
    mean(diff_vol2(day*6+1:day*7,1));mean(diff_vol2(day*7+1:day*8,1));...
    mean(diff_vol2(day*8+1:day*9,1));mean(diff_vol2(day*9+1:day*10,1))];

mean_diffvol_day = [mean(diff_vol2(1:day,1));mean(diff_vol2(day+1:day*2,1));...
    mean(diff_vol2(day*2+1:day*3,1));mean(diff_vol2(day*3+1:day*4,1));...
    mean(diff_vol2(day*4+1:day*5,1));mean(diff_vol2(day*5+1:day*6,1));...
    mean(diff_vol2(day*6+1:day*7,1));mean(diff_vol2(day*7+1:day*8,1));...
    mean(diff_vol2(day*8+1:day*9,1));mean(diff_vol2(day*9+1:day*10,1))];

```

D.2 SCRIPT FOR ANALYZING MODEL RESPONSE TO RAINFALL

```

%% Compare rain vs no rain scenarios

% load Rain Scenarios for April 2009
load ('/Users/andrearyan/Documents/MATLAB/PC2
20110427/Analysis/Nueces_15x15_April2009_withrain/OutData2D_rain.mat');
disp ('*****Finished loading first variable*****')

load ('/Users/andrearyan/Documents/MATLAB/PC2
20110427/Analysis/NuecesApril2009_90s_7days/OutData2D_no_rain.mat');
disp ('*****Finished loading second variable*****')
OutData2D_no_rain = OutData2D; clear OutData2D;

load ('/Users/andrearyan/Documents/MATLAB/PC2

```

```

20110603/NuecesRuns_20110603/Nueces2009_WhR_7d_an_0p/OutData2D.mat');
OutData2D_hR = OutData2D; clear OutData2D;
disp ('*****Finished loading third variable*****')

%% Find volume of water in each time step
length1 = size(OutData2D_rain.depth_time);
mm = length1(2);

sum_volume_rain = zeros(mm,1);
volume_rain = zeros(667,971,mm);
for n = 1:mm
    volume_rain(:,:,n) = OutData2D_rain.depth(:,:,n);
    volume_rain_nonan = volume_rain(:,:,n);
    aa = isnan(volume_rain_nonan);
    volume_rain_nonan(aa) = 0; %get rid of NaNs
    volume_rain(:,:,n) = volume_rain_nonan;

    sum_volume_rain(n,1) = sum(sum(volume_rain(:,:,n)));
end

disp ('*****Finished Summing Volume for Rain Scenario*****')

sum_volume_norain = zeros(mm,1);
volume_norain = zeros(667,971,mm);
for n = 1:mm
    volume_norain(:,:,n) = OutData2D_no_rain.depth(:,:,n);
    volume_norain_nonan = volume_norain(:,:,n);
    aa = isnan(volume_norain_nonan);
    volume_norain_nonan(aa) = 0; %get rid of NaNs
    volume_norain(:,:,n) = volume_norain_nonan;

    sum_volume_norain(n,1) = sum(sum(volume_norain(:,:,n)));
end

disp ('*****Finished Summing Volume for No Rain Scenario*****')

sum_volume_hR = zeros(mm,1);
volume_hR = zeros(667,971,mm);
for n = 1:mm
    volume_hR(:,:,n) = OutData2D_hR.depth(:,:,n);
    volume_hR_nonan = volume_hR(:,:,n);
    aa = isnan(volume_hR_nonan);
    volume_hR_nonan(aa) = 0; %get rid of NaNs
    volume_hR(:,:,n) = volume_hR_nonan;

    sum_volume_hR(n,1) = sum(sum(volume_hR(:,:,n)));
end

disp ('*****Finished Summing Volume for Heavy Rain Scenario*****')

% When does it rain in 2009?
when_rain = ...
[174600 , 0.762 ;...
531000 , 1.27 ;...
534600 , 0.508];

rain_amount = when_rain(:,2);

%% Find inundated area at each time step

```

```

depth_cutoff = 0.02; %this is the depth below which will not be included in
inundated area

sum_area_rain = zeros(mm,1);
area_rain = zeros(667,971,mm);

for n = 1:mm
    depth_rain = volume_rain(:,:,n);
    cc = find(depth_rain < depth_cutoff);
    depth_rain(cc) = 0;
    area_rain(:,:,n) = depth_rain;

    sum_area_rain(n,1) = sum(sum(area_rain(:,:,n))); %gives area inundated at
greater than 2 cm
end

disp ('*****Finished Finding Inundated Area for rain Scenario*****')

sum_area_norain = zeros(mm,1);
area_norain = zeros(667,971,mm);

for n = 1:mm
    depth_norain = volume_norain(:,:,n);
    cc = find(depth_norain < depth_cutoff);
    depth_norain(cc) = 0;
    area_norain(:,:,n) = depth_norain;

    sum_area_norain(n,1) = sum(sum(area_norain(:,:,n))); %gives area inundated
at greater than 2 cm
end

disp ('*****Finished Finding Inundated Area for no rain Scenario*****')

sum_area_hR = zeros(mm,1);
area_hR = zeros(667,971,mm);

for n = 1:mm
    depth_hR = volume_hR(:,:,n);
    cc = find(depth_hR < depth_cutoff);
    depth_hR(cc) = 0;
    area_hR(:,:,n) = depth_hR;

    sum_area_hR(n,1) = sum(sum(area_hR(:,:,n))); %gives area inundated at
greater than 2 cm
end

disp ('*****Finished Finding Inundated Area for no rain Scenario*****')

% difference in inundated area:
diff_area = sum_area_rain - sum_area_norain;
aa = find(diff_area < 0);
diff_area(aa) = 0;

diff_area2 = sum_area_hR - sum_area_norain;
aa = find(diff_area2 < 0);
diff_area2(aa) = 0;

%% Calculate percent diff for rain inundated area & total volume:
max_IA_hR = max(sum_area_hR(:,1));

```

```

max_IA_norain = max(sum_area_norain(:,1));
max_IA_rain = max(sum_area_rain(:,1));

diff_IA_hR = max_IA_hR - max_IA_norain
diff_IA_rain = max_IA_rain - max_IA_norain

max_vol_norain = max(sum_volume_norain(:,1));
max_vol_hR = max(sum_volume_hR(:,1));
max_vol_rain = max(sum_volume_rain(:,1));

perc_vol_hR = (max_vol_hR - max_vol_norain) / (max_vol_norain)
perc_vol_rain = (max_vol_rain - max_vol_norain) / (max_vol_norain)

```

D.3 SCRIPT FOR ANALYZING MODEL RESPONSE TO WIND

```

%% Load Variables for wind analysis

load ('/Users/andrearyan/Documents/MATLAB/PC2
20110603/NuecesRuns_20110603/Nueces2009_SR_7d_an_0p/OutData2D.mat');
OutData2D_nowind = OutData2D; clear OutData2D;
disp ('*****Finished loading first variable*****')

load ('/Users/andrearyan/Documents/MATLAB/PC2
20110427/Analysis/Nueces_15x15_April2009_withrain/OutData2D_rain.mat');
OutData2D_wind = OutData2D_rain; clear OutData2D_rain;
disp ('*****Finished loading second variable*****')

load ('/Users/andrearyan/Documents/MATLAB/PC2
20110603/NuecesRuns_20110603/Nueces2009_2WR_7d_an_0p/OutData2D.mat');
OutData2D_2xwind = OutData2D; clear OutData2D;
disp ('*****Finished loading third variable*****')

%% Find difference in mean depth
depth_cutoff = 0.02; %this is the depth below which will not be included in
inundated area

length1 = size(OutData2D_nowind.depth_time);
mm = length1(2);

% NO WIND
depth_nowind = zeros(667,971,mm);
depth_nonan = zeros(667,971);
area_nowind = zeros(667,971);
area_nowind_time = zeros(667,971,mm);
sum_area_nowind = zeros(mm,1);

for n = 1:mm
    %get rid of NaNs
    depth_nowind(:, :, n) = OutData2D_nowind.depth(:, :, n);
    depth_nonan = depth_nowind(:, :, n);
    aa = isnan(depth_nonan);
    depth_nonan(aa) = 0; %get rid of nans
    depth_nowind(:, :, n) = depth_nonan;

    area_nowind = depth_nonan;
    cc = find(area_nowind < depth_cutoff);
    area_nowind(cc) = 0;

```

```

bb = find(area_nowind > 0);
area_nowind(bb) = 1; % has 0's everywhere depth < cutoff & 1's elsewhere
area_nowind_time(:, :, n) = area_nowind;

sum_area_nowind(n, 1) = sum(sum(area_nowind_time(:, :, n))).*15.*15; %gives
area inundated at greater than 2 cm
end

% WIND
depth_wind = zeros(667, 971, mm);
depth_nnan = zeros(667, 971);
area_wind = zeros(667, 971);
area_wind_time = zeros(667, 971, mm);
sum_area_wind = zeros(mm, 1);

for n = 1:mm
depth_wind(:, :, n) = OutData2D_wind.depth(:, :, n); %get rid of NaNs
depth_nnan = depth_wind(:, :, n);
aa = isnan(depth_nnan);
depth_nnan(aa) = 0; %get rid of nans
depth_wind(:, :, n) = depth_nnan;

area_wind = depth_nnan;
cc = find(area_wind < depth_cutoff);
area_wind(cc) = 0;
bb = find(area_wind > 0);
area_wind(bb) = 1; % has 0's everywhere depth < cutoff & 1's elsewhere
area_wind_time(:, :, n) = area_wind;

sum_area_wind(n, 1) = sum(sum(area_wind_time(:, :, n))).*15.*15; %gives area
inundated at greater than 2 cm
end

% 2x WIND
depth_2xwind = zeros(667, 971, mm);
depth_2xnan = zeros(667, 971);
area_2xwind = zeros(667, 971);
area_2xwind_time = zeros(667, 971, mm);
sum_area_2xwind = zeros(mm, 1);

for n = 1:mm
%get rid of NaNs
depth_2xwind(:, :, n) = OutData2D_2xwind.depth(:, :, n);
depth_2xnan = depth_2xwind(:, :, n);
aa = isnan(depth_2xnan);
depth_2xnan(aa) = 0; %get rid of nans
depth_2xwind(:, :, n) = depth_2xnan;

area_2xwind = depth_2xnan;
cc = find(area_2xwind < depth_cutoff);
area_2xwind(cc) = 0;
bb = find(area_2xwind > 0);
area_2xwind(bb) = 1; % has 0's everywhere depth < cutoff & 1's elsewhere
area_2xwind_time(:, :, n) = area_2xwind;

sum_area_2xwind(n, 1) = sum(sum(area_2xwind_time(:, :, n))).*15.*15; %gives
area inundated at greater than 2 cm
end

```

```

%% Errorbar at last time step through 2D space (u_300D)

points = 48; %how many data points do you want
step = round(971/points)-1; %each point includes this many steps (rounds up to
nearest integer then minus one so we don't go over 971)

% NO WIND
mean_depth_nowind = zeros(points,1);
stddev_depth_nowind = zeros(points,1);

for jj = 1:points
    jj1 = (jj*step) - (step-1);
    jj2 = (jj*step);
    mean_depth_nowind(jj,1) = mean(mean(depth_nowind(:,jj1:jj2,mm)));
    stddev_depth_nowind(jj,1) = std(std(depth_nowind(:,jj1:jj2,mm)));
end

% NORMAL WIND
mean_depth_wind = zeros(points,1);
stddev_depth_wind = zeros(points,1);

for jj = 1:points
    jj1 = (jj*step) - (step-1);
    jj2 = (jj*step);
    mean_depth_wind(jj,1) = mean(mean(depth_wind(:,jj1:jj2,mm)));
    stddev_depth_wind(jj,1) = std(std(depth_wind(:,jj1:jj2,mm)));
end

% 2X WIND
mean_depth_2xwind = zeros(points,1);
stddev_depth_2xwind = zeros(points,1);

for jj = 1:points
    jj1 = (jj*step) - (step-1);
    jj2 = (jj*step);
    mean_depth_2xwind(jj,1) = mean(mean(depth_2xwind(:,jj1:jj2,mm)));
    stddev_depth_2xwind(jj,1) = std(std(depth_2xwind(:,jj1:jj2,mm)));
end

%% Calculate % increase in total volume of water on 7th day

vol_7_wind = sum(sum(depth_wind(:, :, 168)));
vol_7_nowind = sum(sum(depth_nowind(:, :, 168)));
vol_7_2xwind = sum(sum(depth_2xwind(:, :, 168)));

perc_7_vol_wind = (vol_7_wind - vol_7_nowind) / (vol_7_nowind)
perc_7_vol_2xwind = (vol_7_2xwind - vol_7_nowind) / (vol_7_nowind)

%% Calculation % increase in total volume of water throughout time
vol_all_wind = zeros(mm,1);
vol_all_nowind = zeros(mm,1);
vol_all_2xwind = zeros(mm,1);
perc_all_vol_wind = zeros(mm,1);
perc_all_vol_2xwind = zeros(mm,1);

for n = 1:mm
    vol_all_wind(n,1) = sum(sum(depth_wind(:, :, n)));
    vol_all_nowind(n,1) = sum(sum(depth_nowind(:, :, n)));

```



```

    vol_all_2xwind(n,1) = sum(sum(depth_2xwind(:,:,n)));

    perc_all_vol_wind(n,1) = (vol_all_wind(n,1) - vol_all_nowind(n,1)) /
(vol_all_nowind(n,1)).*100;
    perc_all_vol_2xwind(n,1) = (vol_all_2xwind(n,1) - vol_all_nowind(n,1)) /
(vol_all_nowind(n,1)).*100;

end

```

D.4 SCRIPT FOR ANALYZING MODEL RESPONSE TO WIND

```

%% Load Variables for Comparing Roughness (Manning's n)

load ('/Users/andrearyan/Documents/MATLAB/PC2
20110603/NuecesRuns_20110605/Nueces2010_WR_14d_an_0p/OutData2D.mat');
OutData2D_an = OutData2D; clear OutData2D;

load ('/Users/andrearyan/Documents/MATLAB/PC2
20110603/NuecesRuns_20110605/Nueces2010_WR_14d_bn_0p/OutData2D.mat');
OutData2D_bn = OutData2D; %this variable is manning's n * 10
clear OutData2D;

load ('/Users/andrearyan/Documents/MATLAB/PC2
20110603/NuecesRuns_20110605/Nueces2010_WR_14d_cn_0p/OutData2D.mat');
OutData2D_cn = OutData2D; %this variable is manning's n * 100
clear OutData2D;

load ('/Users/andrearyan/Documents/MATLAB/PC2
20110603/NuecesRuns_20110610_outdata/Nueces2010_WR_14d_dn_0p/OutData2D.mat');
OutData2D_dn = OutData2D; %this variable is manning's n * 2 for std dev areas
clear OutData2D;

load ('/Users/andrearyan/Documents/MATLAB/PC2
20110603/NuecesRuns_20110610_outdata/Nueces2010_WR_14d_en_0p/OutData2D.mat');
OutData2D_en = OutData2D; %this variable is manning's n * 10 for std dev areas
clear OutData2D;

%% Total Volume in the Delta for Runs with varying roughness

length1 = size(OutData2D_an.depth_time);
mm = length1(2)-1;%-1 since the OutData2D_dn & en are 1 less time step

sum_volume_an = zeros(mm,1);
volume_an = zeros(667,971,mm);
for n = 1:mm
    volume_an(:,:,n) = OutData2D_an.depth(:,:,n);
    volume_an_nonan = volume_an(:,:,n);
    aa = isnan(volume_an_nonan);
    volume_an_nonan(aa) = 0; %get rid of NaNs
    volume_an(:,:,n) = volume_an_nonan;

    sum_volume_an(n,1) = sum(sum(volume_an(:,:,n)));
end

disp ('*****Finished Summing Volume for Normal Roughness Scenario*****')

sum_volume_bn = zeros(mm,1);

```

```

volume_bn = zeros(667,971,mm);
for n = 1:mm
    volume_bn(:,:,n) = OutData2D_bn.depth(:,:,n);
    volume_bn_nonan = volume_bn(:,:,n);
    aa = isnan(volume_bn_nonan);
    volume_bn_nonan(aa) = 0; %get rid of NaNs
    volume_bn(:,:,n) = volume_bn_nonan;

    sum_volume_bn(n,1) = sum(sum(volume_bn(:,:,n)));
end

disp('*****Finished Summing Volume for 10x Roughness Scenario*****')

sum_volume_cn = zeros(mm,1);
volume_cn = zeros(667,971,mm);
for n = 1:mm
    volume_cn(:,:,n) = OutData2D_cn.depth(:,:,n);
    volume_cn_nonan = volume_cn(:,:,n);
    aa = isnan(volume_cn_nonan);
    volume_cn_nonan(aa) = 0; %get rid of NaNs
    volume_cn(:,:,n) = volume_cn_nonan;

    sum_volume_cn(n,1) = sum(sum(volume_cn(:,:,n)));
end

disp('*****Finished Summing Volume for 100x Roughness Scenario*****')

sum_volume_dn = zeros(mm,1);
volume_dn = zeros(667,971,mm);
for n = 1:mm
    volume_dn(:,:,n) = OutData2D_dn.depth(:,:,n);
    volume_dn_nonan = volume_dn(:,:,n);
    aa = isnan(volume_dn_nonan);
    volume_dn_nonan(aa) = 0; %get rid of NaNs
    volume_dn(:,:,n) = volume_dn_nonan;

    sum_volume_dn(n,1) = sum(sum(volume_dn(:,:,n)));
end

disp('*****Finished Summing Volume for 2x std dev Roughness Scenario*****')

sum_volume_en = zeros(mm,1);
volume_en = zeros(667,971,mm);
for n = 1:mm
    volume_en(:,:,n) = OutData2D_en.depth(:,:,n);
    volume_en_nonan = volume_en(:,:,n);
    aa = isnan(volume_en_nonan);
    volume_en_nonan(aa) = 0; %get rid of NaNs
    volume_en(:,:,n) = volume_en_nonan;

    sum_volume_en(n,1) = sum(sum(volume_en(:,:,n)));
end

disp('*****Finished Summing Volume for 10x std dev Roughness Scenario*****')

% compare total volume of water in the system
x_an = OutData2D_an.depth_time./3600./24;
x_bn = OutData2D_bn.depth_time./3600./24;
x_cn = OutData2D_cn.depth_time./3600./24;

```

```

x_dn = OutData2D_dn.depth_time./3600./24;
x_en = OutData2D_en.depth_time./3600./24;

y_an = sum_volume_an.*15*15;
y_bn = sum_volume_bn.*15*15;
y_cn = sum_volume_cn.*15*15;
y_dn = sum_volume_dn.*15*15;
y_en = sum_volume_en.*15*15;

%% difference in total volume:
diff_totalvol = y_an - y_bn;
diff_totalvol2 = y_an - y_cn;
diff_totalvol3 = y_an - y_dn;
diff_totalvol4 = y_an - y_en;

%% percent diff in total volume
perc_totalvol = (y_an - y_bn)./y_an.*100;
perc_totalvol2 = (y_an - y_cn)./y_an.*100;
perc_totalvol3 = (y_an - y_dn)./y_an.*100;
perc_totalvol4 = (y_an - y_en)./y_an.*100;

%% Find max total volume of water in the system:
max_an_vol = max(sum_volume_an(:,1)).*15*15;
max_bn_vol = max(sum_volume_bn(:,1)).*15*15;
max_cn_vol = max(sum_volume_cn(:,1)).*15*15;
max_dn_vol = max(sum_volume_dn(:,1)).*15*15;
max_en_vol = max(sum_volume_en(:,1)).*15*15;

```

D.5 SCRIPT FOR ANALYZING PUMPING

```

%% Compare Pump Scenarios

load ('/Users/andrearyan/Documents/MATLAB/PC2
20110427/Analysis/Nueces_15x15_April2008/OutData3D_0p.mat');
OutData3D_0p = OutData3D; clear OutData3D;
disp ('*****Finished loading first variable*****')

load ('/Users/andrearyan/Documents/MATLAB/PC2
20110427/Analysis/Nueces_15x15_April2008_1pump/OutData3D_1p.mat');
OutData3D_1p = OutData3D; clear OutData3D;
disp ('*****Finished loading second variable*****')

load ('/Users/andrearyan/Documents/MATLAB/PC2
20110427/Analysis/Nueces_15x15_April2008_2pumps/OutData3D_2p.mat');
OutData3D_2p = OutData3D; clear OutData3D;
disp ('*****Finished loading third variable*****')

load ('/Users/andrearyan/Documents/MATLAB/PC2
20110427/Analysis/Nueces_15x15_April2008_3pumps/OutData3D_3p.mat');
OutData3D_3p = OutData3D; clear OutData3D;
disp ('*****Finished loading fourth variable*****')

%% Find Ai at each time step - considering all spaces with any Blue = 1
length1 = size(OutData3D_1p.Blue_time);
mm = length1(2);

```

```

depth_cutoff = 0.02; %this is the depth below which will not be included in Ai

% 1 PUMP
sum_area_1p = zeros(mm,1);
blue_1p = zeros(667,971,mm);

for n = 1:mm
    blue_1p(:,:,n) = OutData3D_1p.Blue(:,:,1,n);
    blue_1p_nonan = blue_1p(:,:,n);
    aa = isnan(blue_1p_nonan);
    blue_1p_nonan(aa) = 0; %get rid of nans
    bb = find(blue_1p_nonan > 0);
    blue_1p_nonan(bb) = 1; %make all non-zero values = 1 (no fractions)
    blue_1p(:,:,n) = blue_1p_nonan; %blue_1p(:,:,n) now has 1's where there is
blue tracer and 0's elsewhere

    sum_area_1p(n,1) = sum(sum(blue_1p(:,:,n))).*15.*15; %gives area inundated
at greater than 2 cm
end

disp ('*****Finished Finding Inundated Area for 1 Pump Scenario*****')

% 2 PUMPS
sum_area_2p = zeros(mm,1);
blue_2p = zeros(667,971,mm);

for n = 1:mm
    blue_2p(:,:,n) = OutData3D_2p.Blue(:,:,1,n);
    blue_2p_nonan = blue_2p(:,:,n);
    aa = isnan(blue_2p_nonan);
    blue_2p_nonan(aa) = 0; %get rid of nans
    bb = find(blue_2p_nonan > 0);
    blue_2p_nonan(bb) = 1; %make all non-zero values = 1 (no fractions)
    blue_2p(:,:,n) = blue_2p_nonan; %blue_2p(:,:,n) now has 1's where there is
blue tracer and 0's elsewhere

    sum_area_2p(n,1) = sum(sum(blue_2p(:,:,n))).*15.*15; %gives area inundated
at greater than 2 cm
end

disp ('*****Finished Finding Inundated Area for 2 Pump Scenario*****')

% 3 PUMPS
sum_area_3p = zeros(mm,1);
blue_3p = zeros(667,971,mm);

for n = 1:mm
    blue_3p(:,:,n) = OutData3D_3p.Blue(:,:,1,n);
    blue_3p_nonan = blue_3p(:,:,n);
    aa = isnan(blue_3p_nonan);
    blue_3p_nonan(aa) = 0; %get rid of nans
    bb = find(blue_3p_nonan > 0);
    blue_3p_nonan(bb) = 1; %make all non-zero values = 1 (no fractions)
    blue_3p(:,:,n) = blue_3p_nonan; %blue_1p(:,:,n) now has 1's where there is
blue tracer and 0's elsewhere

    sum_area_3p(n,1) = sum(sum(blue_3p(:,:,n))).*15.*15; %gives area inundated
at greater than 2 cm

```

```

end

disp ('*****Finished Finding Inundated Area for 3 Pump Scenario*****')

%% Find inundated area at each time step - with cutoff
length1 = size(OutData3D_1p.Blue_time);
mm = length1(2);

cutoff = 0.4; %this is the fraction of blue tracer required to be included in
Ai

% 1 PUMP
sum_area_1p_cutoff = zeros(mm,1);
blue_1p_cutoff = zeros(667,971,mm);

for n = 1:mm
    blue_1p_cutoff(:,:,n) = OutData3D_1p.Blue(:,:,1,n);
    blue_1p_clean = blue_1p_cutoff(:,:,n);
    aa = isnan(blue_1p_clean);
    blue_1p_clean(aa) = 0; %get rid of nans
    bb = find(blue_1p_clean > cutoff);
    blue_1p_clean(bb) = 1; %make all more than cutoff = 1
    cc = find(blue_1p_clean < cutoff);
    blue_1p_clean(cc) = 0; %make all less than cutoff = 0
    blue_1p_cutoff(:,:,n) = blue_1p_clean; %blue_1p(:,:,n) now has 1's where
there is blue tracer greater than cutoff and 0's elsewhere

    sum_area_1p_cutoff(n,1) = sum(sum(blue_1p_cutoff(:,:,n))).*15.*15; %gives
area inundated at greater than 2 cm
end

disp ('*****Finished Finding Cutoff Inundated Area for 1 Pump Scenario*****')

% 2 PUMP
sum_area_2p_cutoff = zeros(mm,1);
blue_2p_cutoff = zeros(667,971,mm);

for n = 1:mm
    blue_2p_cutoff(:,:,n) = OutData3D_2p.Blue(:,:,1,n);
    blue_2p_clean = blue_2p_cutoff(:,:,n);
    aa = isnan(blue_2p_clean);
    blue_2p_clean(aa) = 0; %get rid of nans
    bb = find(blue_2p_clean >= cutoff);
    blue_2p_clean(bb) = 1; %make all more than cutoff = 1
    cc = find(blue_2p_clean < cutoff);
    blue_2p_clean(cc) = 0; %make all less than cutoff = 0
    blue_2p_cutoff(:,:,n) = blue_2p_clean; %blue_1p(:,:,n) now has 1's where
there is blue tracer greater than cutoff and 0's elsewhere

    sum_area_2p_cutoff(n,1) = sum(sum(blue_2p_cutoff(:,:,n))).*15.*15; %gives
area inundated at greater than 2 cm
end

disp ('*****Finished Finding Cutoff Inundated Area for 2 Pump Scenario*****')

% 3 PUMP
sum_area_3p_cutoff = zeros(mm,1);
blue_3p_cutoff = zeros(667,971,mm);

```

```

for n = 1:mm
    blue_3p_cutoff(:,:,n) = OutData3D_3p.Blue(:,:,1,n);
    blue_3p_clean = blue_3p_cutoff(:,:,n);
    aa = isnan(blue_3p_clean);
    blue_3p_clean(aa) = 0; %get rid of nans
    bb = find(blue_3p_clean >= cutoff);
    blue_3p_clean(bb) = 1; %make all more than cutoff = 1
    cc = find(blue_3p_clean < cutoff);
    blue_3p_clean(cc) = 0; %make all less than cutoff = 0
    blue_3p_cutoff(:,:,n) = blue_3p_clean; %blue_1p(:,:,n) now has 1's where
there is blue tracer greater than cutoff and 0's elsewhere

    sum_area_3p_cutoff(n,1) = sum(sum(blue_3p_cutoff(:,:,n))).*15.*15; %gives
area inundated at greater than 2 cm
end

disp ('*****Finished Finding Cutoff Inundated Area for 3 Pump Scenario*****')

%% Pumping at each hour
ypump_1p = zeros(mm,1);
for bb = 1:mm
    ypump_1p(bb,1) = (0.5).*bb*3600; % flow=0.5 cms/pump & bb is saved hourly
end

ypump_2p = zeros(mm,1);
for bb = 1:mm
    ypump_2p(bb,1) = (1.0).*bb*3600;
end

ypump_3p = zeros(mm,1);
for bb = 1:mm
    ypump_3p(bb,1) = (1.5).*bb*3600;
end

%% Compare Cutoff Scenarios for 2 Pump Scenario
% 2 PUMP
sum_area_2p_cutoff1_multiple = zeros(mm,1);
blue_2p_cutoff_multiple = zeros(667,971,mm);
area_with_cutoff_multiple = zeros(10,mm,1);

for j = 1:10
    cutoff = j.*0.1;
    for n = 1:mm
        blue_2p_cutoff_multiple(:,:,n) = OutData3D_2p.Blue(:,:,1,n);
        blue_2p_clean_multiple = blue_2p_cutoff_multiple(:,:,n);
        aa = isnan(blue_2p_clean_multiple);
        blue_2p_clean_multiple(aa) = 0; %get rid of nans
        bb = find(blue_2p_clean_multiple >= cutoff);
        blue_2p_clean_multiple(bb) = 1; %make all more than cutoff = 1
        cc = find(blue_2p_clean_multiple < cutoff);
        blue_2p_clean_multiple(cc) = 0; %make all less than cutoff = 0
        blue_2p_cutoff_multiple(:,:,n) = blue_2p_clean_multiple;
    %blue_1p(:,:,n) now has 1's where there is blue tracer greater than cutoff and
    0's elsewhere

        sum_area_2p_cutoff1_multiple(n,1) =
sum(sum(blue_2p_cutoff_multiple(:,:,n))).*15.*15; %gives area inundated at
greater than 2 cm
    end
end

```

```

        area_with_cutoff_multiple(j,:,1) = sum_area_2p_cutoff1_multiple;
end

disp ('*****Finished Finding Ai for various cutoffs for 2 Pump Scenario*****')

%% Compare Salinities

%% Find matrix at each time step for salinity less than salinity cutoff
(brackish water)
length1 = size(OutData3D_1p.Salinity_time);
mm = length1(2);

SAL_cutoff = 15; %this is the salinity cutoff

% 0 PUMP
sal_0p = zeros(667,971,mm);

for n = 1:mm
    sal_0p(:,:,n) = OutData3D_0p.Salinity(:,:,1,n);
    sal_0p_nonan = sal_0p(:,:,n);
    aa = isnan(sal_0p_nonan);
    sal_0p_nonan(aa) = SAL_cutoff+1; %get rid of nans - make NaN > cutoff
    cc = find(sal_0p_nonan <= SAL_cutoff);
    sal_0p_nonan(cc) = 1; %make all values <= 15ppt = 1 (no fractions)
    bb = find(sal_0p_nonan > SAL_cutoff); %(this includes the NaNs)
    sal_0p_nonan(bb) = 0; %make all values > 15ppt = 0 (no fractions)
    sal_0p(:,:,n) = sal_0p_nonan; % 1's where there is sal<=15 & 0's elsewhere
end

disp ('*****Finished Finding Salinity matrix for salinity < 15 for 1 Pump
Scenario*****')

% 1 PUMP
sal_1p = zeros(667,971,mm);

for n = 1:mm
    sal_1p(:,:,n) = OutData3D_1p.Salinity(:,:,1,n);
    sal_1p_nonan = sal_1p(:,:,n);
    aa = isnan(sal_1p_nonan);
    sal_1p_nonan(aa) = SAL_cutoff+1; %get rid of nans - make NaN > cutoff
    cc = find(sal_1p_nonan <= SAL_cutoff);
    sal_1p_nonan(cc) = 1; %make all values <= 15ppt = 1 (no fractions)
    bb = find(sal_1p_nonan > SAL_cutoff);
    sal_1p_nonan(bb) = 0; %make all values > 15ppt = 0 (no fractions)
    sal_1p(:,:,n) = sal_1p_nonan; % 1's where there is sal<=15 & 0's elsewhere
end

disp ('*****Finished Finding Sal matrix for sal < 15 for 1 Pump Scenario*****')

% 2 PUMPS
sal_2p = zeros(667,971,mm);

for n = 1:mm
    sal_2p(:,:,n) = OutData3D_2p.Salinity(:,:,1,n);
    sal_2p_nonan = sal_2p(:,:,n);
    aa = isnan(sal_2p_nonan);
    sal_2p_nonan(aa) = SAL_cutoff + 1; %get rid of nans - make NaN > cutoff
    cc = find(sal_2p_nonan <= SAL_cutoff);
    sal_2p_nonan(cc) = 1; %make all values <= 15ppt = 1 (no fractions)

```

```

        bb = find(sal_2p_nonan > SAL_cutoff);
        sal_2p_nonan(bb) = 0; %make all values > 15ppt = 0 (no fractions)
        sal_2p(:, :, n) = sal_2p_nonan; % 1's where there is sal<=15 & 0's elsewhere
    end

disp ('*****Finished Finding Sal matrix for sal < 15 for 2 Pump Scenario*****')

% 3 PUMPS

sal_3p = zeros(667,971,mm);

for n = 1:mm
    sal_3p(:, :, n) = OutData3D_3p.Salinity(:, :, 1, n);
    sal_3p_nonan = sal_3p(:, :, n);
    aa = isnan(sal_3p_nonan);
    sal_3p_nonan(aa) = 120; %get rid of nans - make NaN > cutoff
    cc = find(sal_3p_nonan <= SAL_cutoff);
    sal_3p_nonan(cc) = 1; %make all values <= 15ppt = 1 (no fractions)
    bb = find(sal_3p_nonan > SAL_cutoff);
    sal_3p_nonan(bb) = 0; %make all values > 15ppt = 0 (no fractions)
    sal_3p(:, :, n) = sal_3p_nonan; % 1's where there is sal<=15 & 0's elsewhere
end

disp ('*****Finished Finding Sal matrix for sal < 15 for 3 Pump Scenario*****')

%% Find matrix for fraction of freshwater
ref = 30; %reference level of 30 ppt

% 0 PUMP
frac_0p = zeros(667,971,mm);

for n = 1:mm
    frac_0p(:, :, n) = OutData3D_0p.Salinity(:, :, 1, n);
    frac_0p_nonan = frac_0p(:, :, n);
    aa = isnan(frac_0p_nonan);
    frac_0p_nonan(aa) = ref + 3; %to get rid of nans - make NaN > ref
    F = (ref - frac_0p_nonan)./ref;
    bb = find(F < 0); %anywhere there was higher sal than ref, F < 0
    F(bb) = 0; %make all values > ref or NaN = 0 (no fractions)

    frac_0p(:, :, n) = F;
end

disp ('*****Finished Finding FW fraction matrix for 0 Pump Scenario*****')

% 1 PUMP
frac_1p = zeros(667,971,mm);

for n = 1:mm
    frac_1p(:, :, n) = OutData3D_1p.Salinity(:, :, 1, n);
    frac_1p_nonan = frac_1p(:, :, n);
    aa = isnan(frac_1p_nonan);
    frac_1p_nonan(aa) = ref + 3; %get rid of nans - make NaN > ref
    F = (ref - frac_1p_nonan)./ref;
    bb = find(F < 0); %anywhere there was higher sal than ref, F < 0
    F(bb) = 0; %make all values > ref or NaN = 0 (no fractions)
    frac_1p(:, :, n) = F;
end

```



```

disp ('*****Finished Finding FW fraction matrix for 1 Pump Scenario*****')

% 0 PUMP
frac_2p = zeros(667,971,mm);

for n = 1:mm
    frac_2p(:,:,n) = OutData3D_2p.Salinity(:,:,1,n);
    frac_2p_nonan = frac_2p(:,:,n);
    aa = isnan(frac_2p_nonan);
    frac_2p_nonan(aa) = ref + 3; %get rid of nans - make NaN > ref
    F = (ref - frac_2p_nonan)./ref;
    bb = find(F < 0); %anywhere there was higher sal than ref, F < 0
    F(bb) = 0; %make all values > ref or NaN = 0 (no fractions)
    frac_2p(:,:,n) = F;
end

disp ('*****Finished Finding FW fraction matrix for 2 Pump Scenario*****')

% 0 PUMP
frac_3p = zeros(667,971,mm);

for n = 1:mm
    frac_3p(:,:,n) = OutData3D_3p.Salinity(:,:,1,n);
    frac_3p_nonan = frac_3p(:,:,n);
    aa = isnan(frac_3p_nonan);
    frac_3p_nonan(aa) = ref + 3; %get rid of nans - make NaN > ref
    F = (ref - frac_3p_nonan)./ref;
    bb = find(F < 0); %anywhere there was higher sal than ref, F < 0
    F(bb) = 0; %make all values > ref or NaN = 0 (no fractions)
    frac_3p(:,:,n) = F;
end

disp ('*****Finished Finding FW fraction matrix for 3 Pump Scenario*****')

%% Load OutData2D's for Depth

load ('/Users/andrearyan/Documents/MATLAB/PC2
20110427/Analysis/Nueces_15x15_April2008/OutData2D_0p.mat');
OutData2D_0p = OutData2D; clear OutData2D;
disp ('*****Finished loading first variable*****')

load ('/Users/andrearyan/Documents/MATLAB/PC2
20110427/Analysis/Nueces_15x15_April2008_1pump/OutData2D_1p.mat');
OutData2D_1p = OutData2D; clear OutData2D;
disp ('*****Finished loading second variable*****')

load ('/Users/andrearyan/Documents/MATLAB/PC2
20110427/Analysis/Nueces_15x15_April2008_2pumps/OutData2D_2p.mat');
OutData2D_2p = OutData2D; clear OutData2D;
disp ('*****Finished loading third variable*****')

load ('/Users/andrearyan/Documents/MATLAB/PC2
20110427/Analysis/Nueces_15x15_April2008_3pumps/OutData2D_3p.mat');
OutData2D_3p = OutData2D; clear OutData2D;
disp ('*****Finished loading fourth variable*****')

%% Calculate Volume of Brackish water (volume < SAL_cutoff)

% 0 Pumps:

```

```

vol_brack_0p = zeros(mm,1);

for n = 1:mm
    depth_0p = OutData2D_0p.depth(:,:,n);
    gg = isnan(depth_0p);
    depth_0p(gg) = 0;
    brackish_0p = sum(sum(sal_0p(:,:,n).*depth_0p)).*15.*15;
    %this multiplies the depth by 1 for any cell with salinity < 15ppt and 0 for
    any cell > 15ppt and also takes the sum to find the volume (sum up all the
    depths & multiply by 225)
    vol_brack_0p(n,1) = brackish_0p;
end

% 1 Pumps:
vol_brack_1p = zeros(mm,1);

for n = 1:mm
    depth_1p = OutData2D_1p.depth(:,:,n);
    gg = isnan(depth_1p);
    depth_1p(gg) = 0;
    brackish_1p = sum(sum(sal_1p(:,:,n).*depth_1p)).*15.*15;
    %this multiplies the depth by 1 for any cell with salinity < 15ppt and 0 for
    any cell > 15ppt and also takes the sum to find the volume (sum up all the
    depths & multiply by 225)
    vol_brack_1p(n,1) = brackish_1p;
end

% 2 Pumps:
vol_brack_2p = zeros(mm,1);

for n = 1:mm
    depth_2p = OutData2D_2p.depth(:,:,n);
    gg = isnan(depth_2p);
    depth_2p(gg) = 0;
    brackish_2p = sum(sum(sal_2p(:,:,n).*depth_2p)).*15.*15;
    %this multiplies the depth by 1 for any cell with salinity < 15ppt and 0 for
    any cell > 15ppt and also takes the sum to find the volume (sum up all the
    depths & multiply by 225)
    vol_brack_2p(n,1) = brackish_2p;
end

% 3 Pumps:
vol_brack_3p = zeros(mm,1);

for n = 1:mm
    depth_3p = OutData2D_3p.depth(:,:,n);
    gg = isnan(depth_3p);
    depth_3p(gg) = 0;
    brackish_3p = sum(sum(sal_3p(:,:,n).*depth_3p)).*15.*15;
    %this multiplies the depth by 1 for any cell with salinity < 15ppt and 0 for
    any cell > 15ppt and also takes the sum to find the volume (sum up all the
    depths & multiply by 225)
    vol_brack_3p(n,1) = brackish_3p;
end

%% Calculate V_FW in the system (assuming 30 as the ref salinity)

% 0 Pumps
frac_0p(:,:,n);

```

```

vol_fresh_0p = zeros(mm,1);

for n = 1:mm
    depth_0p = OutData2D_0p.depth(:,:,n);
    gg = isnan(depth_0p);
    depth_0p(gg) = 0;
    fresh_0p = sum(sum(frac_0p(:,:,n).*depth_0p)).*15.*15;
    % this multiplies the fraction of freshwater in each cell by the depth
    % and area to find the volume of freshwater
    vol_fresh_0p(n,1) = fresh_0p;
end

% 1 Pumps
frac_1p(:,:,n);
vol_fresh_1p = zeros(mm,1);

for n = 1:mm
    depth_1p = OutData2D_1p.depth(:,:,n);
    gg = isnan(depth_1p);
    depth_1p(gg) = 0;
    fresh_1p = sum(sum(frac_1p(:,:,n).*depth_1p)).*15.*15;
    % this multiplies the fraction of freshwater in each cell by the depth
    % and area to find the volume of freshwater
    vol_fresh_1p(n,1) = fresh_1p;
end

% 2 Pumps
frac_2p(:,:,n);
vol_fresh_2p = zeros(mm,1);

for n = 1:mm
    depth_2p = OutData2D_2p.depth(:,:,n);
    gg = isnan(depth_2p);
    depth_2p(gg) = 0;
    fresh_2p = sum(sum(frac_2p(:,:,n).*depth_2p)).*15.*15;
    % this multiplies the fraction of freshwater in each cell by the depth
    % and area to find the volume of freshwater
    vol_fresh_2p(n,1) = fresh_2p;
end

% 3 Pumps
frac_3p(:,:,n);
vol_fresh_3p = zeros(mm,1);

for n = 1:mm
    depth_3p = OutData2D_3p.depth(:,:,n);
    gg = isnan(depth_3p);
    depth_3p(gg) = 0;
    fresh_3p = sum(sum(frac_3p(:,:,n).*depth_3p)).*15.*15;
    % this multiplies the fraction of freshwater in each cell by the depth
    % and area to find the volume of freshwater
    vol_fresh_3p(n,1) = fresh_3p;
end

```

References

- Adams, John S., and Jace Tunnell. *Rincon Bayou Salinity Monitoring Project*. Corpus Christi, TX: Coastal Bend Bays & Estuaries Program, 2010.
- Alan Plummer Associates, Inc. "City of Corpus Christi Water Supply Project." 2007.
- Alber, Merryl. "A Conceptual Model of Estuarine Freshwater Inflow Management." *Estuaries* 25, no. 6B (2002): 1262-1274.
- Alexander, Heather D., and Kenneth H. Dunton. "Freshwater Inundation Effects on Emergent Vegetation of a Hypersaline Salt Marsh." *Estuaries*, 2002: 1426-1425.
- Alexander, Heather D., and Kenneth H. Dunton. "Treated Wastewater Effluent as an Alternative Freshwater Source in a Hypersaline Salt Marsh: Impacts on Salinity, Inorganic Nitrogen, and Emergent Vegetation." *Journal of Coastal Research* 22, no. 2 (2006): 377-392.
- Battjes, Jurjen A. "Developments in coastal engineering research." *Coastal Engineering* 53 (2006): 121-132.
- Bisht, Gautam, Virginia Venturini, and Shafiqul Isl. "Estimation of the net radiation using MODIS (Moderate Resolution Imaging Spectroradiometer) data for clear sky days." *Remote Sensing of Environment* 97 (2005): 52-67.
- Bureau of Reclamation. 2000a. *Concluding Report: Rincon Bayou Demonstration Project. Volume I: Executive Summary*. United States Department of the Interior, Bureau of Reclamation, Oklahoma-Texas Area Office, Austin, Texas.
- Bureau of Reclamation. 2000b. *Concluding Report: Rincon Bayou Demonstration Project. Volume II: Findings*. United States Department of the Interior, Bureau of Reclamation, Oklahoma-Texas Area Office, Austin, Texas.

- Casulli, V., and E. Cattani. "Stability, Accuracy and Efficiency of a Semi-Implicit Method for Three-Dimensional Shallow Water Flow." *Computers & Mathematics with Applications* 27, no. 4 (1994): 99-112.
- Casulli, V., and P. Zanolli. "Semi-Implicit Numerical Modeling of Nonhydrostatic Free-Surface Flows for Environmental Problems." *Mathematical and Computer Modelling* 36 (2002): 1131-1149.
- Casulli, Vincenzo, and Ralph T. Cheng. "Semi-Implicit Finite Difference Methods for Three-Dimensional Shallow Water Flow." *International Journal for Numerical Methods in Fluids* 15 (1992): 629-648.
- Charbeneau, Randall J., and Edward R. Holley. *Backwater Effects of Bridge Piers in Subcritical Flow*. Project Summary Report, Center for Transportation Research, University of Texas at Austin, 2001.
- Chen, Changsheng, Hedong Liu, and Robert C. Beardsley. "An Unstructured Grid, Finite-Volume, Three-Dimensional, Primitive Equations Ocean Model: Application to Coastal Ocean and Estuaries." *Journal of Atmospheric and Oceanic Technology* 20 (2003): 159-186.
- Copeland, B.J. "Effects of Decreased River Flow on Estuarine Ecology." *Water Pollution Control Federation* 38, no. 11 (1996): 1831-1839.
- Cunningham, Atlee M. *Corpus Christi Water Supply Documented History 1852-1997. Second Edition*. Corpus Christi, TX: Texas A&M University- Corpus Christi, 1999.
- Gibeaut, J. "Lidar: Mapping a Shoreline by Laser Light." *Geotimes* 48, no. 11 (2003): 22-27.

- Heilman, J.L., F.A. Heinsch, D.R. Cobos, and K.J. McInnes. "Energy Balance of a High Marsh on the Texas Gulf Coast: Effect of Water Availability." *Journal of Geophysical Research* 105, no. D17 (2000): 22371-22377.
- Hodges, Ben R. "Accuracy Order of Crank–Nicolson Discretization for Hydrostatic Free-Surface Flow." *Journal of Engineering Mechanics-ASCE* 130, no. 8 (2004): 904-910.
- Hodges, Ben R., Bernard Laval, and Bridget M. Wadzuk. "Numerical error assessment and a temporal horizon for internal waves in a hydrostatic model." *Ocean Modelling* 13 (2006): 44-64.
- Hossain, AKMA, Yafei Jia, and Xiabo Chao. "Estimation of Manning's Roughness Coefficient Distribution for Hydrodynamic Model Using Remotely Sensed Land Cover Features." *2009 17th International Conference on Geoinformatics*. Fairfax, VA: George Mason University, 2009. 635-638.
- Irlbeck, M.J., and G.H. Ward. "Analysis of the historic flow regime of the Nueces River into the upper Nueces Delta, and of the potential restoration value of the Rincon Bayou Demonstration Project." *In Concluding Report: Rincon Bayou Demonstration Project, Appendix C*. (United States Department of the Interior, Bureau of Reclamation), 2000.
- Ji, Z.-G., M.R. Morton, and J.M. Hamrick. "Wetting and Drying Simulation of Estuarine Processes." *Estuarine, Coastal and Shelf Science* 53 (2001): 683-700.
- Montagna, P.A., E.M. Hill, and B. Moulton. "Role of Science-based and Adaptive Management in Allocating Environmental Flows to the Nueces Estuary, Texas, USA." *WIT Transactions on Ecology and the Environment* 122 (2009): 559-570.
- Montagna, Paul A., Alber Merryl, Doering Peter, and Connor S. Michael. "Freshwater Inflow: Science, Policy, Management." *Estuaries* 25, no. 6B (2002): 1243-1245.

- Montagna, Paul A., Richard D. Kalke, and Christine Ritter. "Effect of Restored Freshwater Inflow on Macrofauna and Meiofauna in Upper Rincon Bayou, TX, USA." *Estuaries* 25, no. 6B (2002): 1436-1447.
- Nicolau, Brien A., John Jr. W. Tunnell, John S. Adams, and Barbara F. Ruth. "Long-Term Monitoring of Estuarine Faunal Use in the Nueces Delta Mitigation Project, Corpus Christi, Texas: 1989 Through 1995." *Annual Ecosystem Restoration Conference*. Tampa, Florida, 1996.
- Nicolau, Terri, et al. "Nueces Estuary Advisory Council Recommended Monitoring Plan For Rincon Bayou, Nueces Delta." 2002.
- Ockerman, D.J. *Water Budget for the Nueces Estuary, Texas, May-October 1998*. Fact Sheet, U.S. Department of the Interior, U.S. Geological Survey, 2001.
- Oey, Lie-Yauw. "An OGCM with movable land-sea boundaries." *Ocean Modelling* 13 (2006): 176-195.
- Palmer, Terry A., Paul A. Montagna, and Richard D. Kalke. "Downstream Effects of Restored Freshwater Inflow to Rincon Bayou, Nueces Delta, Texas, USA." *Estuaries* 25, no. 6B (2002): 1448-1456.
- Pulich, Warren. "Texas Coastal Bend." (USGS) 2006.
- Rasser, Michael Kevin. *The Role of Biotic and Abiotic Processes in the Zonation of Salt Marsh Plants in the Nueces River Delta, Texas*. Dissertation, The University of Texas at Austin, 2009.
- Roman, Charles T., Richard W. Garvine, and John W. Portnoy. "Hydrologic Modeling as a Predictive Basis for Ecological Restoration of Salt Marshes." *Environmental Management* 19, no. 4 (1995): 559-566.

- Rueda, F.J., E. Sanmiguel-Rojas, and B.R. Hodges. "Baroclinic stability for a family of two-level semi-implicit numerical methods for the 3D shallow water equations." *International Journal for Numerical Methods in Fluids* 54, no. 3 (2007): 237-268.
- Sellers, William. *Physical Climatology*. Chicago: The University of Chicago Press, 1965.
- Spillman, C.M., Hamilton, D.P., Hipsey, M.R., Imberger J., (2008). "A spatially resolved model of seasonal variations in phytoplankton and clam (*Tapes philippinarum*) biomass in Barbamarco Lagoon, Italy." *Estuarine Coastal and Shelf Science* 79, no. 2 (2008):187-203.
- Stelling, G.S., H.W.J. Kernkamp, and M.M. Laguzzi. "Delft Flooding System: A powerful tool for inundation assessment based upon a positive flow simulation." *Hydroinformatics*, 1998: 449-456.
- Tolan, JM. "El Nino-Southern Oscillation impacts translated to the watershed scale: Estuarine salinity patterns along the Texas Gulf Coast, 1982 to 2004." *Estuarine Coastal and Shelf Science* 72, no. 1-2 (March 2007): 247-260.
- U.S. Secretary of Commerce. *National Institute of Standards and Technology Chemistry WebBook*. 2008. <http://webbook.nist.gov/chemistry/> (accessed 2011).
- Veilleux, Vicki. *National Geodetic Survey: Frequently Asked Questions*. January 2011. <http://www.ngs.noaa.gov/faq.shtml>.
- Ward, George H. *Processes and Trends of Circulation within the Corpus Christi Bay National Estuary Program Study Area*. Corpus Christi: Texas National Resource Conservation Commission, 1997.
- Ward, George H., Michael J. Irlbeck, and Paul A. Montagna. "Experimental River Diversion for Marsh Enhancement." *Estuaries* 25, no. 6B (2002): 1416-1425.

- Wunderlich, Walter O. *Heat and Mass Transfer Between a Water Surface and the Atmosphere*. Laboratory Report No. 14, Norris: Tennessee Valley Authority, 1972.
- Xia, Junqiang, Roger A. Falconer, and Binliang Lin. "Hydrodynamic impact of a tidal barrage in the Severn Estuary, UK." *Renewable Energy* 35 (2010): 1455–1468.
- Yang, Zhaoqing, and Tarang Khangaonkar. "Modeling tidal circulation and stratification in Skagit River estuary using an unstructured grid ocean model." *Ocean Modelling* 28 (2009): 34-49.
- Zhang, Yinglong, Antonio M. Baptista, and Edward P. III Myers. "A cross-scale model for 3D baroclinic circulation in estuary-plume-shelf systems: I. Formulation and skill assessment." *Continental Shelf Research* 24 (2004): 2187-2214.
- Zheng, Lianyuan, Changsheng Chen, and Frank Y. Zhang. "Development of water quality model in the Satilla River Estuary, Georgia." *Ecological Modelling* 178 (2004): 457-482.